Understanding the Mechanisms of Gas/Particle Partitioning of Semi-Volatile Organic Compounds to Model Inorganic Aerosols, Model Organic Aerosols, and Urban Particulate Material

Cikui Liang
B.S., Zhongshan University, 1991
M.S., Oregon Graduate Institute of Science & Technology, 1993

A dissertation submitted to the faculty of the
Oregon Graduate Institute of Science and Technology
in partial fulfillment of the requirements for the degree
Doctor of Philosophy
in
Environmental Science and Engineering

September 1997

This dissertation "Understanding the Mechanisms of Gas/Particle Partitioning of Semi-Volatile Organic Compounds to Model Inorganic Aerosols, Model Organic Aerosols, and Urban Particulate Material" by Cikui Liang has been examined and approved by the following Examination Committee:

James F. Pankow, Advisor
Department Chairman, Professor

James F. Huntzicker
OGI Sr. Vice President, Professor

Richard L. Johnson
Associate Professor

Matthew S. Sachs
Associate Professor

ACKNOWLEDGEMENTS

Throughout the time I spent in graduate school, many people have helped to make my experience more rewarding, enlightening, productive, and enjoyable. Although too numerous to mention each of them here, I wish to express my thanks to all of those individuals.

I wish to thank my thesis advisor, Jim Pankow, for his insightful direction, encouragement, advice, financial support, patience, and friendship. He has taught me how to be a good scientist, how to write English well, and basically how to be a decent person. I am very grateful for his helping hands when I encounter problems in my research and daily life. I also thank him for giving me the opportunity to work with John Seinfeld's group at Caltech, where I have learned numerous new techniques and how to work with other scientist. I would like to thank the other members of my thesis committee, Jim Huntzicker, Rick Johnson, and Matthew Sachs, for reviewing this work and offering insightful comments. I would also like to thank Paul Tratnyek for giving helpful suggestions on my statistical questions and providing guidance on various aspects.

Lorne Isabelle and Wentai Luo gave me tremendous help in the design and construction of the experimental apparatus. They were never tired of my endless questions. Special thank goes to Lorne Isabelle, whose experience, resourcefulness, and skill keeps the lab running, and whose sense of humor enriches the lives of all around him.

Clinton Church, Brain Mader, and Andrea Pavlick have been great friends as well as important resources for English gammer questions. I specifically thank Clint for editing my thesis chapters and helping me with my thesis defense presentation, and for getting out of my way when I needed to use the GC/MS. I would also like to thank Diane Grady for her helpful suggestions on improving my thesis presentation and Michelle Scherer for her support through the years.

The staff at OGI including Gerhard Boehme, Doug Davis, Margaret Day, Justin Dennis, Jack McCarthy, Donna Reed, Janet Roche, Kristine Roley, and many others have all contributed their extensive talent to this work.

I would like to extend my thanks to Jay Odum, Timothy Jungkamp, and Robert Griffin at Caltech. They helped to make my work there much easier, enjoyable and meaningful. Jay has been a great friend of mine, working with me patiently on the manuscript of our paper and answering a lot of technical questions.

I wish to give special thanks to my grandma, parents, sister, and my dear friend Minru Mo, whose generosity, foresight, caring, and spiritual support helped me to survive this long graduate school journey. They have been proud of my small accomplishments as well as big ones. I thank them warmly for everything they have given me and for having so much confidence in my ability.

Finally I want to thank John for being such a supportive friend to me. He has been a resource of knowledge, comfort, and encouragement. His support has kept me going through a lot of rough times, and he seemed to always believe in my capability even when I did not.

DEDICATION

To my grandma, parents, sister, and John.

TABLE OF CONTENTS

LIST OF TABLES

LIST OF FIGURES

NOTATION

A	gas-phase concentration of a compound (ng/m^3)
$A'(r)$	volumetric concentration of the compound in the micropores of the particle (ng/m^3)
a_{TSP}	specific surface area of suspended particles (m^2/g)
APM	atmospheric particulate material
ATD	adsorption/thermal desorption
b_{p}	intercept in a plot of log K_{p} vs. $1/T$
b_{r}	intercept in a plot of log K_{p} vs. log p_{L}°
$b_{\mathrm{r,om}}$	intercept in a plot of log $K_{\mathrm{p,om}}$ vs. log p_{L}°
$b_{\mathrm{r,s}}$	intercept in a plot of log $K_{\mathrm{p,s}}$ vs. log p_{L}°
C	concentration of water in methylene chloride at a temperature T (mol/m^3)
C_{o}	initial water concentration in a filter extract
C_{extract}	measured concentration of a target compound in the filter extract (ng/µL)
$\mathrm{c_g}$	concentrations in the gas phase
c_{J}	compound and temperature dependent constant
$\mathrm{c_p}$	concentrations in the particulate phase
D_{eff}	effective intraparticle diffusion coefficient (cm^2/s)
D_{m}	molecular diffusion coefficient of the compound in air (cm^2/s)
d_{MeCl}	density of methylene chloride (g/cm^3)
DOP	dioctyl phthalate
EC	elemental carbon (µg/cm^2)
ETS	environmental tobacco smoke

F	particulate-phase concentration of compound (ng/m^3)
f	average flow rate through the filter (m^3/min)
f_{om}	weight fraction of the TSP that comprises the om phase
fb	free base
G	gas
GFF	glass fiber filter
H_{w}	Henry's law constant for water
IC	inorganic carbon
IR	infrared
IS	internal standard
K	experimentally-determined instrument constant by vapor pressure osmometry
K_{p}	gas/particle partitioning coefficient (m^3/μg)
$K_{\mathrm{p}}^{\mathrm{fb}}$	partition coefficient for free-base nicotine
$K_{\mathrm{p,om}}$	om-phase-normalized gas/particle partitioning coefficient (m^3/μg)
$K_{\mathrm{p,s}}$	surface-area-normalized gas/particle partitioning coefficient (m^3/m^2)
$K_{\mathrm{p,w}}$	gas/particle partitioning coefficient for water (m^3/μg)
$K_{\mathrm{p,ww}}$	gas/particle partitioning coefficient for water sorbed to water surfaces (m^3/μg)
M_{DOP}	number-average molecular weight of the DOP phase (g/mol)
M_{e}	total mass of a target compound before desorption experiment (ng)
M_{MeCl}	mass of methylene chloride (g)
M_{om}	number-average molecular weight of the om phase (g/mol)
M_{p}	mass of particles on the filter (μg)
M_{r}	mass of each compound remaining on the filter after a desorption experiment (ng)
M_{ss}	mass of a surrogate standard compound
$MW_{\mathrm{om,dry}}$	number-average molecular weight of the dry organic matter phase (g/mol)
M_{t}	cumulative mass desorbed from a filter (ng)
M_{true}	actual mass of a surrogate standard compound

m	mass of dry ETS particles on a filter sample (mg)
m_p	slope in a plot of log K_p vs. $1/T$
m_r	slope in a plot of log K_p vs. log p_L^o
$m_{r,om}$	slope in a plot of log $K_{p,om}$ vs. log p_L^o
$m_{r,s}$	slope in a plot of log $K_{p,s}$ vs. log p_L^o
MS	mainstream smoke
n	intraparticle porosity of the porous shell (void volume in the shell per total volume of the shell)
N_s	surface concentration of sorption sites (mol/cm^2)
OC	organic carbon (µg/cm^2)
OC_{pri}	primary organic carbon
OC_{sec}	secondary organic carbon
OH	organic hydrogen
OO	organic oxygen
om	organic matter
P	partial vapor pressure (atm)
P	particle
p_L^o	vapor pressure of pure subcooled liquid (torr)
PAHs	polycyclic aromatic hydrocarbons
pK_a	dissociation constant
ppbV	part per billion (10^9) by volume
PUF	Polyurethane foam
QFF	quartz fiber filter
Q_l	enthalpy of desorption from the surface (kJ/mol)
Q_v	enthalpy of vaporization from the pure subcooled liquid phase(kJ/mol)
R	gas constant ($= 8.206 \times 10^{-5}$ m^3 atm mol^{-1} K^{-1})
r	distance from the center of a particle
r^2	square of correlation coefficient
RF	response factor

RF_{avg}	average value of response factors
RH	relative humidity
$S(r)$	total volumetric concentration of a compound at a radial distance r from the center of a particle (ng/m^3)
SOA	secondary organic aerosol
SOCs	semi-volatile organic compounds
SS	sidestream smoke
T	temperature (K)
ΔT	change of temperature (K)
t	time (s)
T_D	the diffusion reaction time (min)
T_M	mass-transfer time scale (min)
T_{min}	minimum time for vaporizing desired amount of water from a filter extract (min)
TC	total carbon (μg/cm^2)
TCD	thermal conductivity detector
tc-GFF	Teflon-coated glass fiber filter
TMF	Teflon membrane filter
TSP	concentration of total suspended particulate material (μg/m^3)
UPM	urban particulate material
V_s	initial volume (mL)
V_{ATD}	ATD sample volume (L)
V_g	total volume of methylene-chloride-saturated nitrogen gas needed to achieve a desired C/C_0 in a filter extract (mL)
V_{filter}	volume of air passing through the filter during the same sampling period (L)
VOP	vapor pressure osmometry
W	mass of water taken up by ETS particles at a given relative humidity (mg)

Greek:

α^{fb}	fraction of particle-phase nicotine that is in the free base form
ζ	mole-fraction-scale activity coefficient of a compound in organic matter phase
ζ_w	mole-fraction-scale activity coefficient of water in ETS organic matter phase
ϕ	the fraction associated with the particulate phase

Abstract

Understanding the Mechanisms of Gas/particle Partitioning of
Semi-volatile Organic Compounds to Model Inorganic Aerosol, Model
Organic Aerosols, and Urban Particulate Material

Cikui Liang

Oregon Graduate Institute of Science & Technology, 1997

Supervising Professor: James F. Pankow

Gas/particle (G/P) partitioning is an important process that affects the deposition, chemical reactions, long-range transport. and human and ecosystem health effects of semi-volatile organic compounds (SOCs) in the environment. The dominant mechanism for G/P partitioning of SOCs in both outdoor and indoor air has been uncertain. Non-specific physical *ad*sorption has been considered to be the dominant mechanism by most of the researchers in this field. While this sorption mechanism is important when atmospheric particulate material is comprised solely of mineral materials, urban particulate material (UPM) generally contains a significant amount of amorphous organic carbon. Thus, it seems likely that *ab*sorptive partitioning must be playing at least some role in urban air, and also in air affected by urban sources.

The purpose of this research was to provide some understanding of the controlling mechanisms of G/P partitioning of SOCs to various aerosols in both indoor and outdoor air. Several organic aerosols were studied, including environmental tobacco smoke (ETS) in an indoor setting, chamber-generated secondary organic aerosols (SOA) formed from whole gasoline vapor, and chamber-generated aerosol composed of liquid dioctyl phthalate (DOP). The G/P partitioning to an inorganic aerosol composed of ammonium sulfate was also investigated in the chamber. Furthermore, the G/P partitioning studies were also carried out for the urban air samples collected during summer smog episodes in the Los Angeles metropolitan area.

Comparison of SOCs partitioning to ammonium sulfate and smog urban particulate matter (UPM) containing significant secondary organic carbon demonstrated that adsorption to inorganic surfaces cannot account for the sorption to the smog UPM that was observed. On the other hand, the partitioning to the UPM was highly similar to that found with the three model organic aerosol studied here. These observations suggest that absorption is the dominant mechanism for sorption of SOCs to aerosol containing a significant amount of organic or amorphous organic carbon. According to the absorption theory, the weight fraction of total suspended particulate material that comprised the organic matter phase and the number-average mean molecular weight of the organic matter phase are the two major factors affecting G/P partitioning to UPM. The results also support the application of SOA yield data generated from smog chamber experiments to predict the extent of SOA formation during summer midday smog episodes.

CHAPTER 1

INTRODUCTION

1.1 Gas/Particle (G/P) Partitioning and G/P Partitioning Coefficient K_p

1.1.1 General

Both the ambient atmosphere and indoor air contain a great variety of organic compounds. These compounds originate from both natural and anthropogenic sources, and differ greatly in their typical concentrations as well as their physical and chemical properties. Knowledge of the transport and the fate of these compounds is essential if one is to understand their effects. The fate of an organic compound depends on where and in what physical state it was emitted, and on how it partitions between various phases in the environment. In this context, gas/particle (G/P) partitioning is an important process which affects the deposition, chemical reactions, transport, and the health effects of organic compounds. With vapor pressures between 10^{-4} and 10^{-11} atm at the ambient temperature, semi-volatile organic compounds (SOCs) are of special interest because their intermediate volatilities allow them to be present in significant concentration in both the gas and particulate phases.

G/P partitioning affects the residence times and fates of SOCs in many ways (Bidleman, 1988; Pankow, 1993). For example, adsorption and absorption can promote catalyzed chemical reactions or sensitize photochemical conversions (McDow *et al.* 1994). Strong adsorption and/or absorption to aerosol particles may even change the wavelength of maximum light absorption for the direct photochemical reaction of a given SOC. Some pollutants found in indoor air can be absorbed onto surface materials, then desorbed from the surfaces either unchanged or altered. In addition, a fundamental understanding of G/P partitioning will benefit local, regional, and global transport modeling efforts.

1.1.2 Definition of G/P Partitioning Coefficient K_p

An equation that has been used successfully to parameterize G/P partitioning is (Yamasaki, *et al.*, 1982; Pankow, 1991)

$$K_p = \frac{F/\mathrm{TSP}}{A} \tag{1-1}$$

where K_p (m^3/μg) is the G/P partitioning coefficient for a given compound of interest, F and A are the P- and G-phase concentrations (ng/m^3) of the compound, respectively, and TSP (μg/m^3) is the total suspended particulate material concentration. K_p may be considered to be the equilibrium constant for the reaction

$$A + \mathrm{TSP} \rightleftharpoons F \tag{1-2}$$

1.1.3 Collection of Particulate- and Gas-Phase SOCs

1.1.3.1 Sampling for Particulate-Phase SOCs

Collecting particles on filter media is by far the most popular method for the sampling of particulate matter (PM) in both outdoor and indoor air. This is probably due to the fact that the equipment required for such sampling tends to be relatively inexpensive and easy to operate. The collection of PM is usually carried out by drawing a certain volume of air through a fiber or membrane filter with a sampling pump. A number of different types of filter media have been used, including glass fiber filters (GFFs), Teflon-coated GFFs (tc-GFFs), quartz fiber filters (QFFs), and Teflon membrane filters (TMFs).

For TSP measurements, most investigators sample for periods up to a few hours in order to collect air particles on a pre-weighed filter. The filter is then weighed again at the end of the sampling period. While the methods and equipment required to make a gravimetric mass measurement may be straightforward, great care must be taken if small quantities of collected particles are to be weighed accurately. Typically, for filter loadings of only a few tens of micrograms, filters must be equilibrated prior to weighing at a constant temperature and humidity for several hours (24-48 h in some procedures) both before and after sampling (Conner *et al.*, 1990).

The value of F measured on a filter for a given compound is usually taken to equal the particulate-phase concentration in the atmosphere at the time of sampling. Unfortunately, a variety of mechanisms can lead to artifacts during sampling. Two of the most important mechanisms are volatilization loss ("blow off") from a particle-laden filter (Hart and Pankow, 1994), and adsorption from the gas phase to a filter ("blow on") (Turpin and Huntzicker, 1994).

Early investigations (Konig *et al.,* 1980; Schwartz *et al.*, 1981; Van Vaeck *et al.*, 1984; Van Vaeck *et al.*, 1985) concluded that loss by volatilization was the primary source of artifacts when sampling with filters, especially for relatively volatile compounds on heavily-loaded filters. Volatilization can be caused by two distinct mechanisms. First, due to the pressure gradient that exists through a filter, particles deep within a filter will be exposed to gas-phase concentrations that are lower than at the front of the filter (Zhang and McMurry, 1991). Compounds will therefore tend to be stripped from the filtered particles. Second, volatilization can occur if contamination levels decrease or if the temperature increases during sampling. These changes will cause the partitioning to be shifted in favor of the gas phase, and organic compounds will desorb from the collected particles. Volatilization losses lead to artificially-low K_p values because the F values are underestimated and the A values are overestimated. It should be kept in mind that gases adsorbed on a filter can also be volatilized during sampling. Keeping the sampling time as short as possible can minimize volatilization losses from filters due to fluctuations in temperature and concentration during sampling (Hart and Pankow, 1994; Pankow *et al.*, 1994). Van Vaeck *et al.* (1984) have suggested placing a fresh clean filter surface into an air sample stream at frequent intervals for the purpose of minimizing volatilization losses. However, doing so will maximize the sorptive importance of the filter itself relative to the collected TSP (Hart and Pankow, 1994).

As noted above, adsorption on a filter during a sampling period ("blow-on") has also been identified as a possible sampling artifact (Bidleman *et al.* 1986; Coutant *et al*, 1988; McDow and Huntzicker, 1990; Zhang and McMurry, 1991; Kaupp and Umlauf, 1992;

Turpin and Huntzicker, 1994). The adsorption of gaseous polycyclic aromatic hydrocarbons (PAHs) to a QFF was found to cause an overestimation of measured K_p values by a factor of 1.2-1.6 (Hart and Pankow, 1994). The magnitude of adsorption artifacts depends on the compound of interest, the face velocity, the sampling period, and the filter type (McDow, 1986). The magnitude of this artifact tends to increase with decreasing face velocity and sampling time. The surface areas for QFFs, GFFs, and TMFs have been reported to be 126, 125, and 26 m^2/m^2, respectively (Turpin, 1989). Since a TMF has ~ 1/5 of the surface area of a QFF or a GFF of the same projected area, the severity of the filter sorption artifact may be less with a TMF than with a QFF or a GFF (McDow and Huntzicker, 1990). A number of studies (Ligocki and Pankow, 1989; McDow and Huntzicker, 1990; Hart and Pankow, 1994) have suggested that backup filters be used to correct for adsorption artifacts during G/P partitioning measurements. Since elemental carbon is present only in the particulate phase and since no elemental carbon is detected on a backup filter from carbon analyses (McDow and Huntzicker, 1990), it therefore rules out significant transmission of particles through the front filters, and the presence of organic compounds on a backup filter is considered to be adsorption from the gas phase. Hart and Pankow (1994) have suggested that one can correct for gas adsorption on a QFF by using two QFFs in series or by using a second sampler with a TMF followed by a QFF. On the other hand, the typically higher blank levels of SOCs on a TMF (Ligocki and Pankow, 1989) and the lower maximum cleaning temperature for TMF (300 °C *vs.* 500 °C for QFF) (McDow, 1986) indicate that the scheme of two QFFs in series is preferable.

1.1.3.2. Sampling for Gas-Phase SOCs

The most common method for sampling gas-phase SOCs in both outdoor and indoor air is to use some type of sorbent trap to collect the analytes of interest. The ideal sorbent will permit low blank levels, quantitative collection of the analytes of interest, and easy recovery of the trapped analytes. The type of sorbent used depends on the chemical and physical properties of the target compounds as well as the concentration range of the compounds of interest.

A variety of sorbents have been used to sample the more volatile constituents in ambient air. Activated carbon was one of the first sorbents used. However, it did not permit quantitative recovery for many compounds (West *et al.*, 1958). Chromatographic packing materials (*e.g.* Porapak Q and S, the Chromsorb series, and Tenax) were next studied for the collection of a variety of compounds (Williams and Umstead, 1968; Dravnieks *et al.*, 1971). Tenax-GC, a 2,6-diphenylene oxide porous polymer, was found to be very useful in trace gas analysis as it exhibited low blank levels and high thermal stability (Zlatkis et al., 1973; Bertisch et al., 1974; Pellizari et al., 1975 a,b). Several years later, Tenax-TA became available. This sorbent offers even lower blank levels than Tenax-GC, as well as a higher specific surface area for adsorption.

The measurement of compounds which are present at relatively low concentrations requires large sample volumes, which in turn can require a large sorbent bed volume. While large Tenax-GC and -TA traps can be used, the cost is usually considered prohibitive. In addition, the pressure drop through beds of these sorbents is not compatible with sampling at the flow rates needed to obtain a large sample volume in a relatively short sampling period (hours). When large sample volumes are used, significant breakthrough of the more volatile constituents will occur. Retention volume data on Tenax-GC for a wide variety of compounds have been compiled by Gallant *et al.* (1978) and Pankow (1988).

Polyurethane foam (PUF) is an alternative to Tenax-GC and Tenax-TA that has been used successfully to sample a large variety of compounds in the atmosphere (Bidleman and Olney, 1974; Turner and Glotfelty, 1977; Ligocki and Pankow, 1985). PUF is inexpensive, easy to handle, easy to recover the trapped analytes from, and able to sustain high flow rates. These features make PUF very attractive for compounds where large volumes must be sampled. Unfortunately, the more volatile SOCs exhibit low breakthrough volumes on PUF. Analytes trapped by PUF sheets or plugs can be recovered by solvent extraction. Subsequent concentration of an extract prior to GC/MS analysis can lead to additional losses of the more volatile analytes.

The Amberlite XAD resins (XAD-2 and XAD-4) comprise another class of widely-used porous resins that have been employed for the collection of both volatile and semi-volatile constituents in air (Adams *et al.*, 1977; Ogden *et al.*, 1989a; Chuang *et al.*, 1991). XAD-4 has a larger surface area per unit mass than XAD-2. XAD resins have the advantage of a somewhat greater capacity for the more volatile constituents than does Tenax , but exhibit somewhat higher background levels when used in dry atmospheres (Guerin *et al.*, 1992). In addition, they have a lower temperature stability, which precludes desorption by thermal means. Instead, the resin bed is eluted with a solvent, and the eluate is then usually concentrated prior to analysis. As noted above, there is a potential for losses of the more volatile analytes during this process.

An interesting yet incompletely evaluated family of trapping media is the high-purity carbon molecular sieves. These materials, which are made from synthetic polymer starting materials, possess very uniform carbon surfaces with excellent adsorptive/desorptive and hydrophobic characteristics (Betz and Firth, 1988; Supelco, 1990). Because of their inherent thermal stabilities, unlike PUF and XAD resins, they are excellent candidates for thermal desorption analysis, and may even be superior to Tenax (Sheldon *et al.*, 1985).

In order to quantitatively determine compounds in the gas phase with a wide range of volatilities, this study employed an integrated approach using both Tenax-TA for more volatile compounds and PUF for the less volatile compounds. An advantage of this system is that there is sufficient overlap of compounds of intermediate volatility that each method can be used as an independent check on the other to determine the overall recovery efficiencies of the sorbents. While Bidleman and Olney (1974) were the first group to employ this sampling approach, others have adopted this method (Cautreels and Van Cauwenberghe, 1978; Thrane and Mikalsen, 1981; Yamasaki *et al.*, 1982; Keller and Bidleman, 1984; Pankow *et al.*, 1994).

1.1.3.3 Simultaneous Gas- and Particulate Phase Sampling

A traditional way to simultaneously sample gas- and particulate-phase compounds is to place one or more filters in front of one or more beds of one of the sorbent materials described above. The filter(s) and the sorbent bed(s) are analyzed separately. As implied above, these filter/sorbent systems are prone to artifacts. The adsorption of gaseous substance on deposited particles or on the filter material itself, as well as substance losses from the gas trap, will lead to an overestimation of the particle-bound fraction (Bidleman *et al.*, 1986; Coutant *et al.*, 1988). As an alternative, a denuder technique can be used so that the gas-phase compounds are collected before the particulate-phase compounds are collected (Possanzini *et al.*, 1983; Johnson *et al.*, 1986; Coutant *et al.*, 1989; Cake *et al.*, 1990; Ye *et al.*, 1991; Krieger and Hites, 1994). A denuder consists of an adsorbent-coated multi-tube or annular adsorption unit which removes the gaseous substances from the flowing airstream. Because the diffusion coefficients of particles and gas-phase molecules differ by a factor of 10^3 - 10^6, particles tend to pass through the denuder while the gas-phase compounds diffuse to the denuder walls, where they are accumulated. The majority of the particles remain in the airstream and are collected on a filter downstream from the denuder. Recovery of the analytes from a denuder typically occurs by solvent extraction. Because the gas-phase compounds are collected before the particles are removed from the sample stream, denuders are not susceptible to the same sampling artifacts present with the filter/sorbent samplers. However, denuders have their own problems, such as volatilization of SOCs from the particles and trapping of small particles by the denuder. Additionally, the small flow rates at which denuders are operated (≈ 1 m^3/h) require long sampling times (Kaupp and Umlauf, 1992).

1.2. Nature, Source, and Toxicity of Pollutants in Indoor Air

1.2.1 General

Indoor air contains a great variety of physical, biological, and chemical contaminants from multiple sources. They differ greatly in quality, and usually vary both temporally and spatially in concentration. The contaminants of current concern can be divided into two general categories (Guerin *et al.*, 1992) : 1) those most commonly associated with occupant discomfort or acute illness; and 2) those thought to be carcinogenic or to contribute to other chronic illnesses. Microorganisms, carbon dioxide (CO_2), formaldehyde, petroleum-derived solvents, halogenated solvents, and a variety of other volatile organic compounds are most frequently the cause of discomfort and acute illness (the "Sick Building Syndrome").

Microorganisms, volatile organic compounds, airborne fibers, and respirable suspended particulate matter are likely the contributors to allergic reactions and other forms of chronic poor health. Tobacco smoking contributes to the indoor air burden of some of the suspect chemicals. Materials viewed as posing a cancer threat in indoor air are asbestos, radon-222, environmental tobacco smoke (ETS), a large variety of organic chemicals, and several heavy metals (Gold *et al.*, 1990). Chemicals of particular concern include formaldehyde, benzene, methylene chloride, selected PAHs, selected pesticides, N-nitrosamines, cadmium, and nickel.

An important characteristic of indoor air contaminants is that their concentrations vary both spatially and temporally to a greater extent than the contaminants found in outdoor air (Guerin *et al.*, 1992). This is due to the large variety of sources present, the intermittent nature of some of those sources, and different types and quantities of "sinks" (materials which absorb the constituents). Changes in concentration are caused by changes in temperature, emission rates, ventilation conditions, and the air exchange rate.

The common principal sources of indoor air contaminants are outdoor air, the building itself, and occupant activities (Maroni *et al.*, 1995; Robertson, 1990). Incursion of outdoor air includes the air that enters the indoor environment through the ventilation system, windows, doors, and many imperfectly-sealed points typical of common construction. Residential attached garages and commercial underground parking garages are important sources. Contributions from the building itself can be traced to the construction materials, furnishings and decorations, heating and cooling systems, water heaters, refrigerator/freezers, and humidification devices. While occupants themselves contribute to indoor air constituents (*e.g.* CO_2, other exhaled breath constituents, and dander), it is their activities which are the principal problem. The most obvious example is tobacco smoking, which can lead to visibly obvious ETS. Another example is painting or wood staining where emissions can be obviously detected by their odors. Maintenance and repair activities (e.g. polishing, cleaning, vacuuming), daily activities (e.g. cooking), and the use of personal care products (e.g. deodorants, hair spray) all lead to various constituents in different quantities in indoor air.

1.2.2 ETS and Its Contribution to Indoor Air Contaminant Levels

1.2.2.1 ETS Definition

ETS is a term used to describe the contaminants released into indoor air when tobacco products burn and smokers exhale. Pipe-, cigar-, and cigarette-smoking all contribute to ETS, but cigarette smoking is of principal interest because it is by far the most common form of tobacco smoking. ETS is composed of exhaled mainstream smoke (MS) from the smoker, sidestream smoke (SS) emitted from the smoldering tobacco between puffs, contaminants emitted into the air during the puff, and contaminants that diffuse out of the cigarette the through cigarette paper and mouth end between puffs (NRC, 1986; U.S. Department of Health and Human Services, DHHS, 1986; Guerin *et al.*, 1992).

1.2.2.2. Differences Between MS and SS

Differences in SS and MS are due to differences in the temperature of combustion of the tobacco, pH, and the degree of dilution with air, which is accompanied by a corresponding rapid decrease in temperature. Compared to MS, SS is generated at a lower temperature (approximately 600 °C between puffs vs. 800-900 °C for MS during puffs) (Johnson, 1970; Baker, 1980) and has a higher pH (6.7-7.5 vs. 6.0-6.7) (Brunnemann and Hoffmann, 1974) than MS. Being slightly more alkaline, SS contains more ammonia and organic bases, and is depleted of acids (Johnson *et al.*, 1973; Brunnemann and Hoffmann, 1975; Sakuma *et al.*, 1983; Sakuma *et al.*, 1984). Differences in MS and SS can also be ascribed to differences in the oxygen concentration (16% in MS vs. 2% in SS). Therefore, SS contaminants are generated in a more reducing environment than those generated in MS. Nitrosamines, for example, are present in greater concentrations in SS than in MS (NRC, 1986; DHHS, 1986; Guerin *et al.*, 1992).

SS is rapidly diluted in air, which results in a lower TSP as well as a SS particle size distribution that is smaller than that for MS (Benner *et al.*, 1989; Eatough *et al.*, 1989). As a result, nicotine, for example, while predominantly in the particle phase in MS, is found predominately in the gas phase in SS (Eudy *et al.*, 1985). Also, nicotine can exist in both unprotonated (free) and protonated forms. Free nicotine is volatile and protonated nicotine is not. The greater alkalinity of SS would be expected to increase the proportion of nicotine existing in the more volatile, free form (Johnson *et al.*, 1973; Browne *et al.*, 1980). In addition, free nicotine in the gas phase is also more readily absorbed through the oral mucosa of ETS-exposed individuals than is protonated nicotine (Armitage and Turner, 1970, Schievelbein and Eberhardt, 1972). SS particle sizes are typically in the range of 0.01-0.1 µm, while MS particle sizes are in the range of 0.1-1.0 µm. The SS size distribution shifts to smaller sizes when the particles lose mass by evaporation and become smaller as the smoke is diluted (Ingebrethsen and Sears, 1985; Guerin *et al.*, 1992). The differences in size distribution for MS and SS particles, as well as the different breathing patterns of smokers and nonsmokers, will affect the deposition of the particle-bound contaminants in the respiratory tract for the two groups. It has been estimated that 47 to 90% of the total inhaled MS particles can be deposited in the respiratory tract, while only 10% of the total inhaled SS particles are deposited (DHHS, 1986).

ETS is not the same as fresh SS. The differences will depend on the degree of dilution with room air and the availability of surfaces for particle deposition. In general, the phase distribution of the various components of ETS is shifted in favor of gas phase by dilution, with a greater proportion of higher molecular weight species in the gas phase in ETS than for the fresh SS. Ramsey *et al.* (1990) demonstrated that a significant fraction of the straight chain saturated hydrocarbons above C_{25} are predominantly in the gas phase in ETS. Also, studies employing ^{123}I-label iodohexadecane (boiling point 380 °C) as a tracer added to cigarettes indicated that while 95% of the tracer was present in the particle phase of SS when it was freshly generated, about 70% of the tracer was found in the gas phase when the SS was diluted to particulate levels typically for ETS (Black *et al.*, 1987; Pritchard *et al.*, 1988; Proctor *et al.*, 1988). The ratio of particulate matter to CO_2 drops by 50% when SS is diluted to ETS (R. J. Reynolds, 1988). One of the most significant factors in the aging of ETS is the loss nicotine to surfaces. The longer that ETS remains within a given volume (lower ventilation rate), the more likely that nicotine will be depleted through surface adsorption (Thompson *et al.*, 1989). Chemical reactions with surfaces or airborne components may be responsible for reductions with time of other ETS components. For example, the ratio of formaldehyde and acrolein increases from 0.58 to 2.03 when sidestream smoke is diluted to the typical ETS particulate level in a large chamber (R. J. Reynolds, 1988). The most plausible explanation for this is the reactivity of acrolein with airborne components, such as ozone, OH radical. Studies using sulfur hexafluoride as a tracer for leaks in a controlled environmental chamber have demonstrated that nicotine, vinylpyridine, nitric oxide, hydrocarbons, and carbon monoxide all had shorter half-lives than what could be accounted for by leaks from the chamber (Eatough *et al.*, 1989). Of course, the loss of nitric oxide (NO) is to be expected, due to its conversion to nitrogen dioxide (NO_2) through reaction with atmospheric oxygen. The reaction is well known for atmospheric chemistry (Seinfeld, 1986), and has also been confirmed for MS (Jenkins and Gill, 1980) and postulated for ETS (Baker and Proctor, 1990). Ingebrethsen and Sears (1989) have found that there is a small increase in the average particle size as ETS ages. This is most likely due to the losses of the smaller particles through impaction on surfaces (the smaller particles can diffuse somewhat more rapidly than the larger ones) and the coagulation of smaller droplets into larger ones.

A few studies have reported changes in the chemical composition of ETS as it ages in an indoor environment. In the absence of external oxidizing agents or UV light, NO in ETS is only slowly converted to NO_2, HNO_2, and possible organic nitrogen-oxide compounds (Benner *et al.*, 1989). In the presence of a strong UV light source, this conversion is rapid (Benner *et al.*, 1989). In addition, under these extreme conditions, the photochemistry leads to doubling of total particulate matter, lower concentrations of basic compounds in the gas phase, loss of solanesol, and photochemical alternations of the nitrogen-containing bases of ETS (Benner *et al.*, 1989; Tang *et al.*, 1990). Since almost all public buildings have fluorescent lamps with a measurable UV component, UV-induced aging of ETS could be common.

1.2.2.3 ETS Composition

ETS is composed of aged exhaled MS and diluted SS. Thus, ETS most likely contains all of the constituents present in MS and SS, plus any constituents which may form during the aging process by oxidation or photochemical transformation (Guerin *et al.*, 1992). Extensive analyses (*e.g.* Johnstone and Plimmer, 1959; Stedman, 1968; Schmeltz and Hoffmann, 1977; Hammond *et al.*, 1987; Benner *et al.*, 1989; Eatough *et al.*, 1989; Löfroth *et al.,* 1989) have shown ETS to be a major source of human exposure to tobacco-specific N-nitrosamines, PAHs, aromatic amines, and some other carcinogens. ETS is a mixture of thousands of compounds in both the gas- and particulate-phases. Over 4000 compounds have been identified in laboratory-based studies (Dube and Green, 1982; Robert, 1988) including 1) alkanes; 2) alkenes and alkynes; 3) aromatic hydrocarbons; 4) sterols and oxygenated isoprenoid compounds; 5) alcohol and esters; 6) aldehydes, ketones, and quinones; 7) acids; 8) phenols and phenolic ethers; 9) alkaloids and other bases; 10) brown pigments; 11) carbohydrates; 12) amino acids, proteins, and related compounds; 13) inorganic constituents; 14) agricultural chemicals; and 15) other constituents. Some detailed information on the composition of ETS is given in Table 1.1.

1.2.2.4 Health Effects of ETS

Tobacco smoke affects not only people who smoke, but also people who are exposed to the combustion products of other people's smoking. Since the constituents of MS and SS are different, the effects produced are not necessarily the same. On the other hand, MS and SS both contain chemicals that are carcinogenic and mutagenic (Sakuma *et al.*, 1983; Sakuma *et al.*, 1984; Löfroth and Lazaridis, 1986; Grimmer *et al.*, 1987; Evan *et al.*, 1993), including known human carcinogens (benzene, 2-naphthylamine, 4-aminobiphenyl, nickel, and ^{210}polonium), probable human carcinogens (formaldehyde, hydrazine, N-nitrosodimethylamine, N-nitrosodiethylamine, N-nitrosopyrrolidine, 1,3-butadiene, aniline, benzo(a)pyrene, nitrosodiethanolamine, and cadmium), and animal carcinogens (benzo(a)anthracene, γ-butyrolactone, and N-nitrosonornicotine) (Vainio *et al.*, 1985). Knowledge of the nature of MS and SS, of the materials absorbed during "passive" smoking, and of the quantitative relationships between dose and effect that are commonly observed from exposure to carcinogens leads to the conclusion that passive smoking gives rise to risk of cancer (World Health Organization (WHO), 1987).

Table 1.1 Composition of ETS[a]

Name	Characteristics
Alkanes	(1) branched-chain compounds comprise about 24%-45% of the total alkanes; (2) odd-numbered homologs predominate, with the C_{31} compounds presenting in the largest overall amounts; and (3) the levels of C_{12} to C_{33} paraffins are about 0.5-1.4 mg/cigarette in tobacco smoke totally
Alkenes and alkynes	neophytadiene is the most abundant compound in this group
Aromatic Hydrocarbons	(1) the levels of benzene, naphthalene, and alkyl derivatives vary from 0.17 to 46 μg/cigarette in the tobacco smoke; (2) many of these compounds are carcinogenic; benzo(a)pyrene is the major PAH of biological significance, and occurs at a level of about 1-2 ppm by weight in the particulate phase; other biologically active PAHs are generally present in lower concentrations with the possible exception of chrysene; (3) PAHs form complexes with nitro-aromatic compounds and purines; and (4) PAHs and their heterocyclic analogs are tumor initiators
Sterols and oxygenated isoprenoid compounds	(1) may play some role in the biological effects of smoke either through *in situ* autoxidation to hydroperoxides and related compounds during leaf curing and aging, or through pyrolysis to PAHs during burning of a cigarette; (2) a hydroperoxide of cholesterol has been shown to be carcinogenic; stigmasterol has been pyrolyzed to benzo(a)pyrene at 750°C; and (3) solanesol may be a source, or at least in part, of dipentene in cigarette smoke, and thereby influences the smoke aroma indirectly; and it has been suggested as a tracer for ETS

Table 1.1 Cont'd

Alcohols and Esters	(1) fatty alcohols have been found in small tobacco particles with 1-heptadecanol being the major representative of this class; (2) glycols, glycerol, and menthol arise mostly from the humectants and flavoring additives used in domestic cigarettes, although significant amounts of naturally-occurring glycerol are found in tobacco; (3) more than 300 esters have been identified in tobacco smoke, and bulk of these compounds consist of sterols, terpenes, and fatty alcohols esterified with higher fatty acids; and (4) the primary source of the benzoate and cinnamate ester in tobacco smoke may be derived from the flavoring agents used in tobacco
Aldehydes and Ketones	(1) aldehydes and ketones may contribute to the organoleptic properties of tobacco smoke; and (2) the total carbonyl levels in tobacco have been shown to be related indirectly to the moisture content, specially for the low-boiling-point aldehydes and ketones in tobacco smoke: a fivefold increase of acetaldehyde in smoke may occur on reducing the moisture content by one-half
Nitriles, Cyclic ethers, and Sulfur Compounds	(1) aliphatic nitriles and cyclic ethers have been found in both the gas- and particulate-phases; and (2) the sulfur compounds in tobacco smoke may influence the flavor and aroma even though they are present at very low concentrations
Acids	(1) significant amounts of C_1-C_{10} fatty acids including branched-chain isomers are found in tobacco smoke; (2) the volatile fatty acids are believed to contribute to the over-all leaf aroma and smoke flavor; (3) formic and acetic acids comprise about 75% of the volatile acids in the cigarette or cigar smoke; (4) the C_{16}-C_{18} saturated and unsaturated compounds are the major higher fatty acids in tobacco smoke; (5) approximately 90% of the total acids have 10-34 carbon atoms, 4.1% are methyl-(C_{15}-C_{26}) or cyclohexyl-(C_{22}-C_{25}) substituted compounds, and 5.9% are more complex in structure; (6) the polar acids are mainly hydroxylated derivatives of palmitic and stearic acids; and (7) the nonvolatile acids vary widely with tobacco types, cultivation, and curing practices

Table 1.1 Cont'd

Phenols and phenolic ethers	(1) the major polyphenols in tobacco leaf are chlorogenic acid and rutin; (2) the *in vitro* or *in vivo* oxidation of polyphenols produces a variety of products which may condense with alkaloids or amino acids in "browning" or analogous reactions; (3) bulk of the phenols in smoke are formed by pyrolysis of the cellular constituents; and (4) phenol, eugenol, and related compounds in cigarette smoke may act as ciliostats and cocarcinogens
Alkaloids and Other bases	(1) nicotine is the major alkaloid and makes up to 69% of the N-heterocyclic compounds; (2) the autooxidation of nicotine occurs through a free-radical mechanism, and produces myosmine, nicotyrine, cotinine, nicotine N-oxides, nicotinic acid, and possibly some high molecular weight components; (3) the levels of alkaloids in tobacco smoke are about 40 to 100-fold greater than those in the leaves, indicating that pyrosynthesis of the bases occurs during burning; (4) benzacridine and 7H-dibenzo[c,g]carbazole in cigarette smoke are carcinogenic and may contribute to the weak tumorigenic activity of the basic fraction; (5) aromatic secondary amines are found in the smoke condensates and occur in low levels (0.013-0.1 μg/cigarette); (6) relatively low-boiling-point bases in cigarette smoke consist of the aliphatic amines, saturated heterocyclic bases, and simple pyridine derivatives; and (7) nitrosamines are known to be carcinogenic
Brown Pigment	all pigments contain chlorogenic acids, amino acids, and some fraction of iron and rutin
Carbohydrates	these components enter into tobacco smoke by thermal cellular eruptions during combustion
Inorganic elements	(1) over 40 elements are found in the tobacco smoke; and (2) nickel and ^{210}polonium are known to be human carcinogens
Other constituents	(1) CO_2 makes up 80% of the gas- phase of tobacco smoke; and (2) 60% of the CO_2 and 47% of CO are derived from oxidation of CO and carbon, respectively

[a] summarized from Stedman, 1968.

The most common acute effects associated with exposure to ETS are irritation of the eye, nose, and throat. Smoke also contains immunogens, which can activate the immune system (NRC, 1986). ETS exposure has been claimed to be associated with health effects as diverse as childhood respiratory diseases, lung cancer, and cardiovascular diseases (Repace and Lowrey, 1985; DDHS, 1986; NRC, 1986; Wells, 1988; Glantz and Parmley, 1991). Cigarette smoking is the predominant source of airborne genotoxicity in indoor environments (Löfroth *et al*., 1983; Houdt *et al*., 1984). A review of indoor byproducts of cigarette smoking (Sterling *et al.*, 1982) reported that the difference in carbon monoxide (CO) values between smoking and non-smoking sections of cafeterias ranged from 0.8 mg/m^3 to about 5 mg/m^3. Cigarette smoke is also recognized as a significant source of volatile organic compounds (Berglund *et al.*, 1986) and particulate materials (Goyer, 1990) in indoor air. Particles in tobacco smoke are especially hazardous due to their chemical composition and because they are inhalable (0.1-1.0 μm) and remain airborne for hours after smoking stops. In one instance, cigarette smoke was found to be responsible for 87% of the total mass of indoor PAHs (Mitra and Ray, 1995).

Many of the genotoxic and carcinogenic organic compounds in ETS can be found in both the gas- and particulate-phases. In this context, G/P partitioning is a very significant process affecting the forms in which organic compounds are dosed to the lungs. Therefore, G/P partitioning plays an important role in determining the health effects of inhaling organic compounds. Unfortunately, there has been very little study of the mechanisms controlling the G/P partitioning of organic compounds to ETS.

1.3 SOCs in Outdoor and Indoor Environments

1.3.1 Sources of SOCs

SOCs are introduced into the atmosphere by many anthropogenic activities, including motor vehicle usage, agricultural applications, chemical manufacturing, transportation, and storage. Although volcanic emissions, forest fires, and other natural processes can contribute SOCs to the atmospheric environment, anthropogenic activities have been considered to be the main source of SOCs to the environment. Many SOCs have been detected in urban air (Yamasaki *et al.*, 1982; Foreman and Bidleman, 1990; Nakano *et al.*, 1990; Halshall *et al.*, 1993), remote air (Cautreels and Cauwenberghe, 1980; Bidleman *et al.*, 1995), natural waters (Fletcher and McKay, 1995; Loganathan, 1995), soil (Wu and Gschwend., 1986; Jones *et al.*, 1989), sediments (Brumley *et al.*, 1991; Means *et al.*, 1980), plants (Bjorseth, 1983; Rogge *et al.*, 1993), and human milk (Glausch *et al.*, 1995).

SOCs are also ubiquitous in indoor air. Although there are some prominent indoor sources of SOCs, such as tobacco smoking, daily activities (*e.g.* cooking and cleaning), and emissions from building materials, there can be significant contribution from outdoor air. Indoor air quality will therefore respond to changes in outdoor air quality with a response rate that depends on the permeability of the structure and the nature of the pollutants (Yocom, 1982). Many studies have been carried out to investigate the relationship between indoor and outdoor levels of SOCs. For example, Ando *et al.* (1991) found that the concentration of suspended particulate matter and some PAHs in indoor air increased in proportion to the concentrations of these compounds in outdoor air. Kado *et al.* (1994) suggested that outdoor sources contribute significantly to indoor particle concentrations, and that the chemical compositions of indoor and outdoor particles were similar.

1.3.2 Studies of SOCs in Outdoor and Indoor Air

Poor outdoor air quality in large urban areas due to vehicular emissions, street dust, and assorted industrial sources has been a concern for several decades, and many countries have implemented regulations to control ambient air pollution. The US Clean Air Act (1971) is probably the most widely cited. It led to the enactment and enforcement of National Ambient Air Quality Standards set by the US Environmental Protection Agency (1972). The standards are designed to protect the public from many outdoor air pollutants. Much work has been carried out to determine the composition of both non-polluted and highly-polluted outdoor air. The sources, transport characteristics, lifetimes, fates, and sinks of commonly-occurring outdoor air pollutants have been studied extensively. While these are important to human health, in the developed world indoor air quality may be of as much or greater concern because a majority of the people in such countries spend most of their time (70-90%) inside buildings (Lebowitz *et al.*, 1985; Wiley *et al.*, 1991). Therefore, an appraisal of both outdoor and indoor air quality is very important in understanding the effects of air pollution on human health.

In the past, both active and passive sampling have been employed to collect SOCs in outdoor and indoor air. The sampling materials and techniques have been similar for both circumstances. Active sampling involves drawing air through a collection medium by means of a pump. Passive sampling involves placing a material which sorbs, or chemically fixes the chemical of interest from the environment being sampled (Guerin *et al.*, 1992). Active sampling is used to sample small volumes of air over relatively short durations or to sample large volumes of air. Passive sampling is primarily used to sample small volumes of air over long periods of time. In contrast to active sampling, passive samplers collect analytes by diffusion.

Passive systems offer the advantages of being relatively simple and inexpensive, and requiring no elaborate pumping apparatus to obtain quantitative results. They are also quiet and can be employed unattended for days, which is very attractive in an indoor air monitoring program. But their effective sampling rates are typically low (tens of mL per minute). The operational theory of passive samplers has been reviewed in detail elsewhere (Fowler, 1982).

Several investigators have evaluated different passive sampler designs and their uses in indoor air sampling (Coutant *et al.*, 1986; Hammond and Leaderer, 1987; Ogden *et al.*, 1989b; Cohen *et al.*, 1990). For active sampling, both low-volume and high-volume samplers have been used to sample outdoor and indoor air (Lewis and Jackson, 1982; Wallace *et al.*, 1985; Griest *et al.*, 1988; Hart *et al.*, 1992; Pankow *et al.*, 1994). Some of the air sampling devices that collect adequate quantities of material for chemical and microbioassay analyses are not suitable for indoor air sampling because of their large size, high noise levels, and lack of portability (Mumford *et al.*, 1987; Wilson *et al.*, 1989). Indoor air samplers should be quiet, transportable, relatively unobtrusive, and capable of operating at a flow rate high enough to collect sufficient quantities of both the particulate- and gas-phase compounds of interest for chemical analyses. Caution should be exercised when using high-volume sampling in small enclosed areas (Griest *et al.*, 1988). It is possible to oversample the environment - essentially scrub the air in the room of its particulate matter - and yield lower apparent overall concentrations. As opposed to outdoor studies, data on indoor air are relatively scarce. If one can find some similarities in the physicochemical characteristics of SOCs in both outdoor and indoor air, it might be possible to extrapolate what has been learned from outdoor studies to indoor air.

1.4 Objectives

The dominant mechanism for G/P partitioning of SOCs in both outdoor and indoor air has been uncertain. Non-specific physical *ad*sorption has been considered to be the dominant mechanism by most of the researchers in this field. However, Pankow (1994) has proposed that absorption into organic matter could also be an important mechanism in many cases. The purpose of this research has been to provide some understanding of the mechanisms of G/P partitioning of SOCs in indoor and outdoor air. This was accomplished by studying the G/P partitioning of : 1) PAHs, n-alkanes, and nitrogen-containing compounds to ETS particles in an indoor environment; 2) PAHs and *n*-alkanes to urban particulate materials (UPM); and 3) PAHs and *n*-alkanes to three different types of model aerosol materials (ammonium sulfate particles, liquid dioctyl-phthalate (DOP) droplets, and amorphous SOA generated from the photooxidation of whole gasoline vapor). A comparison of G/P partitioning of the same compound classes in both indoor and outdoor air can help provide an understanding of whether the results obtained outdoors can be extrapolated to indoor air.

1.5 Model Semi-Volatile Organic Compounds

A group of *n*-alkanes and PAHs was chosen as model compounds (Table 1.2). Both compounds classes have natural and anthropogenic sources, and are found in both outdoor and indoor air (Foreman and Bidleman, 1990; Chuang *et al.*, 1991; Menzie *et al.*, 1992; Rogge *et al.*, 1993; Pankow *et al.*, 1994). *n*-Alkanes were chosen because they are relatively

Table 1.2 List of Model Compounds

Compounds	Abbreviation	Formula	MW (g/mol)	log p_L^o (torr)[a]
***n*-Alkanes**				
Hexadecane	C_{16}	$C_{16}H_{34}$	206	-3.17
Heptadecane	C_{17}	$C_{17}H_{36}$	240	-3.70
Octadecane	C_{18}	$C_{18}H_{38}$	254	-4.23
Nonadecane	C_{19}	$C_{19}H_{40}$	268	-4.76
Eicosane	C_{20}	$C_{20}H_{42}$	282	-5.28
Heneicosane	C_{21}	$C_{21}H_{44}$	296	-5.81
Docosane	C_{22}	$C_{22}H_{46}$	310	-6.34
Tricosane	C_{23}	$C_{23}H_{48}$	324	-6.87
Tetracosane	C_{24}	$C_{24}H_{50}$	338	-7.40
PAHs				
Naphthalene	NAP	$C_{10}H_8$	128	-0.56
Acenaphthene	ACE	$C_{12}H_{10}$	154	-1.98
Fluorene	FLU	$C_{13}H_{10}$	166	-2.42
Phenathrene	PHE	$C_{14}H_{10}$	178	-3.23
Anthracene	ANT	$C_{14}H_{10}$	178	-3.26
Fluoranthene	FLA	$C_{16}H_{10}$	202	-4.42
Pyrene	PRY	$C_{16}H_{10}$	202	-4.61
Chrysene	CHR	$C_{18}H_{12}$	228	-5.90
N-containing compounds				
Quinoline	Q	C_9H_7N	129	-1.25
Isoquinoline	IQ	C_9H_7N	129	-1.38
Nicotine	NIC	$C_{10}H_{14}N_2$	162	-1.48
Carbazole	CZ	$C_{12}H_9N$	167	-4.82

[a] 20 °C data

inert under typical sampling, extraction, concentration, and analysis conditions. They are also typically found at concentrations that are relatively easy to determine analytically. By monitoring PAHs along with *n*-alkanes, comparisons can be made between the partitioning behaviors of these two compound classes. Several nitrogen-containing compounds were included in the ETS studies because: 1) there are very few studies on G/P partitioning have been carried out for this compound class; 2) some of the N-containing compounds (*e.g.* nicotine) are specific indicator for tobacco smoke pollution; 3) the behavior of nicotine in tobacco smoke is of considerable contemporary interest.

The subcooled liquid vapor pressure (p_L^o) values for the model SOCs at 20 °C are given in Table 1.2. For the PAHs, the log p_L^o values were calculated from a regression equation between log p_L^o (Hinckley *et al.*, 1990) and Kovats retention index (Vassilaros *et al.*, 1982). For the *n*-alkanes, the log p_L^o values were obtained from a regression equation between log p_L^o extrapolated from the Riedel equation (McGarry, 1983) using data from Zwolinski and Wilhoit (1971) and carbon number (Luo *et al.*, 1996). Log p_L^o values for the N-containing compounds were extrapolated from the reported data in the literature (Timmermans, 1950; Prausnitz, 1980; Boulik *et al.*, 1984; Rostyne, and Das *et al.*, 1993).

1.6 Overview

In Chapter Two, the theories of adsorption and absorption are reviewed, and the differences between these two approaches are discussed in detail. A few existing kinetics sorption models are also reviewed.

In Chapter Three, the G/P partitioning of a range of *n*-alkanes, PAHs, and N-containing compounds to ETS are described. The ETS particles were collected on a QFF in an indoor setting. Desorption experiments were carried out under controlled temperature and relative humidity conditions. The K_p values for the model SOCs were derived by using a radial intraparticle diffusion model developed by Rounds *et al.* (1993).

Chapter Four discusses the G/P partitioning for a range of *n*-alkanes and PAHs to various model inorganic and organic aerosols that were generated in an outdoor smog chamber on the Caltech campus. The G/P partitioning was also measured for UPM collected during two heavy smog episodes in the Los Angeles metropolitan area at a sampling site in the City of Pasadena. The UPM data were then compared to the data for model aerosols to obtain information about both the operative G/P partitioning mechanisms during summer smog episodes and the physical and chemical nature of UPM.

Chapter Five describes a method for the removal of water from the ETS filter extracts prior to attempts to determine the number-average molecular weight of the ETS organic-matter phase. It also describes the procedures used in the carbon/hydrogen/nitrogen/sulfur/oxygen analyses for the ETS particles and the Los Angeles aerosols.

Chapter Six compares the G/P partitioning of *n*-alkanes and PAHs to different model inorganic and organic aerosols obtained in this study with that found for UPM by a range of investigators in different locations. The operative G/P partitioning mechanisms to UPM are then discussed.

Chapter Seven is a summary of the conclusions reached in each of the previous chapters. In addition, areas of further needed research are identified.

The material discussed in Chapter Three was published in a modified form in the September, 1996 issue of *Environmental Science & Technology*. The work presented in Chapter Four has been submitted to *Environmental Science & Technology*. Therefore, Chapters Three and Four are written as research papers; each chapter contains an independent abstract, introduction, references, and acknowledgements section. The research presented in Chapter Five and Chapter Six has not yet been prepared for publication.

CHAPTER 2

THE THEORY OF GAS/PARTICLE PARTITIONING FOR SEMI-VOLATILE ORGANIC COMPOUNDS

2.1 Introduction

Semi-volatile organic compounds (SOCs) are always present, to some extent, in both the gas- and particulate-phases. The partitioning of a compound between these two phases depends on the temperature, the saturation vapor pressure of the compound (p_L°), and the amount and type of particulate material present. The values of the gas/particle partitioning coefficient (K_p) for a compound class which have been measured in different urban areas and by different researchers tend to be similar in magnitude at a given temperature. The variations in K_p that do exist could be due to the differences in particle compositions and environmental conditions. By definition, K_p is an overall equilibrium partitioning coefficient, and does not by itself provide information about the underlying partitioning mechanism(s). However, an understanding of the dependence of K_p on partitioning mechanism will facilitate the prediction of K_p values of SOCs in both outdoor and indoor air.

Atmospheric particulate material (APM) is a very complex mixture which is composed of many organic and inorganic compounds, including water. Gas/particle (G/P) partitioning of SOCs can take place by: 1) *ad*sorption onto particle surfaces; 2) *ab*sorption into organic material present in the particles; or 3) some combination of adsorption and absorption (Pankow, 1987; Pankow, 1994).

2.2 Equilibrium Sorption Theories

2.2.1 Adsorption of SOCs to Surfaces of Atmospheric Particles

Junge (1977) used the Langmuir isotherm to develop an equation for predicting the extent of physical adsorption of SOCs as a function of the concentration of aerosol surface area (θ_J, cm^2/cm^3) and p_L° at a temperature of interest

$$\phi = \frac{c_J \theta_J}{p_L^\circ + c_J \theta_J} \tag{2-1}$$

where ϕ is the fraction associated with the particulate phase, and c_J is a compound and temperature dependent constant. The value of ϕ can be determined experimentally according to

$$\phi = \frac{c_p}{c_p + c_g} \tag{2-2}$$

where c_p and c_g are the concentrations in the particulate- and gas-phases, respectively.

Pankow (1987) has derived an equation for c_J as

$$c_J = 760 R T N_s e^{(Q_l - Q_v)/RT} \tag{2-3}$$

where R is the gas constant (8.206×10^{-5} m^3 atm mol^{-1} K^{-1}), T (K) is the temperature, N_s (mol/cm^2) is the surface concentration of sorption sites, Q_l (kJ/mol) is the enthalpy of desorption from the surface, and Q_v (kJ/mol) is the enthalpy of vaporization from the pure subcooled liquid phase. K_p is therefore to be given by (Pankow, 1987)

$$K_p = \frac{N_s a_{TSP} T e^{(Q_l - Q_v)/RT}}{1600 p_L^\circ} \tag{2-4}$$

where a_{TSP} (m^2/g) is the specific surface area of the adsorbing solid.

Observed log K_p vs. log p_L° data for sorption to urban particulate material (UPM) and other types of APM tend to be well correlated according to

$$\log K_p = m_r \log p_L^\circ + b_r \tag{2-5}$$

Equation (2-4) predicts that for a given temperature and for a given sample of APM, when the group $N_s e^{(Ql-Qv)/RT}$ remains nearly constant within a compound class of interest (*e.g.* PAHs and *n*-alkanes), then a plot of measured log K_p values vs. log p_L° will be linear with a slope

$m_r \approx -1$ and a y-intercept $b_r \approx \log (N_s a_{TSP} T e^{(Ql-Qv)/RT} / 1600)$ (Pankow, 1987). Pankow (1991) has explained why the group $N_s e^{(Ql-Qv)/RT}$ can be expected to exhibit this type of constancy, and Pankow and Bidleman (1992) have discussed the fact that many field and laboratory studies of specific compound classes have obtained m_r values that are in fact quite similar to -1.

The temperature dependence of K_p for a given compound sorbing to a given type of particulate material can be expressed as (Yamasaki *et al.*, 1982; Pankow, 1987)

$$\log K_p = \frac{m_p}{T} + b_p \tag{2-6}$$

Most of the temperature dependence of K_p that is explicitly present in equation (2-6) is implicitly present in equation (2-5) since p_L° values are temperature dependent.

If adsorption is the dominant partitioning mechanism, a surface-area-normalized constant $K_{p,s}$ can be defined as (Storey *et al.*, 1995)

$$K_{p,s}\ (\mathrm{m}^3/\mathrm{m}^2) = \frac{K_p}{a_{TSP}\, 10^{-6}\mathrm{g}/\mu\mathrm{g}} \tag{2-7}$$

Thus,

$$\log K_{p,s} = m_{r,s} \log p_L^\circ + b_{r,s} \tag{2-8}$$

where $m_{r,s} = m_r$ and $b_{r,s} = b_r - \log (a_{TSP}/10^6)$.

2.2.2 Absorption of SOCs into Liquid Organic Material in Atmospheric Particles

To date, most of the modeling of G/P partitioning of SOCs in the atmosphere has been carried out under the assumption that the partitioning process involves mainly simply physical adsorption (Junge, 1977; Yamasaki *et al.*; 1982; Pankow, 1987). When APM is mainly mineral material of continental origin, it does seem likely that simple physical adsorption will dominate the sorption process. However, it also seems clear that phase partitioning of an absorptive nature must be playing at least some role in many circumstances; in some subset of circumstances, it might even play a dominant role (Pankow, 1994). Indeed, even suspended particulate material found far from urban sources areas will contain some organic phase material (*e.g.* particles of plant wax). Also, we know that urban particulate matter (UPM) always contains amorphous organic carbon from primary emissions (Turpin and Huntzicker, 1991), and from the formation of secondary organic aerosol (Pandis *et al.*, 1992). Some absorption of SOCs of interest into these types of particulate organic matter seems certain to occur. Therefore, it is of interest to determine how important absorptive partitioning can be.

For equilibrium partitioning between the gas phase and an absorptive organic matter (om) phase, Pankow (1994) has derived that

$$\log K_{\mathrm{p}} = -\log p^{\circ}_{\mathrm{L}} + \log \frac{f_{\mathrm{om}} 760\,RT}{MW_{\mathrm{om}}\,\zeta\,10^{6}} \qquad \textbf{(2-9)}$$

where f_{om} is the weight fraction of the TSP that comprises the om phase, MW_{om} is the number-average molecular weight of the om phase, and ζ is the mole-fraction-scale activity coefficient of the compound of interest in that phase. Equation (2-9) predicts that a plot of log K_{p} vs. log p°_{L} will be linear with a slope $m_{\mathrm{r}} \approx -1$ and an intercept $b_{\mathrm{r}} \approx \log (f_{\mathrm{om}} 760RT / MW_{\mathrm{om}}\zeta 10^{6})$ when $1/\zeta$ remains constant within the compound class of interest. This result indicates that a plot of log K_{p} vs. log p°_{L} will tend to have a slope near -1 for absorptive partitioning just as with adsorptive partitioning (Pankow, 1994).

When absorption into a liquid (or at least amorphous) om phase is the dominant sorption mechanism, an om-phase-normalized constant $K_{\mathrm{p,om}}$ can be defined as (Odum *et al.*, 1996; Pankow, In press)

$$K_{\mathrm{p,om}} = \frac{K_{\mathrm{p}}}{f_{\mathrm{om}}} \qquad \textbf{(2-10)}$$

where f_{om} is the weight fraction of the TSP that comprises the om phase. In this case,

$$\log K_{\mathrm{p,om}} = m_{\mathrm{r,om}} \log p^{\circ}_{\mathrm{L}} + b_{\mathrm{r,om}} \qquad \textbf{(2-11)}$$

Where $m_{\mathrm{r,om}} = m_{\mathrm{r}}$ and $b_{\mathrm{r,om}} = b_{\mathrm{r}} - \log f_{\mathrm{om}}$.

2.2.3 Summary of Partitioning Mechanism

In any given situation, both adsorptive and absorptive partitioning may be operative. The observed value of K_{p} will then contain contributions from both mechanisms so that for a given compound

$$K_{\mathrm{p}} = \frac{N_s a_{\mathrm{TSP}} T e^{(Q_1 - Q_v)/RT}}{1600 p_{\mathrm{L}}^{\circ}} + \frac{f_{\mathrm{om}} 760 RT}{MW_{\mathrm{om}} \zeta 10^6} \tag{2-12}$$

Thus, regardless of the relative importance of adsorptive vs. absorptive partitioning, a plot of log K_{p} vs. log p_{L}° may be expected to be well correlated with a slope of near -1. The actual relative importance of these two partitioning mechanisms in a given situation depends on the values of various parameters in equation (2-12). Increasing a_{TSP} and $e^{(Ql-Qv)/RT}$ will favor adsorption; increasing f_{om}, decreasing MW_{om}, and ζ will favor absorption.

2.3 Kinetics

2.3.1 Existing Kinetic Models

Sorption kinetic models can explain the basic equilibrium aspects of partitioning as well as slow, reversible, nonequilibrium behaviors. Table 2.1 provides a comparison of some existing sorption kinetics models.

Among many models that have been developed to simulate sorption kinetics, one-box model is the simplest in which the sorption rate is a first-order function of concentration difference between the sorbent (viewed as a completely mixed box) and the solution, and is quantified by a single rate constant, k_{d} (Kasten *et al.*, 1952; Oddson *et al.*, 1970). This mathematical formulation implies that sorptive exchange is limited by only one of many conceivably important processes including binding by single class of sorbing site or mass transfer across a boundary. However, the one-box model does not fit experimental data well. The improved two-box model typically divides a sorbent into two compartments (Wu and Gschwend, 1986): 1) an exterior part which is easily accessible, permits rapid surface adsorption , and requires only minutes to reach equilibrium; and 2) an interior part which exchanges mass slowly and requires weeks or even months to reach full equilibrium (Wu and Gschwend, 1986). The two-box model utilizes three independent fitting parameters. These parameters cannot be evaluated easily, and there is no fundamental basis on which to predict their values. It is also widely recognized that natural porous materials can contain many different types of sorption sites (Connaughton *et al.*, 1993). Even though the obtained kinetics fitting parameters could correspond to the actual rates for the mixture of the sorption

Table 2.1 Comparison of Sorption Kinetics Models

Name	Conceptual model	Fitting parameter	Reference
One-box model	$S \xleftrightarrow{K_d} C$	k_d	Coates and Elzerman, 1986
Two -box model	$S_1 \xleftrightarrow{X, K_p} C \xleftarrow{k_d} S_2$	k_d, K_p, and X	Wu and Gschwend, 1986
Time-varying Γ model	$S \xrightarrow{k_d} C$ mean $k_d = \alpha/\beta$, standard deviation = $\alpha^{0.5}/\beta$	α and β	Connaughton *et al.* 1993
Radial diffusion model 1 (gas-phase pore diffusion)	$S \xleftrightarrow{K_p} C \xrightarrow{D_{eff}} C$ $D_{eff}{}^{a} = \frac{f(n, \text{tortuosity})\, D_m n}{(1-n)\, K_p \rho_s}$	D_{eff}	Wu and Gschwend, 1986 Rounds and Pankow, 1990
Radial diffusion model 2 (liquid-like organic phase diffusion)	$S \xleftrightarrow{K_p, \alpha} C \xrightarrow{D} C$	D and α	Odum *et al.* 1994

Abbreviations:

α = surface mass transfer coefficient
C = concentration of the bulk fluid-phase (ng/m^3)
C_s = concentration of the analyte at the surface
C' = concentration of the compound in the pore fluid (ng/m^3)
D = diffusion coefficient in liquid-like organic phase (cm^2/s)
D_{eff} = effective diffusion coefficient (cm^2/s)
D_m = molecular diffusion coefficient of the compound in air (cm^2/s)
f (n, tortuosity) = pore geometry factor
k_d = first-order desorption rate constant coefficient (min^{-1})
K_p = sorption equilibrium partitioning coefficient (m^3/μg)
n = intraparticle porosity of the sorbent (cm^3 of void shell /cm^3 total)
ρ_s= specific density of the sorbent (g/cm^3)
S = concentration of the bulk sorbed compound (g/g)
S_1 = concentration of the compound that is in equilibrium with the bulk fluid-phase concentration (g/g)
S_2 = concentration of the sorbed compound that is rate limited (g/g)
X = fraction of the bulk sorbed compound that is in equilibrium with the fluid concentration
[a] K_p, D_m, and ρ_s can be determined independently

sites, there might not be a direct relationship between the mean strength of the sites and the fitting parameter for partition strength.

A time-varying Γ model (Connaughton *et al.*, 1993) is a variation of a two-box model. Such a model invokes the concept of multiple regions or sites, and assumes a continuum of compartments with varying desorption rate constants. This type of model seems to be able to predict the long-term release of pollutants from contaminated soils.

Radial diffusion models were established to describe the kinetics of ion exchange and absorption in batch reactor (Eagle and Scott, 1950). The application of such models to environmental problems has taken place only recently (Wu and Gschwend, 1986; Ball and Roberts, 1991; Rounds and Pankow, 1990; Rounds *et al.*, 1993; Farrell and Reinhard, 1994), with diffusion into and out of the particles assumed to be the only rate-limiting process. For particles coated with amorphous liquid-like organic compounds, Cotham (1990) has demonstrated that the coating can enhance sorption, and has proposed that sorption to some atmospheric particles might be better described by the partitioning of compounds into a liquid phase rather than adsorption to solid surface. Odum *et al.*(1994) have developed a modified radial diffusion model to simulate the sorption kinetics of SOCs to diesel combustion aerosols with a liquid organic layer, and concluded that the rate limiting process is the mass transfer at the surface and that diffusion is only limiting for the larger particles. This result is somewhat different from the early radial diffusion models which assumed that gas-phase pore diffusion is the limiting factor for intraparticle transport.

2.3.2 Theories of Intraparticle Radial Diffusion Model

Rounds and Pankow (1990) have applied a intraparticle radial diffusion model to describe the diffusive uptake or release of a gas-phase organic compound by atmospheric particles. In their study, gas-phase pore diffusion was assumed to be the predominant mechanism for intraparticle transport. Transport due to surface diffusion was assumed to be negligible. Particles were assumed to be fractionally porous and to have a nonporous, non-sorbing inner core surrounded by a uniformly porous, sorbing outer shell.

A governing equation (Crank, 1950; Wu and Gschwend, 1986; Rounds and Pankow,

1990) for intraparticle diffusion in spherical coordinates is given by

$$\frac{\partial S(r)}{\partial t} = D_{\mathrm{m}} n [\frac{\partial^2 A'(r)}{\partial r^2}] + \frac{2}{r}\frac{\partial A'(r)}{\partial t} \tag{2-13}$$

Where $S(r)$ is the total volumetric concentration of a compound at a radial distance r from the center of the particle (ng/m^3), $A'(r)$ is the volumetric concentration of the compound in the micropores of the particle (ng/m^3), D_{m} is the molecular diffusion coefficient of the compound in air (cm^2/s), n is the intraparticle porosity of the porous shell (void volume in the shell per total volume of the shell), and t is the time (s).

When a filter is used to sample particles, the physical distribution of the particles loaded on the filter should be considered (Rounds *et al.*, 1993). The spatial separation of particles leads to the possibility that particles deeper in the filter might be exposed to a gas-phase concentration that is different from that at the front edge of the filter. Mathematically separating the filter into more than one layer is a logical way to describe sorption kinetics under such conditions. In such a case, the behavior of the intraparticle radial diffusion model is controlled by three parameters (Rounds *et al.*, 1993): 1) the number of filter layers N; 2) the mass-transfer time scale T_{M}; and 3) the diffusion reaction time T_{D} where

$$T_{\mathrm{M}} = \frac{K_{\mathrm{p}} M_{\mathrm{p}}}{f} \tag{2-14}$$

$$T_{\mathrm{D}} = \frac{(\text{diffusion length})^2}{D_{\mathrm{eff}}} \tag{2-15}$$

M_{p} (μg) is the mass of particles on the filter, f (m^3/min) is the average flow rate through the filter, and D_{eff} is the effective intraparticle diffusion coefficient (cm^2/s). The diffusion reaction time scale for a polydisperse size distribution can be defined as an average T_{D} for each size, weighted by the mass fraction. For a fully porous particle, the diffusion length is equal to the particle radius.

2.4 Summary of K_{p} Measurements

K_{p} can be measured by using either an equilibrium or a kinetics approach. In the equilibrium approach, K_p for compounds of interest are estimated with equation (1-1) by simultaneous gas- and particle-phase sampling. In the kinetics approach, desorption experiments are carried out, and K_p values for compounds of interest are estimated using equation (2-14) and the compound release profiles as a function of time.

The advantage of using the desorption method for K_p measurements is the ability to closely control temperature and relative humidity. In addition, for a heavily-loaded filter, there is little potential that sorption to the filter matrix itself will affect the measured K_p values. Finally, in contrast to uncontrolled ambient sampling, artifacts due to "blow-off" and "blow-on" will not arise. Indeed, controlled blow-off is the whole basis of a desorption experiment, and blow-on cannot occur at all. A potential disadvantage of the desorption method is the possible alteration of the collected particle phase by volatilization during an extended experiment.

Reprinted in part with permission from Environmental Science and Technology, 1996, 30, 2800-2805. Copyright 1996 American Chemical Society.

CHAPTER 3

GAS/PARTICLE PARTITIONING OF ORGANIC COMPOUNDS TO ENVIRONMENTAL TOBACCO SMOKE AND COMPARISON TO URBAN PARTICULATE MATTER

3.1 Abstract

Certain organic compounds in environmental tobacco smoke (ETS) can cause respiratory diseases and lung cancers. The behavior and health effects of ETS will depend upon how each of these compounds is distributed between the gas and particulate phases. ETS particles were collected on a filter. Semivolatile organic compounds were desorbed from the filter at 20 °C using a flow of clean nitrogen at 60% relative humidity. The desorption was followed with time. Volatile, lower molecular weight compounds were released quickly; less volatile compounds were desorbed slowly. A diffusion model was used to estimate gas/particle partition coefficient (K_p) values. The *n*-alkane and polycyclic aromatic hydrocarbon (PAH) data agreed with prior measurements for ETS by another method. New data for four nitrogen-containing compounds were obtained. At a given pure compound vapor pressure, PAHs were sorbed more strongly than the *n*-alkanes. The K_p value for nicotine was unusually large, probably due to a significant degree of protonation of the nicotine in the ETS phase. For carbazole, however, which cannot be protonated, K_p was very similar to what would be predicted for a PAH of the same vapor pressure. After normalization for the fraction of organic matter in the particulate phase, the ETS data for PAHs agreed well with data for PAHs sorbing to urban particulate material (UPM). This is consistent with the interpretation that partitioning to both ETS and UPM is absorptive in nature.

3.2 Introduction

Some of the organic compounds in environmental tobacco smoke (ETS), such as certain polycyclic aromatic hydrocarbons (PAHs), nitrosamines, amines, and some other nitrogen-containing compounds, are known to be genotoxic and carcinogenic, and to cause respiratory diseases and lung cancers (Guerin and Jenkins, 1984; Arey *et al.*, 1987; Lewtas *et al.*, 1987). The transport, fate, and health effects of ETS will certainly depend upon how each of these compounds is distributed between the gas and particulate phases. Semi-volatile organic compounds (SOCs) are of special interest in this context because their intermediate volatilities allow them to be present in both the gas and particulate phases. Pankow *et al.* (1994) have examined the characteristics of gas/particle (G/P) partitioning to ETS by concurrently sampling the gas and particulate phases in an indoor environment. As is discussed below, in addition to being of interest for health reasons, ETS may serve as a useful model material in the continuing study of gas/particle partitioning to urban particulate material (UPM).

An equation that has been used successfully to parameterize G/P partitioning is (Yamasaki *et al.*, 1982; Pankow, 1991; Pankow, 1992):

$$K_p = \frac{F/\mathrm{TSP}}{A} \tag{3-1}$$

where K_p (m^3/μg) is the G/P partitioning coefficient for a given compound of interest; F (ng/m^3) and A (ng/m^3) are the particle-associated and gaseous concentrations, respectively; and TSP (μg/m^3) is the level of total suspended particulate material in the air. Theory predicts that K_p values within a given compound class will depend on the pure sub-cooled liquid vapor pressure p_L° according to (Pankow, 1987; Yamasaki *et al.*, Pankow, 1991)

$$\log K_p = m_r \log p_L^\circ + b_r \tag{3-2}$$

The temperature dependence of K_p for a given compound sorbing to a given type of atmospheric particulate material can be expressed as (Yamasaki *et al.*, 1982; Pankow, 1994):

$$\log K_p = \frac{m_p}{T} + b_p \tag{3-3}$$

Most of the temperature dependence explicitly present in equation (3-3) is implicitly present in equation (3-2) since p_L^o values depend on temperature.

The constants m_r and b_r depend on the compound class and on the nature of the particulate material. The constants m_p and b_p depend on the specific compound and the particulate material of interest, though for UPM, there is evidence that b_p values tend to be constant within a given compound class (Pankow, 1994). Pankow *et al.* (1994) have found that on ETS, as on UPM, *n*-alkanes and PAHs exhibit m_r values near -1; b_r values, however, were found to be significantly larger for ETS than for UPM, making sorption to ETS significantly stronger than sorption to UPM.

The purpose of this work was to confirm the ETS results of Pankow *et al.* (1994) by another method, and also to expand the list of compounds for which K_p values are available. Rounds *et al.* (1993) conducted desorption experiments with UPM, and successfully simulated the resulting experimental data using an intraparticle diffusion model; estimated K_p values were obtained for a range of both *n*-alkanes and PAHs. In the experiment conducted here, compounds were desorbed from ETS particles using a flow of clean nitrogen. The desorbed gaseous compounds were collected continuously using adsorption/thermal desorption (ATD) cartridges. As in Rounds *et al.* (1993), an intraparticle diffusion model was used to estimate K_p values.

The advantages of the desorption method for the measurement of K_p values include the ability to closely control the temperature and relative humidity. In addition, for a heavily-loaded filter, there is little potential that sorption to the filter matrix itself will affect the measured K_p values. Finally, in contrast to uncontrolled ambient sampling, artifacts due to "blow-off" and "blow-on" will not arise. Indeed, controlled "blow-off" is the whole basis of a desorption experiment, and "blow-on" cannot occur at all. A potential disadvantage of the desorption method is the possible alteration of the collected particle phase by volatilization during an extended experiment. As a result, the method may not be well-suited to the study of compounds which possess high K_p values, and which therefore require large volumes of gas to remove measurable amounts from the particle phase.

3.3 Experimental Section

3.3.1 Sampling

ETS sampling was carried out at the same local business place used earlier (Pankow *et al.*, 1994). An 8 inch × 10 inch quartz fiber filter (QFF) was used in a high-volume sampler to collect the particles. The QFF was pre-cleaned by baking overnight at 370 °C, then kept in a constant relative humidity (RH) chamber (RH = 66%) that contained a saturated solution of $NaNO_2$ at room temperature until use. After RH-equilibration, each QFF was weighed, wrapped in aluminum foil and transported to the sampling site. (The aluminum foil was washed with methylene chloride and baked at 320 °C overnight before use.) The sampling period was 3.5 hours with a constant flow though the filter. The total volume of air sampled was 262 m^3. After sampling, the inlet and outlet ports of the filter holder were wrapped with baked aluminum foil. The QFF was equilibrated again in the constant-humidity chamber and then weighed. The total mass of particulate matter collected was 119.2 mg (TSP=454.8 $\mu g/m^3$), including the particulate-phase water. The QFF was stored at -20 °C until further use.

3.3.2 Filter Desorption Apparatus and Procedure

A 102 mm-diameter filter was cut from the 8 inch × 10 inch filter and mounted in a filter holder of the same size. The mass of particles on the filter was calculated to be 22.49 mg. A schematic diagram of the filter desorption apparatus is given in Figure 3.1. The desorption experiment was carried out over 49 days. During that time, the temperature was maintained at 20 °C ± 0.2 °C by enclosing the apparatus in an environmental chamber. The RH of the clean nitrogen gas passing through the filter was maintained at 60%, which was similar to the 52% measured at the time of the original sampling. The N_2 gas was cleaned by first passing it through a hydrocarbon trap which contained molecular sieve 13X and activated carbon, and then through a baked quartz filter (Pallflex Corp, Putnam, CT) to obtain particle-free gas stream. The desired RH was obtained by bubbling the N_2 through de-ionized water in a humidifier with a controlled flow rate. ATD cartridges containing ~1 g each of Tenax-TA were used to sample the gas stream exiting from the filter, and also to

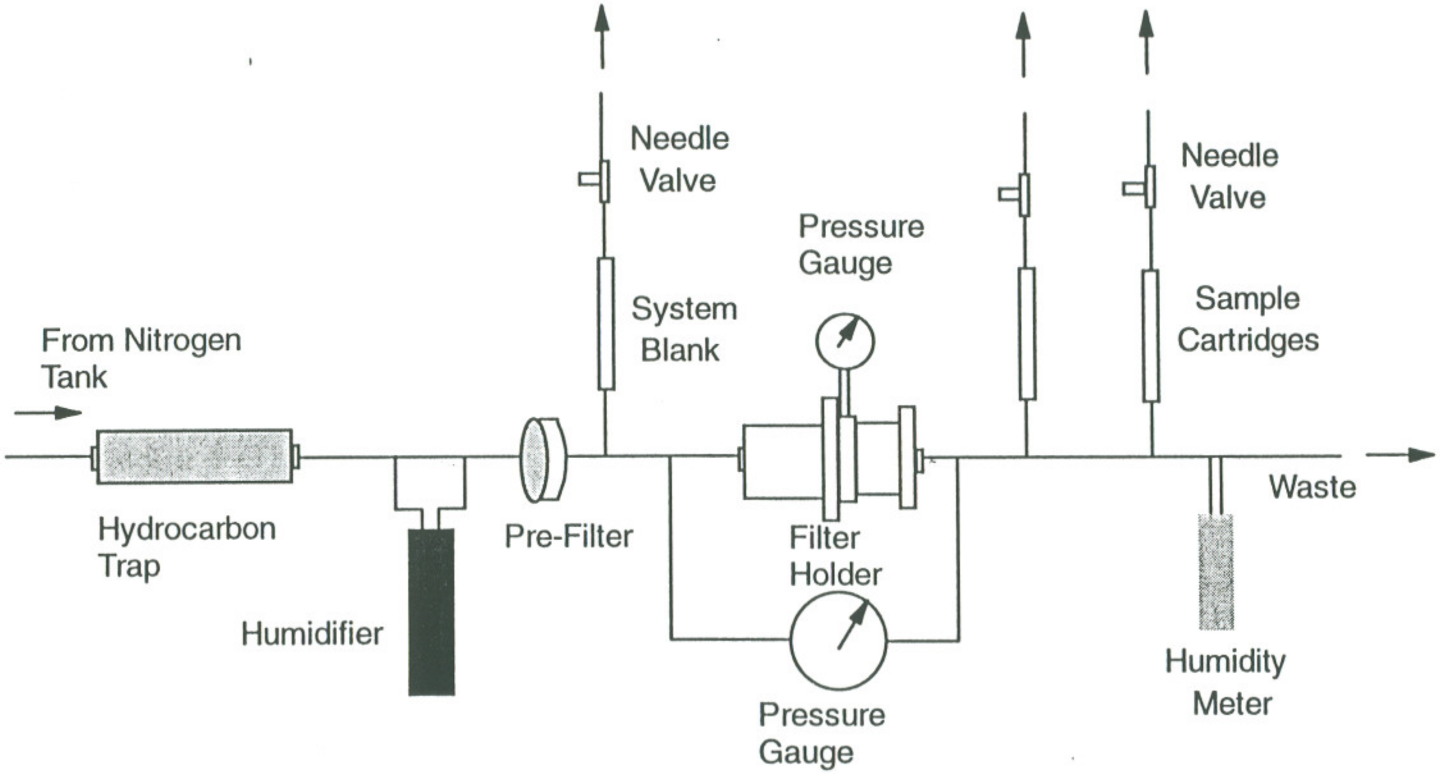

Figure 3.1 Schematic diagram of the experimental filter desorption apparatus.

collect system blanks for the nitrogen gas. Each ATD cartridge was pre-cleaned by pumping one liter of 1:1 hexane:acetone through the cartridge at 2 mL/min. The solvents were purged with ultra-pure helium at 50 °C for 20 min. Each cartridge was then conditioned at 300 °C for 2 h with a 1 mL/min flow of ultra-pure helium. The total flow rates through the filter were measured with a wet test meter periodically over the course of desorption, and the flow rates through the ATD cartridges were also measured with a bubble flow rate meter. The average flow rates were: filter, 4.79; system blank cartridge, 0.03; sample cartridges, 0.7 each; and waste, 3.36 L/min. Because the gas-phase concentrations of the more volatile compounds were expected to decrease rapidly, the sample ATD cartridges were initially replaced at short time intervals, and thereafter at increasingly longer intervals. Each used ATD cartridge was capped, sealed in a screw cap tube, and stored at -20 °C until further analysis. Figure 3.2 presents the experimental data for selected *n*-alkanes, PAHs, and nitrogen-containing compounds.

3.3.3 Analytical Methods

All ATD cartridges were analyzed by thermal desorption with capillary GC/MS as described by Pankow *et al.* (1988). Each cartridge was first spiked with internal standard (IS) compounds (naphthalene-d_8, anthracene-d_{10}, and perylene-d_{12}), and then desorbed with ultra-pure helium for 30 min at 270 °C. Whole-column cryotrapping at 0°C was employed during the thermal desorption. At the conclusion of the 30-min desorption, the GC temperature program was 0-100 °C at 25 °C/min, 100-300 °C at 10 °C/min, then hold at 300 °C for 2 min.

At the end of the desorption experiment, the filter was removed from its holder and extracted to determine the masses of the compounds that were incompletely desorbed. The QFF was first spiked with surrogate standard (SS) compounds (acenaphthene-d_{10} and phenanthrene-d_{10}), then Soxhlet-extracted overnight with 200 mL of methylene chloride. The extract was reduced to ~3 mL via evaporation using a three-ball Synder column. After cooling, the extract was passed through a cleanup/drying column packed with 0.5 g silica gel and 4 g anhydrous sodium sulfate (Na_2SO_4) to remove polar compounds and traces of water.

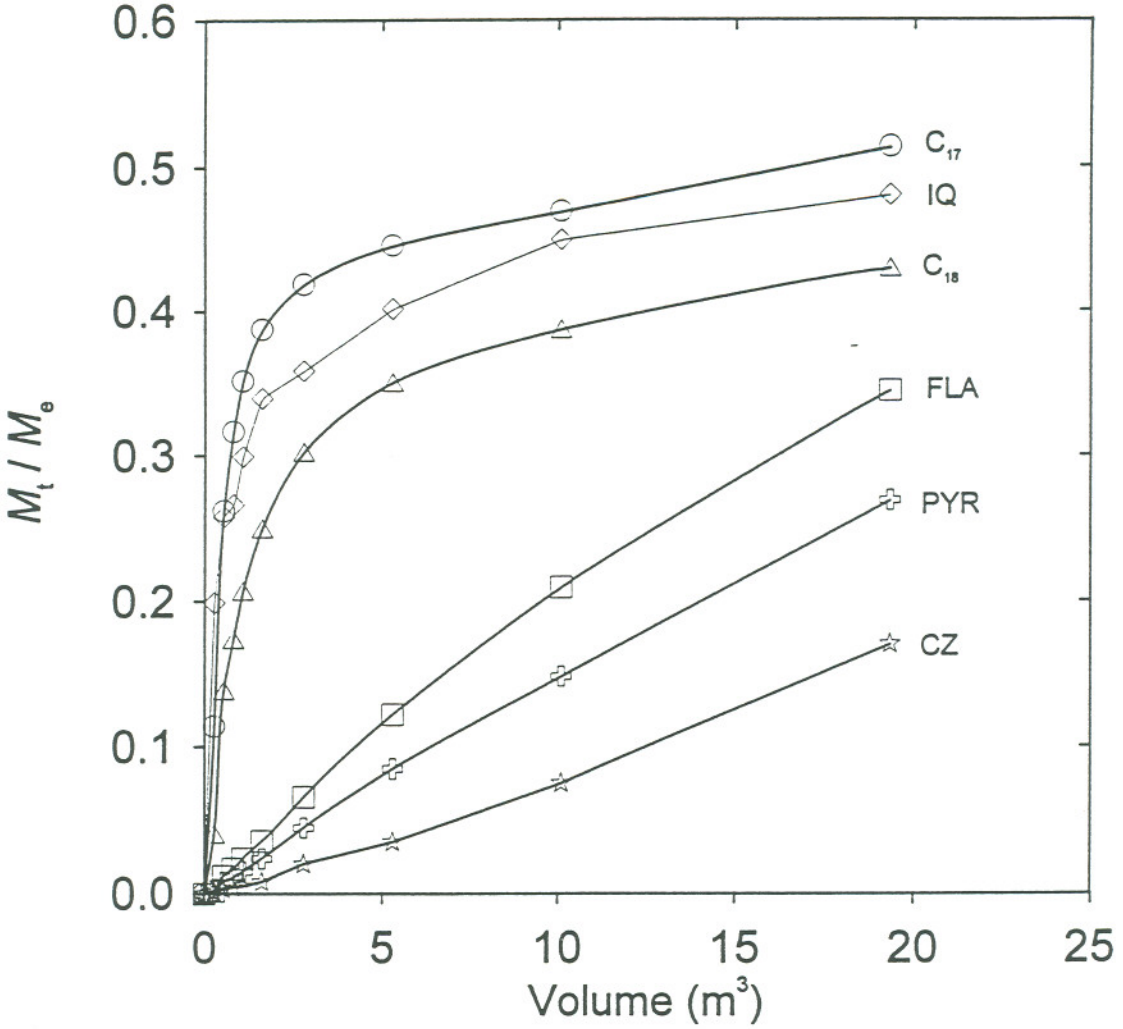

Figure 3.2 Fractional approach to equilibrium data for selected compounds plotted against volume. IQ = isoquinoline; FLA = fluoranthene; PYR = pyrene; CZ = carbazole. Solid lines do not represent model fits to the data, but rather just connect the points.

The silica gel and Na_2SO_4 were pre-cleaned by baking at 205 °C for 12 hr and 370 °C for 2 hr, respectively. The column was rinsed with 100 mL of methylene chloride before use. The filter extract was first passed through the column, and then gently blown down to ~400 µL with N_2. The column was then rinsed with a ~10 mL aliquot of methylene chloride. The rinse was combined with the extract, and the volume was blown down again. This rinse/blowdown cycle was carried out three times. The extract was stored at -20 °C. Immediately prior to analysis, the extract was weighed and spiked with IS compounds (naphthalene-d_8, anthracene-d_{10}, and perylene-d_{12}). The extract was analyzed using GC/MS with a splitless injection of 1 µL. A 30-m, 0.32-mm-i.d., 0.25-µm film thickness DB-5 capillary column (J&W Scientific, Folsom, CA) was used. The GC temperature program used was: hold at 50 °C for 2 min, 50-100 °C at 25 °C/min, 100-300 °C at 10 °C/min, then hold at 300 °C for 2 min.

3.3.4 Recovery Studies

In order to compensate for any loss of the target compounds during the analytical process, a recovery efficiency (R) is defined as

$$R(\%) = \frac{M_{SS}}{M_{true}} \qquad \textbf{(3-4)}$$

where M_{ss} is the mass of a SS compound calculated using equation (3-6) and M_{true} is the actual mass of the SS compound spiked onto the filter before Soxhlet extraction. The actual mass of a target compound is estimated by normalizing the calculated value obtained by equation (3-6) with a corresponding R value as demonstrated in equation (3-8).

The compound-dependent extraction recoveries were measured by extracting blank QFFs spiked with seventeen model compounds and two SS compounds (acenaphthene-d_{10} and phenanthrene-d_{10}). Table 3.1 and 3.2 summarize the recovery results. The average recoveries (%) for the *n*-alkanes, PAHs, and N-containing compounds were 94 ± 6, 93 ± 8, and 93 ± 7 (±1sd), respectively. The average recoveries (%) for acenaphthene-d_{10} and phenanthrene-d_{10} were 100 ± 6 and 94 ± 4 (±1sd), respectively.

Table 3.1 Recovery Efficiencies of Target SOCs from the Extraction of QFFs

Compounds		Recovery (%) (±1sd)
***n*-Alkanes**		
Hexadecane (C_{16})		87 ± 2
Heptadecane (C_{17})		91 ± 10
Octadecane (C_{18})		86 ± 6
Nonadecane (C_{19})		97 ± 8
Eicosane (C_{20})		99 ± 5
Heneicosane (C_{21})		100 ± 9
Docosan (C_{22})		101 ± 4
	n-Alkanes, Average	94 ± 6
PAHs		
Fluorene (FLU)		86 ± 6
Phenanthrene (PHE)		103 ± 8
Fluranthene (FLA)		90 ±12
PyrenE (PYR)		87 ± 7
Chrysene (CHR)		99 ± 12
	PAHs, Average	93 ± 8
N-containing compound		
Quinoline (Q)		91 ± 14
Isoquinoline (IQ)		92 ± 11
Nicotine		87 ± 7
Carbazole (CZ)		103 ± 18
	N-compounds, Average	93 ± 7

Table 3.2 Recovery Efficiencies of Surrogate Standard Compounds from the Extraction of QFFs

Experiment	Recovery Efficiency of Acenaphthene-d_{10} (%)	Recovery Efficiency of Phenanthrene-d_{10} (%)
Blank	105	98
Filter extraction before desorption	103	91
Filter extraction after desorption	93	92
Average	100 ± 6	94 ± 4

3.3.5 Quantitation

Compounds of interest were quantified by comparing retention times, mass spectra, and mass intensities with those observed from runs of external standard solutions. Each standard solution contained all of the target, SS, and IS compounds. The SS compounds were used for correction of mass loss during analytical procedure as described above. The IS compounds were used to estimate masses of the target or SS compounds in both the standard and sample runs, and also used to correct for any daily variations of instrument responses or differences of injected mass for on-column injections among sample runs. A five-step process was involved for quantitation:

1) External standard solutions were prepared over concentration ranges bracketing the expected concentrations in the sample extracts;

2) Retention times and mass spectra were recorded for all the target, SS, and IS compounds;

3) A response factor (*RF*) for each target or SS compound was calculated using the GC/MS software according to

$$RF = \frac{(area)(IS\ amt)}{(IS\ area)(amt)} \tag{3-5}$$

where *area* and *amt* are the peak area and the mass (ng) of a target or SS compound for the external standard runs, respectively; *IS area* and *IS amt* are the peak area and the mass (ng) of the referential IS compound in the same runs;

4) A response curve for each of the target and SS compound was generated using the external standards (any standard which caused more than 10% scatter in the response curve was removed), and an average RF (RF_{avg}) for each compound was then calculated. (note: the filter extracts and the ATD cartridges were analyzed by different methods, separate sets of response curves and RF_{avg} values for the compounds of interest are recommended for these two methods)

5) The scan numbers of the compound peaks in the GC runs were recorded, and the peak areas were integrated using a Galaxy 2000 (X-spec Inc. San Jose, CA) data system. The corresponding mass M (ng) of a target or SS compound in a sample run was calculated according to

$$M = \frac{(Area)(IS\ amt)}{(IS\ area)\ (RF_{avg})} \tag{3-6}$$

where *Area* is the peak area of a target or SS compound.

The M_i (ng) mass of a target compound desorbed from the filter during a given sampling period i was calculated according to

$$M_i = M_{\text{ATD}} \frac{V_{\text{filter}}}{V_{\text{ATD}}} \tag{3-7}$$

where M_{ATD} (ng) is the mass of a target compound detected on a ATD cartridge, V_{ATD} (L) is the ATD sample volume, and V_{filter} (L) is the volume of air passing through the filter during the same sampling period. The mass of each compound remaining on the filter M_r (ng) after the desorption experiment was estimated by

$$M_r = \frac{1000\ C_{\text{extract}}\ M_{\text{MeCl}}}{d_{\text{MeCl}}\ R} \tag{3-8}$$

where M_{MeCl} (g) and d_{MeCl} (g/cm^3) are the mass and density of the methylene chloride in the filter extracts, respectively; and C_{extract} (ng/µL) is the measured concentration of a target compound in the filter extract.

3.3.6 Quantitation Limits

For the purposes of this study, a conservative method was used to estimate the method quantitation limits. A quantitation limit of 200 ion counts above the baseline in the chromatographic region of interest was determined to be appropriate. While this criterion was used for the quantitation ion, three other major characteristic fragment ions were required to be present (but not necessarily ≥200 counts) in the correct ratios in order for a compound to be considered present and then quantitated. The number of ion counts depended on the compound, and the sensitivity and cleanness of the MS source. For the GC/MS conditions utilized in this study, this typically corresponded to ~0.5 ng for each of the target compounds.

3.3.7 Data Analysis

For each compound, the desorption data were analyzed using the variable

$$\frac{M_t}{M_e} = \frac{(\text{cumulative mass desorbed})_t}{\text{total mass of compound}} \qquad \textbf{(3-9)}$$

The subscript t refers to the total elapsed time at the end of a given sampling period; the subscript e refers to equilibrium. M_t is the sum of the corresponding M_i values up to the end of a given sampling period. The quantity M_e includes the total amount desorbed over the course of the entire desorption experiment, plus the mass extracted from the filter after completion of the experiment. M_t / M_e therefore gives the fractional approach to equilibrium; it equals unity when equilibrium (*i.e.* total desorption) is reached. It is assumed here that for each compound, 100% of the mass of any given compound found on the filter at the end of the desorption was available for exchange with the gas phase. The value of M_e for the various compounds on the 102 mm-diameter filter section are given in Table 3.3.

3.4 Results and Discussion

3.4.1 General

Rounds *et al.* (1993) have illustrated that the compound-dependent minimum time T_M to reach equilibrium with the clean nitrogen is related to K_p, the mass of particles on the

Table 3.3 Estimated log K_p Values by Desorption Using Least-Regressions of M_t /M_e Values vs. V (20 °C and 60% relative humidity)

Compound	log p^o_L (Torr)	M_e (ng)	slope of M_t/M_e *vs.* V regression (m^{-3})	r^2 for M_t/M_e *vs.* V regression	log K_p ($m^3/\mu g$)
			n-Alkanes		
C_{16}	-3.17	210	0.405	0.689	-3.96[a]
C_{17}	-3.70	319	0.427	0.910	-3.98
C_{18}	-4.23	396	0.227	0.922	-3.71
C_{19}	-4.76	493	0.102	0.912	-3.36
C_{20}	-5.28	491	0.0257	0.913	-2.76
C_{21}	-5.81	506	0.00945	0.952	-2.33
C_{22}	-6.34	1590	0.00199	0.967	-1.65
			PAHs		
fluorene (FLU)	-2.42	19.0	1.94	0.853	-4.64
phenanthrene (PHE)	-3.23	78.6	0.0673	0.895	-3.18
fluoranthene (FLA)	-4.42	72.2	0.00767	0.943	-2.24
pyrene (PYR)	-4.61	72.9	0.00647	0.954	-2.16
chrysene (CHR)	-5.90	193	0.000201	0.983	-0.66
			N-Containing Compounds		
quinoline (Q)	-1.25[b]	6.93	0.637	0.960	-4.16
isoquinoline (IQ)	-1.38[c]	19.0	0.338	0.806	-3.88
nicotine	-1.48[d]	35300	0.0300	0.996	-2.83
carbazole (CZ)	-4.82[e]	467	0.00498	0.986	-2.26

[a] Not considered reliable due to the low degree of correlation in the M_t / M_e *vs.* V plot (see text).

[b] Calculated based on the data in Van de Rostyne and Prausnitz (1980).
[c] Calculated based on the data in Das *et al.* (1993).
[d] Calculated based on the data in Timmermans (1950).
[e] Calculated based on the data in Boulik *et al.* (1984)

filter M_p, and the flow rate f through the filter:

$$T_M = \frac{K_p M_p}{f} \tag{3-10}$$

A useful way to analyze filter desorption data is to plot M_t / M_e vs. the volume V that has passed through the filter (Rounds *et al.*, 1993). For infinitely fast desorption kinetics, $M_t / M_e = 1$ when $T_M = 1$, and a plot of M_t / M_e vs. V will be a straight line from the origin to $V = K_p M_p$ and $M_t / M_e = 1$. Since the slope of such a line will be $1/K_p M_p$, measurement of the slope for such fast kinetics will yield the value of K_p for the compound of interest. However, even when the desorption kinetics are not extremely fast, since there will be no intraparticle concentration gradients at $t = 0$, the data points obtained near $t = 0$ will asymptotically approach the infinitely fast kinetics line. In this work, a least-squares regression was therefore carried out using the early data points for each compound, forcing a zero intercept. Note that the adjective "early" is compound dependent. For very volatile compounds like n-C_{16}, it referred to points collected in the first few hours of the experiment. For high K_p compounds like pyrene, a time like 20 hours could still be considered "early". Since M_p was known (22.49 mg), the K_p values were obtained from the slopes of the regressions. This method is applicable regardless of the nature of the sorption mechanism. The only requirement is that the sorption isotherm be linear.

3.4.2 Log K_p values

Table 3.3 gives the estimated log K_p values for compounds of interest as derived from the initial slopes. All of the log K_p values are considered reliable except that for C_{16} (note the low r^2 value for that compound). Table 3.4 compares the log K_p values obtained here by desorption at 20 °C with those obtained at 25 °C using simultaneous gas and particle-phase

Table 3.4 Comparison of Log K_p Values Measured at 20 °C by Desorption for ETS Particles (This Work) and at 25 °C by Gas/Particle Sampling (from Pankow *et al.*, 1994)

Compound	20 °C (this work)		25 °C (from Pankow *et al.*, 1994)	
		n-Alkanes		
	log p_L^o (Torr)	log K_p ($m^3/\mu g$)	log p_L^o (Torr)	log K_p ($m^3/\mu g$)
C_{16}	-3.17	-3.96[a]	-2.91	-4.93
C_{17}	-3.70	-3.98	-3.43	-4.35
C_{18}	-4.23	-3.71	-3.94	-3.95
C_{19}	-4.76	-3.36	-4.45	-3.49
C_{20}	-5.28	-2.76	-4.96	-3.01
C_{21}	-5.81	-2.33	-5.48	-2.52
C_{22}	-6.34	-1.65	-5.99	-2.24
		PAHs		
fluorene (FLU)	-2.42	-4.64	-2.23	-5.09
phenanthrene (PHE)	-3.23	-3.18	-3.02	-3.66
anthracene (ANT)	NA[b]	NA	-3.05	-3.35
fluoranthene (FLA)	-4.42	-2.24	-4.19	-2.76
pyrene (PYR)	-4.61	-2.16	-4.37	-2.59
chrysene (CHR)	-5.90	-0.66	-5.64	-1.55

[a] Not considered reliable due to the low degree of correlation in the M_t / M_e *vs.* V plot (see text).

[b] Not available

sampling (Pankow *et al.*., 1994). The two data sets are plotted together in Figure 3.3 in a log K_p vs. log p_L^o format. The expectation here is that the majority of the temperature dependence of the log K_p values is implicitly compensated for by the temperature dependence of the log p_L^o values. In general, the two data sets are in excellent agreement. This confirms the conclusion of Pankow *et al.* (1994) that on a weight for weight basis, sorption of SOCs to ETS is considerably stronger than sorption to UPM.

As seen in Figure 3.3, for a given vapor pressure, certain of the N-containing compounds exhibit very strong sorption to ETS. The correlation line for the PAHs lies below these points, followed by the line for the *n*-alkanes. Such compound class differences are not unexpected, and have their origins in class-dependent physical and chemical properties. The presence of acidic compounds in the ETS particle phase may explain the strong sorption of certain N-containing compounds like nicotine (see below). Similarly, interactions between aromatic electrons in the PAHs and polar compounds in the ETS particles could be responsible for the stronger sorption of the PAHs as compared to the *n*-alkanes.

The pK_a values for the protonated forms of isoquinoline and quinoline are 5.4 and 4.5, respectively (see Figure 3.4) (Windholz, 1976). The two pK_a values for nicotine are $pK_{a1} = 3.12$ and $pK_{a2} = 8.12$ (Windholz, 1976). The pK_a for the protonated nitrogen on the pyrrolidine ring in nicotine is very much higher than the pK_a for the protonated nitrogen on the pyridine ring. The pK_a value for protonated carbazole is -6.0 (Katritzky and Rees, 1984). The exceedingly acidic nature of protonated carbazole is due to the aromatic nature of non-protonated carbazole. Indeed, carbazole is very difficult to protonate because doing so destroys its aromaticity. As seen in Figure 3.3, the point for carbazole lines near the correlation line for PAHs. This is not unexpected since carbazole is fully aromatic, and electronically very similar to anthracene. However, the carbazole point may lie somewhat above the PAH correlation line rather than below it since the vapor pressure of $10^{-4.82}$ Torr in Table 3.3 may be too low for this three-ringed compound.

The pH of fresh smoke from domestic blend-cigarettes has been estimated by Morrie (1972) to range from 5.2 to 6.2. Over this pH range, nicotine exists mainly in its mono-

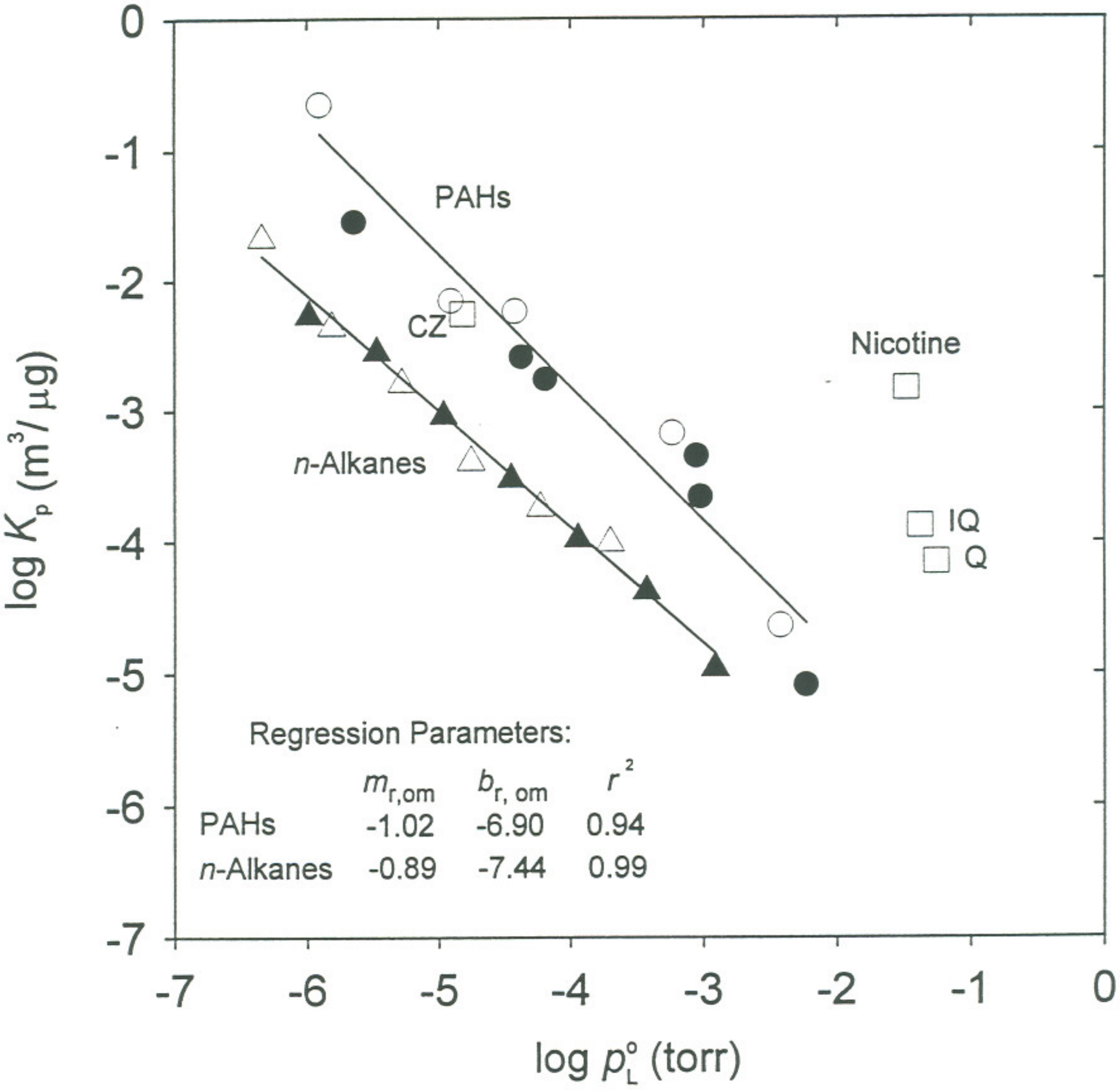

Figure 3.3 Comparison of log K_p vs. log p_L^o correlation among different compound classes. Filled circles and triangles are data from Pankow *et al.*(1994). Open circles, triangles, and squares are data obtained in this study.

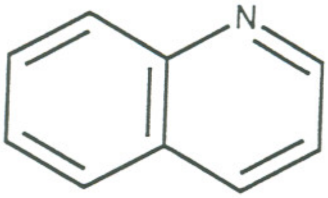

Quinoline
$\mathrm{p}K_a = 4.5$
$\log p_L^{\circ} = -1.25$

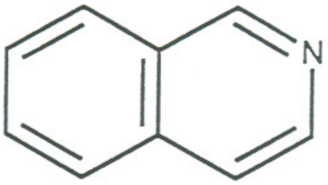

isoquinoline
$\mathrm{p}K_a = 5.4$
$\log p_L^{\circ} = -1.38$

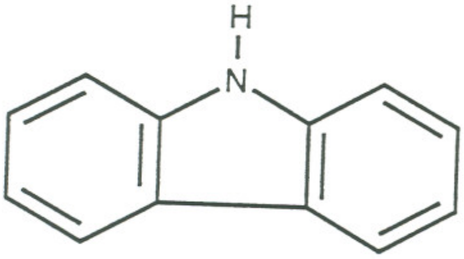

Carbazole
$\mathrm{p}K_a = -6.0$
$\log p_L^{\circ} = -4.82$

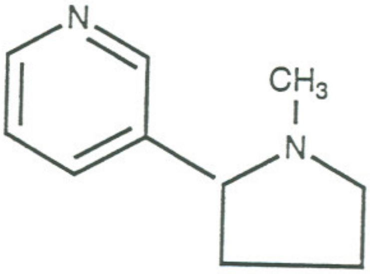

Nicotine
first $\mathrm{p}K_a = 3.12$
second $\mathrm{p}K_a = 8.02$
$\log p_L^{\circ} = -1.48$

Figure 3.4 Structures and properties (20 °C) for four N-containing compounds found in environmental tobacco smoke (ETS).

protonated form. It seems likely that this is the reason the aerosol phase is favored for nicotine so that this compound exhibits a large K_p value despite its high pure-compound vapor pressure. We also note that since the pH of ETS particles may be subject to considerable variability, so too may be the log K_p value for nicotine (see below). Whether or not there are pH effects for quinoline and isoquinoline is not known. Indeed, the pH=5.2-6.2 results of Morrie (1972) were obtained for fresh tobacco smoke, not ETS. Moreover, the pH electrode used was not calibrated for a tobacco smoke matrix.

3.4.3 Effects of K_p and TSP on ϕ

At equilibrium, the fraction ϕ of a compound that is associated with particles is given by:

$$\phi = \frac{F}{F + A} = \frac{K_p \mathrm{TSP}}{1 + K_p \mathrm{TSP}} \tag{3-11}$$

Figures 3.5a and 3.5b uses the regressions from Figure 3.3 to illustrate how ϕ depends on log p_L^o and TSP for the PAHs and the *n*-alkanes, respectively. For given values of log p_L^o and TSP, ϕ will be larger for the PAHs than the *n*-alkanes. As the TSP value is reduced by dilution, there will be a shift to the gas phase for both compound classes. Figure 3.6 plots ϕ vs. log TSP for nicotine under the assumption that the K_p value for nicotine does not change as TSP changes.

3.4.4 Absorptive Partitioning

Scanning electron microscopy examination of a QFF used to sample ETS did not reveal the presence of any single particles on the QFF surface (see Figure 3.7). Rather, the quartz fibers appeared to have become coated with the ETS material, especially at the intersections of fibers where liquid-looking material clearly wetted those intersections. Based on these observations, and the fact that QFF punches sent to Sunset Labs (Forest Grove, OR) revealed that 97% of the carbon in the ETS was organic (only 3% elemental carbon could be detected), we conclude that the partitioning mechanism for ETS involves

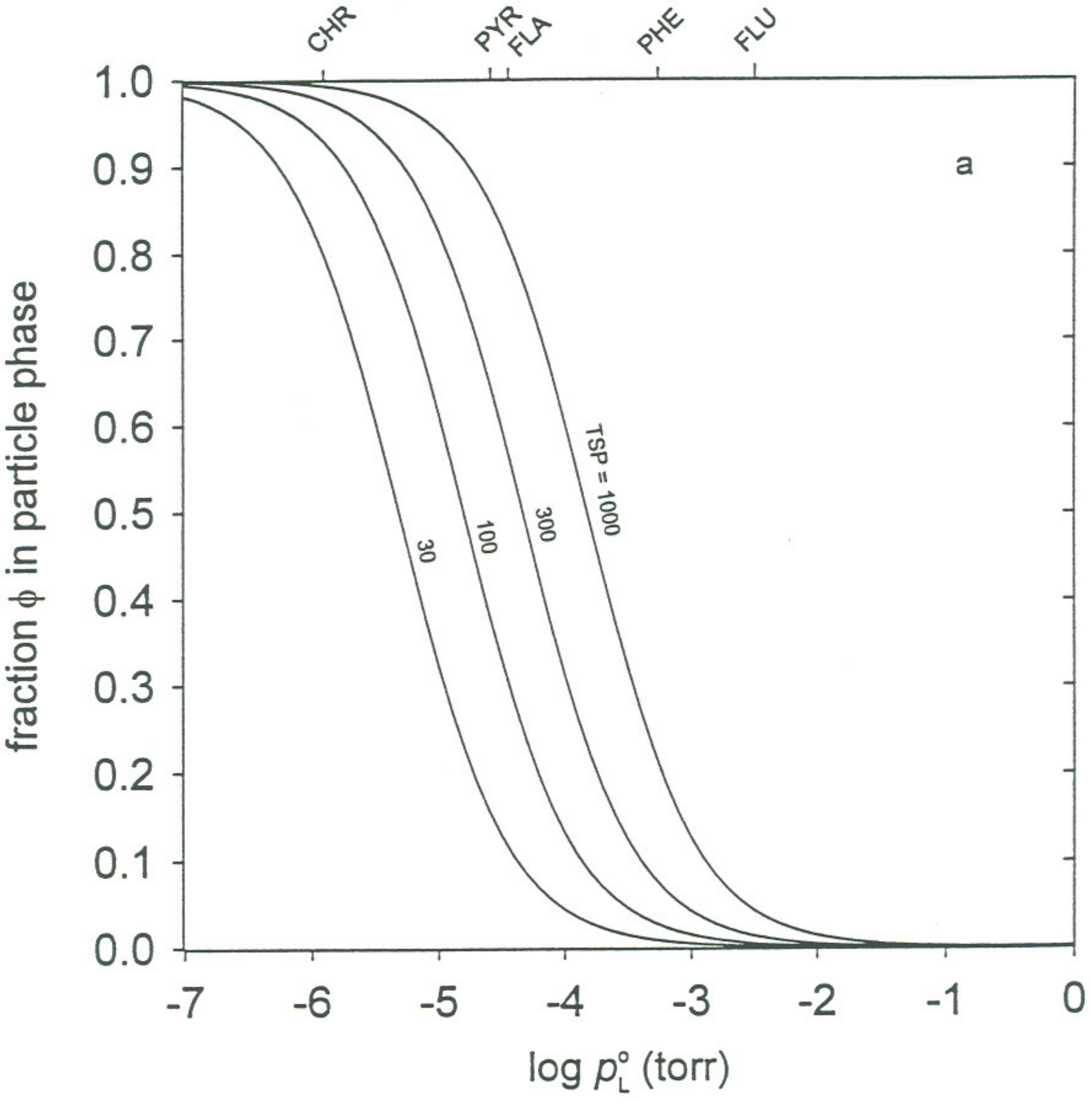

Figure 3.5a Calculated values of ϕ as a function of log p_L° and TSP at 20 °C for PAHs at 20 °C. CHR = chrysene; PRY = pyrene; FLA = fluoranthene; PHE = phenantheren; FLU = fluorene.

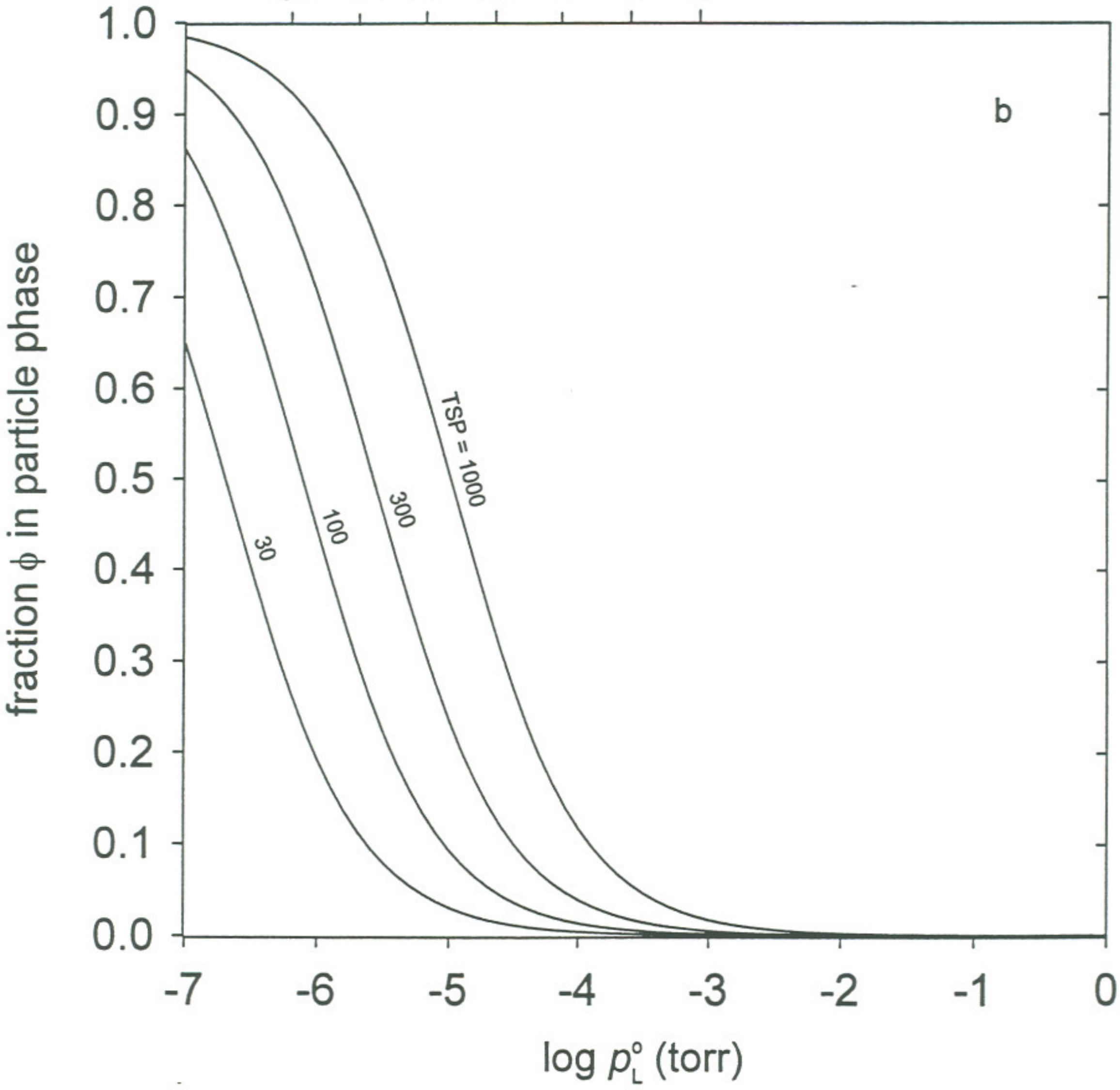

Figure 3.5b Calculated values of ϕ as a function of log p_L^o and TSP at 20 °C for *n*-alkanes at 20 °C.

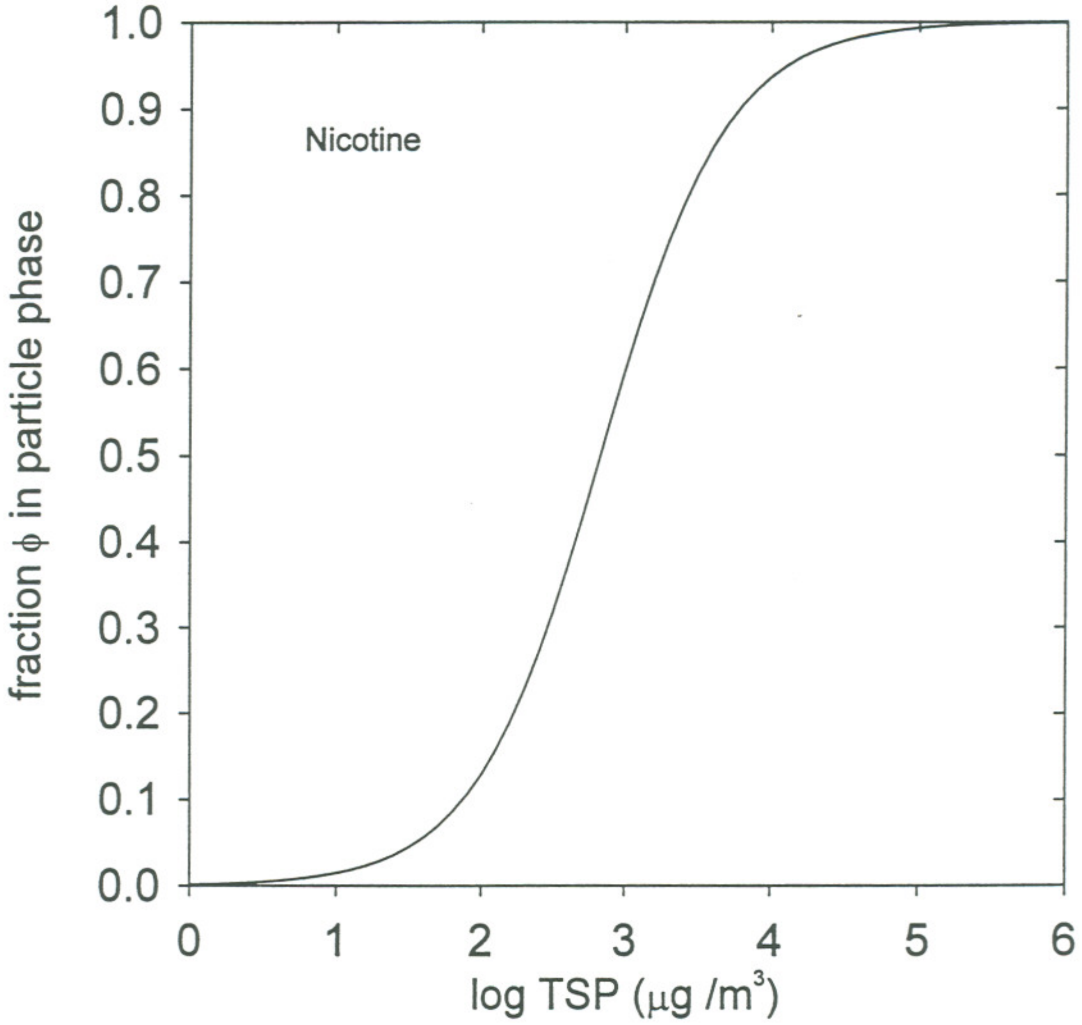

Figure 3.6 Calculated values of ϕ vs. log TSP for equilibrium partitioning of nicotine to ETS at 20 °C.

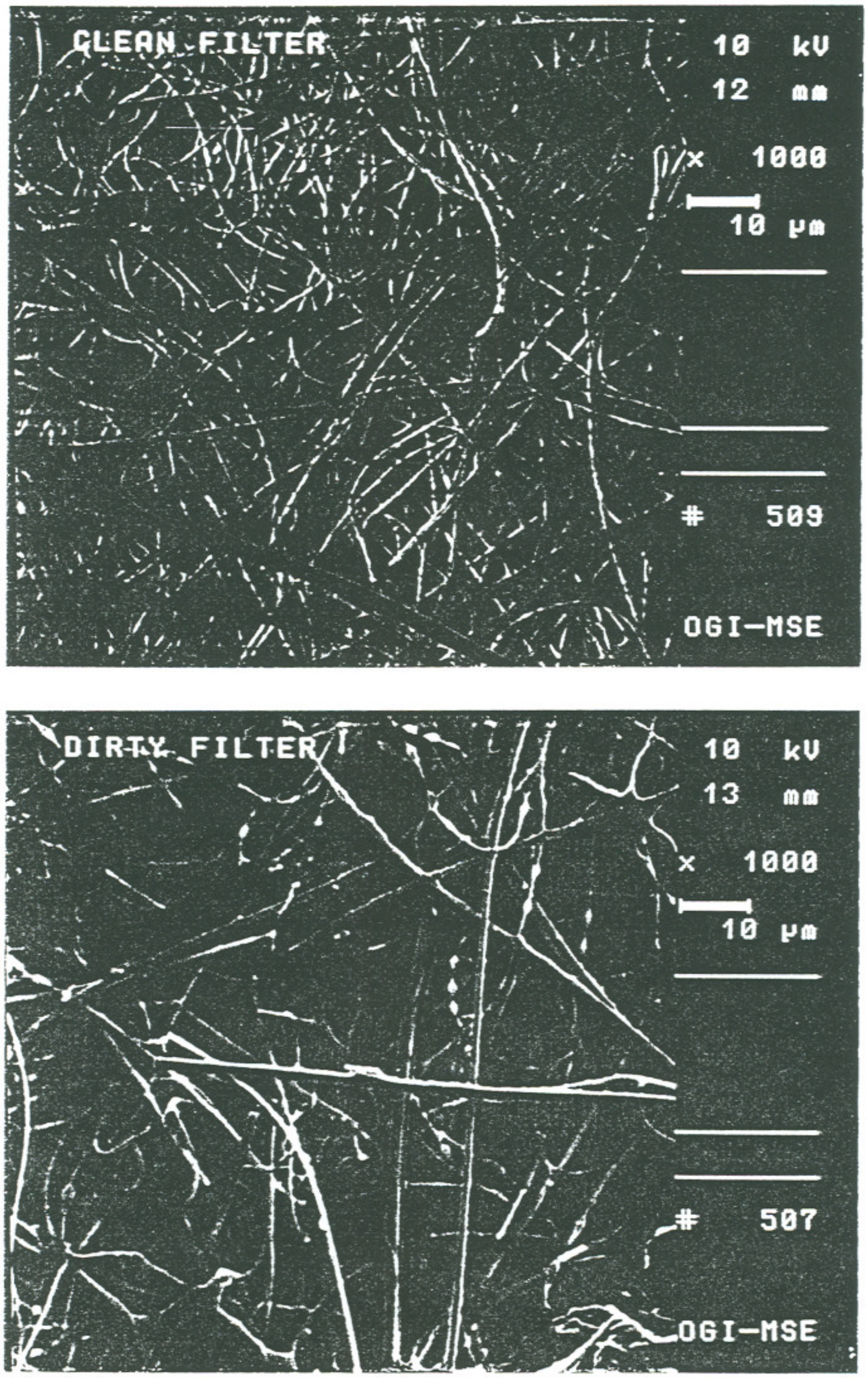

Figure 3.7 Scanning electron microscopy (SEM) image for QFFs: a) clean QFF surface; and b) QFF after sampling for ETS (496 μg/cm^2).

*ab*sorptive uptake into a liquid ETS phase.

For absorptive partitioning, Pankow (1994) has derived that

$$K_p = \frac{f_{om}\ 760\ RT}{MW_{om}\ \zeta\ p_L^o\ 10^6} \tag{3-12}$$

Eq (3-12) assumes that the absorptive phase is primarily organic in nature; f_{om} is the weight fraction of the TSP making up that primarily organic matter (om) phase. The parameter MW_{om} is the number-average molecular weight of the om phase, ζ is the mole-fraction-scale activity coefficient of the compound of interest in that phase, and R is the gas constant (8.2×10^{-5} m^3-atm/mol-K). Any presence of water in the om phase will contribute to the value of f_{om}, and will also affect MW_{om}. When $\zeta = 1$, then the partitioning is simple, gas/liquid, Raoult's Law partitioning.

Eq (3-12) together with the data in Figure 3.3 can be used to calculate ζ values in the ETS material for the compounds studied here. Since ETS particles are essentially totally liquid in nature, we take $f_{om} = 1$ for this material. A rough estimate for MW_{om} might be about 85. While the organic compounds present in the om phase are likely to have MW values much higher than 85, we have found that ETS can be ~15% by weight water. That much water has a large effect on the value of MW_{om}, and will also make the ETS phase at least somewhat polar. (For 15% by weight water, if the average MW for the organic compounds is 250, then $MW_{om} = 85$.) Using the correlation equations given in Figure 3.3 to calculate K_p values for $\log p_L^o = -3$, we obtain $\log K_p = -3.92$ and -4.77 for the PAH and *n*-alkane compound classes, respectively. These values yield $\zeta = 1.79$ and 12.66, respectively, for the two compound classes at that $\log p_L^o$ value. This trend as well as the specific values are consistent with what has been observed in polar organic solvents. Indeed, the activity coefficients for benzene and *n*-nonane in ethanol have been found to be 5.4 (23.6 °C) and 20.8 (27.9 °C) respectively (Tiegs *et al.*, 1986).

When considering adsorption-dominated partitioning, Storey and Pankow (1992) and Storey *et al.*(1995) have found it useful to normalize K_p values using the specific surface area of the particulate material. In the case of absorption-dominated partitioning, Odum *et al.*(1996) have proposed normalizing K_p by f_{om} to obtain an om-phase-based partition coefficient $K_{\mathrm{p,om}}$ according to:

$$K_{\mathrm{p,om}}\ (\mathrm{m}^3/\mu g) = \frac{K_{\mathrm{p}}}{f_{\mathrm{om}}} \tag{3-13}$$

For any given compound, using Eq (3-13) to normalize the K_{p} values for two different samples of absorbing atmospheric particulate material will yield similar $K_{\mathrm{p,om}}$ values insofar as the samples are characterized by: 1) similar MW_{om} values; and 2) similar ζ values for the compound of interest (Pankow, 1997). It seems possible that both assumptions might be approximately valid for ETS material and the organic material found in urban particulate material (UPM). Now, if $f_{\mathrm{om}} = 1.0$ for ETS, then $\log K_{\mathrm{p,om}} = \log K_{\mathrm{p}}$. These Log $K_{\mathrm{p,om}}$ values for the PAHs sorbing to ETS material are plotted *vs.* $\log p_{\mathrm{L}}^{\mathrm{o}}$ in Figure 3.8. We now compare the position of that line to what might be deduced for UPM.

Based on year-long data for 46 U.S. cities, Shah *et al.* (1986) report that the organic carbon fraction of urban TSP averages 0.084 (as carbon). Allowing for the presence of other elements (*e.g.*, hydrogen and oxygen) in the organic compounds as well as 10-15% water in the om phase, a reasonable estimate for typical UPM might be $f_{\mathrm{om}} = 0.1$. (Though UPM can contain significant water, unlike in ETS, we are assuming that most such water is present as a second, primarily inorganic phase.) For the Yamasaki *et al.* (1982) dataset for Osaka, Japan, for PAHs, it has been found that $\log K_{\mathrm{p}} = -0.98 \log p_{\mathrm{L}}^{\mathrm{o}} - 7.87$ (see Storey and Pankow, 1992). Using $f_{\mathrm{om}} = 0.1$, this equation becomes $\log K_{\mathrm{p,om}} = -0.98 \log p_{\mathrm{L}}^{\mathrm{o}} - 6.87$, which is plotted in Figure 3.8. Subject to the validity of the assumptions discussed above regarding MW_{om} and ζ, the good agreement between the ETS and UPM lines in this figure is supportive of the hypothesis that absorptive partitioning is the dominant mechanism for partitioning to UPM.

3.4.5 Effects of Acid/Base Equilibria on Gas/Particle Partitioning of Nicotine

Based on the two $\mathrm{p}K_{\mathrm{a}}$ values given in Figure 3.4, nicotine can exist as a diprotonated +2 form, a monoprotonated +1 form, and as a neutral "free-base" (fb) form. The presence of significant water in the ETS phase will allow both of the acid/base equilibria for nicotine to be well established. However, since ETS particles are not expected to have pH values approaching or below 3, only the mono-protonated and free-base forms are expected to be

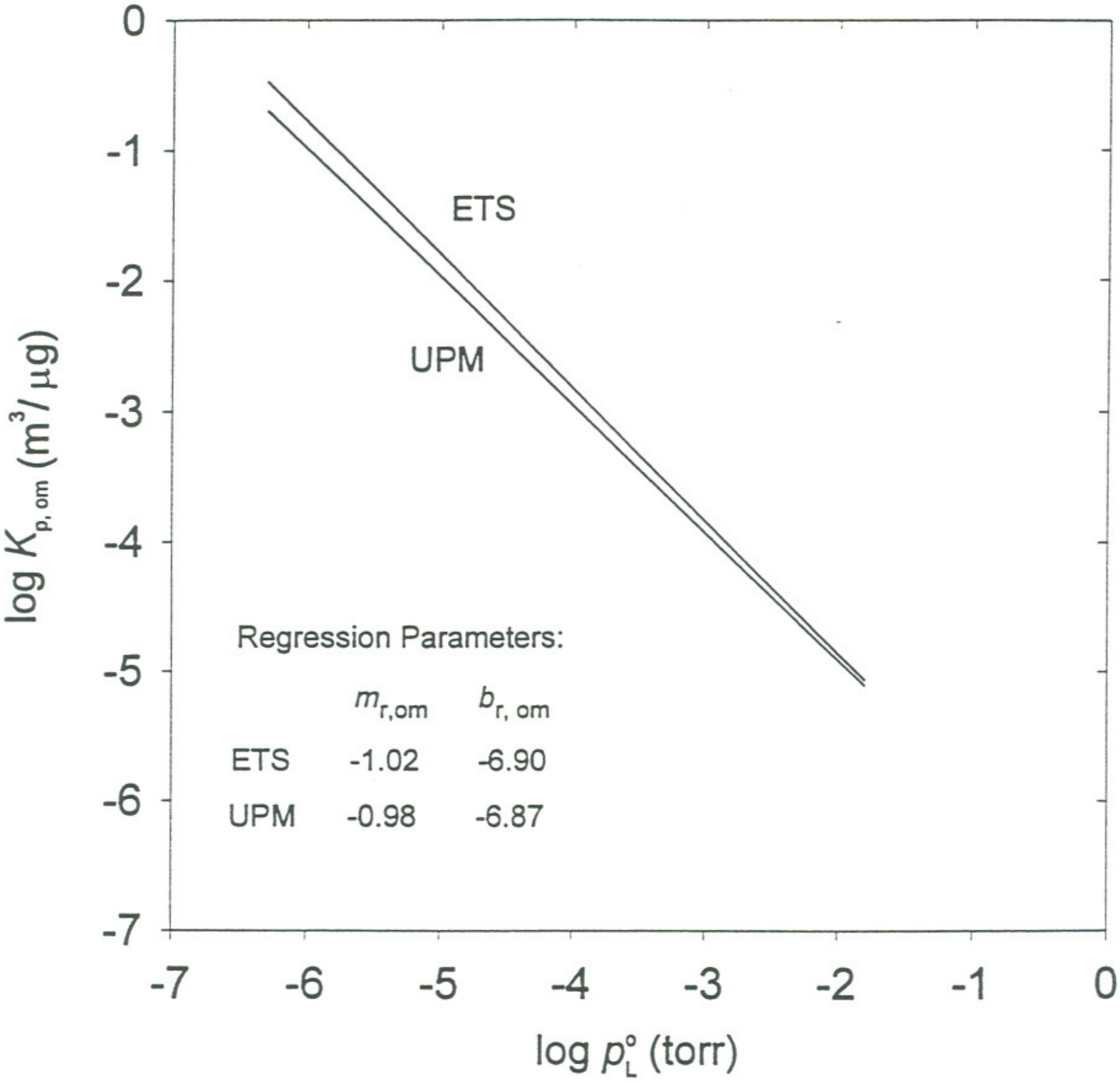

Figure 3.8 Comparison of log K_p vs. log p_L^o correlation parameters for PAHs sorbing to urban particulate material (UPM) (based on data of Yamasaki *et al.* (1982) and Storey and Pankow (1992)) with that to environmental tobacco smoke (ETS) particles at 20 °C.

important for the gas/particle partitioning of nicotine to ETS.

It is only the neutral, free base form of nicotine that is: 1) volatile from the ETS phase; 2) present in the gas phase; and 3) able to participate directly in partitioning equilibrium between the two phases. Let α^{fb} = fraction of particle-phase nicotine that is in the free base form. Thus,

$$\alpha^{fb} \times F = \text{ng/m}^3 \text{ of free-base nicotine in particle phase} \qquad \textbf{(3-14)}$$

When the pH of the ETS phase is significantly below 8 so that the monoprotonated species dominates the nicotine chemistry, then α^{fb} will be significantly less than 1.0; when pH > 8 so that the free base species dominates, then $\alpha^{fb} \approx 1$.

Since it is only the free-base form of nicotine that is volatile, the <u>intrinsic</u> K_p value for the partitioning of free-base nicotine between the gas and particle phases will be given by

$$K_p^{fb} = \frac{\alpha^{fb} \times F/TSP}{A} = \alpha^{fb} \times K_p \qquad \textbf{(3-15)}$$

Rearranging, we obtain

$$K_p = \frac{K_p^{fb}}{\alpha^{fb}} \qquad \textbf{(3-16)}$$

Eq (3-16) reveals that at acidic pH values, when $\alpha^{fb} \ll 1.0$, the protonation of nicotine enhances its ability to partition to the ETS phase. Eq (3-16) explains how the addition of ammonia-releasing chemicals to cigarette tobacco (Freedman, 1995) could represent an effort to decrease K_p for nicotine through the manipulation of α^{fb}. Indeed, adding a base such as ammonia to tobacco smoke will drive α^{fb} towards 1.0, thereby reducing K_p towards K_p^{fb}. This increases the fraction of the nicotine that is in the gas phase (*i.e.*, it increases $1-\phi$), and this might increase the absorption of the nicotine by a smoker. Under these conditions, the smoker can be said to be "free-basing" nicotine, with clear similarities to how cocaine is free-based when crack cocaine is smoked.

3.5 Acknowledgments

This work was supported in part by a grant from the U.S. Environmental Protection

Agency's Office of Exploratory Research (U.S. EPA/OER) under Grant R822312-01-0. We gratefully acknowledge the technical assistance of Lorne M. Isabelle and Wentai Luo in the design and analysis phases of the experimental work. We also appreciate the Columbia Empire Volleyball Association, Douglas B. Reeves, Andrea Pavlick, and Clinton Church for assistance in the sampling. Finally, the authors would like to thank Jay R Odum for several helpful conversations during the finalization of this work.

3.6 Abbreviations

ANT = anthracene; C_{16}= hexadecane; C_{17}= heptadecane; C_{18}= octadecane; C_{19}= nonadecane, C_{20} = eicosane; C_{21} = heneicosane; C_{22}= docosane; CZ = carbazole; CHR = chrysene; FLA = fluoranthene; FLU = fluorene; IQ = isoquinoline; PHE = phenanthrene; PYR = pyrene; QL = quinoline.

3.7 Literature Cited

Arey J., Zielinska B., Atkinson R., and Winer A. M. (1987) Polycyclic aromatic hydrocarbons and nitroarene concentration in ambient air during a wintertime high NO2 episode in the Los Angeles Basin. *Environ. Sci. Technol.* **21**, 1437-1444.

Boulik T., Fried V., and Hala E. (1984) *The Vapor Pressure of Pure Substances: Selected Values of the Temperature Dependence of the Vapor Pressure of Some Pure Substances in the Normal and Low Pressure Region*, 2nd Ed; Elsevier Scientific Pub. Co.: New York.

Das A., Frenkel M., Gadalla N. A. M., Kudchadker S., Marsh K. N., Rodger A. S., and Wilhoit R. C. (1993) Thermodynamic and thermophysical properties of organic nitrogen compounds. Part II. 1- and 2-butanamine, 2-methyl-1-propanamine, 2-methyl-2-propanamine, pyrrole, 1-, 2-, and 3-methylpyrrole, pyridine, 2-, 3-, and 4-methylpyridine, pyrrolidine, piperidine, indole, quinoline, isoquinoline, acridine, carbazole, phenanthridine, 1-and 2-naphthalenamine, and 9-methylcarbazole *J. Phys. Chem. Ref. Data* **22**, 659-782.

Freedman A. M. (1995) Tobacco firm shows how ammonia spurs delivery of nicotine. *Wall Street Journal.* A1, Oct. 18.

Guerin M. R. and Jenkins R. A. (1984) Analytical chemical methods for determination of environmental tobacco smoke constituents. *Eur J. Resp. Dis. Suppl.* **133**, 33-46.

Katritzky A. R. and Rees C. W. (1984) *Comprehensive Heterocyclic Chemistry,* vol. IV; Pergamon Press: New York.

Lewtas J., Goto S., Williams K., Chuang J. C., Petersen B. A., and Wilson, N. K. (1987) The mutagenicity of indoor air particles in a residential pilot field study: application and evaluation of new methodologies. *Atmos. Environ.* **21**, 443-449.

Morie G. P.(1972) Fraction of protonated and unprotonated nicotine in tobacco smoke at various pH values. *Tobacco Sci.* **16**, 167.

Pankow J. F. (1987) Review and comparative analysis of the theories on partitioning between the gas and aerosol particulate phases in the atmosphere. *Atmos. Environ.* **21**, 2275-2283.

Pankow J. F. (1991) Common y-intercept and single compound regression of gas-particle partitioning data vs 1/T. *Atmos. Environ.* **25A**, 2229-2239.

Pankow J. F (1992) Application of common y-intercept regression parameters for log K_p vs 1/T for predicting gas-particle partitioning in the urban environment. *Atmos. Environ.* **26A**, 2489-2497.

Pankow J. F. (1994) An absorption model of gas/particle partitioning of organic compounds in the atmosphere. *Atmos. Environ.* **28**, 185-188.

Pankow J. F. In *Gas and Particle Partitioning Measurements of Atmospheric Organic Compound*; Lane D.A. Ed; Gordon and Breach:Newark, in press.

Pankow J. F., Isabelle L. M., Buchholz D. A., Luo W., and Reeves B. D. (1994) Gas/particle partitioning of polycyclic aromatic hydrocarbons and alkanes to environmental tobacco smoke. *Environ. Sci. Technol.* **28**, 363-365.

Rounds S.A., Tiffany B. A., and Pankow J. F. (1993) Description of gas/particle sorption kinetics with an intraparticle diffusion model: Desorption experiments. *Environ. Sci. Technol.* **27**, 366-377.

Shah J. J., Johnson R. L., Heyerdahl E. K., and Huntzicker J. J. (1986) Carbonaceous aerosol at urban and rural sites in the United State. *J. Air Pollut. Control Assoc.* **36**, 254-257.

Storey J. M. E. and Pankow J. F. (1992) Gas-particle partitioning of semi-volatile organic compounds to model atmospheric particulate materials - Part I. Sorption to graphite, sodium chloride, alumina, and silica particles under low humidity conditions. *Atmos. Environ.* **26A**, 435-443.

Storey J. M. E., Luo W., Isabelle L. M., and Pankow J. F. (1995) Gas/solid partitioning of semivolatile organic compounds to model atmospheric solid surfaces as a function of relative humidity. Part 1. Clean Quartz. *Environ. Sci. Technol.* **29**, 2420-2428.

Tiegs D., Gmehling J., Medina A., Soares M., Bastos J., Alessi P., and Kikic I. (1986) *Activity Coefficients at Infinite Dilution.* Vol. IX, Part 1 & Part 2; DECHEMA: Germany.

Timmermans, J. (1950) *Physico-chemical Constants of Pure Organic Compounds*; Elsevier Pub. Co.: New York.

Van de Rostyne C. and Prausnitz J. M. (1980) Vapor pressure of some nitrogen-containing, coal-derived liquids. *J. Chem. Eng. Data* **25**, 1-3.

Windholz M. (1976) *The Merck Index,* 9th ed.; Merck & Co. Inc: New Jersey.

Yamasaki H., Kuwata K., and Miyamoto K. (1982) Effect of temperature on aspects of airborne polycyclic aromatic hydrocarbons. *Environ. Sci. Technol.* **16**, 189-194.

Reprinted with permission from Environmental Science and Technology, in press.

CHAPTER 4

GAS/PARTICLE PARTITIONING OF SEMI-VOLATILE ORGANIC COMPOUNDS TO MODEL INORGANIC, MODEL ORGANIC, AND AMBIENT SMOG AEROSOL

4.1 Abstract

Gas/particle (G/P) partitioning is an important process that affects the deposition, chemical reactions, long-range transport, and impact on human and ecosystem health of atmospheric semi-volatile organic compounds (SOCs). Gas/particle partitioning coefficients (K_p) were measured in an outdoor chamber for a group of polynuclear aromatic hydrocarbons (PAHs) and *n*-alkanes sorbing to three types of model aerosol materials: solid ammonium sulfate, liquid dioctyl-phthalate (DOP), and secondary organic aerosol (SOA) generated from the photooxidation of whole gasoline vapor. K_p values were also measured for ambient *n*-alkanes sorbing to urban particulate material (UPM) during summer smog episodes in the Los Angeles metropolitan area. Based on the K_p values obtained for the aerosols studied here, for environmental tobacco smoke (ETS), and for a quartz surface, we conclude that G/P partitioning of SOCs to UPM during summer smog episodes is dominated by absorption into the organic fraction in the aerosol. Comparisons of the partitioning of SOCs to three different types of aerosols demonstrate that: 1) DOP aerosol may be a good surrogate for ambient aerosol that consists mainly of organic compounds from primary emissions; 2) ETS particles may be a good surrogate for SOA; and 3) the sorption properties of ambient smog aerosol and the chamber-generated SOA from gasoline are very similar. The similarities observed between ambient smog aerosol and chamber-generated SOA from gasoline support the use of literature SOA yield data from smog chamber studies to predict the extent of SOA

formation during summer midday smog episodes.

4.2 Introduction

Gas/particle (G/P) partitioning is an important process that affects the deposition, chemical reactions, long-range transport, and human and ecosystem health effects of atmospheric semi-volatile organic compounds (SOCs). Much of the thinking about the G/P partitioning of SOCs has involved the assumption that the partitioning process involves simple physical adsorption (Junge, 1977; Yamasaki *et al.*, 1982; Pankow, 1987). While this sorption mechanism will be important when atmospheric particulate material is comprised solely of mineral materials, urban particulate material (UPM) generally contains a significant amount of amorphous organic carbon (Gray *et al.*, 1984; Shah *et al.*, 1986). Thus, it seems likely that absorptive partitioning must be playing at least some role in urban air, and also in air affected by urban sources.

An equation that has been used successfully to parameterize G/P partitioning is (Yamasaki *et al.*, 1982; Pankow, 1991; Pankow 1992)

$$K_p = \frac{F/\mathrm{TSP}}{A} \qquad \textbf{(4-1)}$$

where K_p (m^3/μg) is the G/P partitioning coefficient for a given compound, F and A are the P- and G-phase concentrations (ng/m^3) of the compound, respectively, and TSP (μg/m^3) is the total suspended particulate material concentration. When both *ad*sorptive and *ab*sorptive partitioning are operative, K_p can be parameterized as (Pankow, 1994)

$$K_p = \frac{C_1 + C_2}{p_L^\circ} \qquad \textbf{(4-2)}$$

where p_L° (torr) is the pure-compound subcooled liquid vapor pressure. The terms C_1 / p_L° and C_2 / p_L° represent the adsorptive and absorptive contributions to K_p, respectively. Detailed theoretical expressions for C_1 and C_2 are given by Pankow (1994). Within a given compound class (*e.g.* polycyclic aromatic hydrocarbons (PAHs), *n*-alkanes, etc.), C_1 and C_2 will be only weakly compound-dependent, and log (*F*/TSP) /*A* value will tend to be correlated with log p_L° according to

$$\log K_p = m_r \log p_L^\circ + b_r \qquad \textbf{(4-3)}$$

where m_r is usually near -1.

The temperature dependence of K_p for a given compound sorbing to a given type of atmospheric particulate material can be expressed as (Yamasaki *et al.*, 1982; Pankow, 1994)

$$\log K_p = \frac{m_p}{T} + b_p \qquad \textbf{(4-4)}$$

Most of the temperature dependence explicitly present in equation 4 is implicitly present in equation 3 due to the the temperature-dependence of p_L^o.

Based on a comparison of organic matter-phase-normalized K_p values that were measured for PAHs partitioning to environmental tobacco smoke (ETS) and estimated for partitioning to UPM, Liang and Pankow (1996) have suggested that absorption may frequently be the dominant G/P partitioning mechanism for SOCs in urban air. In addition, Odum *et al.* (1996) recently showed from smog chamber studies that the condensation of the photooxidation products which form secondary organic aerosol (SOA) is very well described by an absorptive G/P partitioning model. In this chapter we discuss smog chamber experiments that were performed to examine the partitioning of two classes of SOCs (PAHs and *n*-alkanes) to three different model aerosol materials: solid ammonium sulfate; non-polar, liquid dioctyl-phthalate (DOP); and polar, amorphous SOA generated from the photooxidation of whole gasoline vapor. G/P partitioning was also measured for UPM collected during two heavy smog episodes in the Los Angeles metropolitan area at a sampling site in the City of Pasadena. The UPM data were then compared to the data for model aerosols to obtain information about both the operative G/P partitioning mechanism during summer smog episodes and the nature of UPM.

4.3 Experimental Section

4.3.1 Smog Chamber Experiments

Five experiments were conducted in the Caltech 60-m^3 flexible Teflon smog chamber described in detail elsewhere (Pandis *et al.*, 1991; Wang *et al.*, 1992; Odum *et al.*, 1996). Prior to each experiment, the chamber was flushed with four to five bag volumes of purified compressed air while being allowed to warm to 31-38 °C under sunlight for at least 12 h. The purified compressed air was obtained by passing laboratory compressed air through four consecutive packed sorbent beds which contained (in order) Purafil, Drierite, 13X molecular sieve, and activated charcoal. After purification, but before entering the chamber, the air was rehumidified to a relative humidity (RH) of approximately 10% for the chamber temperature of 31-36 °C using distilled/deionized water. The warm temperatures prevented the use of higher RH values because such use would have led to condensation in the sample lines between the chamber and the instrumentation.

Solid, inorganic aerosol was generated by atomizing an aqueous solution of 5 g/L ammonium sulfate using a stainless steel, constant rate atomizer (Odum *et al.*, 1996). Before entering the Teflon chamber, the aerosol was passed via heated copper tubing first through a diffusional dryer packed with indicating silica gel, then through a ^{85}Kr charge neutralizer. The initial number concentration in the chamber was $\sim 7 \times 10^4/\text{cm}^3$. The geometric mean diameter was 111 ± 1.5 nm.

Liquid DOP aerosol was generated by atomizing a 0.005 % by weight solution of DOP in pentane using a stainless steel, constant rate atomizer. Before entering the Teflon chamber, the DOP aerosol was passed through a diffusional dryer packed with activated charcoal to remove pentane, then through a ^{85}Kr charge neutralizer. The initial number concentration in the chamber was $\sim 10^4/\text{cm}^3$. The geometric mean diameter was 480 ± 1.6 nm.

Amorphous SOA was generated by first adding seed $(NH_4)_2SO_{4(s)}$ particles at a concentration in the chamber of $10^4/\text{cm}^3$ (total aerosol volume is $\sim 20\ \mu\text{m}^3/\text{cm}^3$). These particles served as condensation nuclei. The chamber was then covered with a black tarpaulin so that photochemical reactions would not begin until all reactants had been added and given time to become well mixed. This was followed by injections of propene, NO, and NO_2 into the chamber to obtain initial concentrations of 300, 640, and 340 ppbV, respectively. These chemicals led to the generation of sufficient hydroxyl radicals and ozone to sustain the subsequent photochemical reactions. SOA was generated using "Industry-Average" gasoline obtained from the Auto/Oil Air Quality Research Improvement

Program (Hochhauser *et al.*, 1991). 700 μL of the gasoline was completely volatilized in a glass dilution bulb that was gently heated while being purged with purified lab air that was in turn directed into the chamber through Teflon lines. The initial total carbon concentration in the chamber was 9000 $\mu g/m^3$. Convective mixing, advective mixing caused by wind agitation of the chamber walls, and diffusion were allowed to mix the chamber for 20 min. The tarpaulin was then removed to initiate the photooxidation. After 2 h, the photochemical reactions were halted by covering the chamber again with the tarpaulin. Approximately 500-600 $\mu g/m^3$ of SOA (total aerosol volume of 500-600 um^3/cm^3 and geometric mean diameter of 520 ± 1.2 nm) and more than 1 ppm of ozone were generated during this period. This ozone was titrated down to a mixing ratio of 150 ppb by slowly vaporizing 330 μL of liquid tetramethylethylene into the chamber. This precaution was taken in order to avoid excessive destruction of the SOC model compounds, which were added next. Most of the SOCs were added by injecting ~300 μL of a 250 ng/μL per component mixture of PAHs and *n*-alkanes in methylene chloride through a hot (300 °C) injector located at the base of the chamber. Two *n*-alkanes (C_{16} and C_{17}) were added to the chamber by injecting individual 50 μL aliquots of these compounds at ~10^4 ng/μL in methylene chloride.

Sampling of the SOCs was commenced approximately one hour after their injection into the chamber. Available information on G/P partitioning kinetics (Kamens *et al.*, 1995) suggests that this was long enough to allow G/P equilibrium to be reached . G- and P-phase organic compounds were collected through a copper tube (i.d. = 0.5 in) which extended ~30 cm into the chamber. Sampling event durations and conditions are listed in Table 4.1. The sampler utilized a 102 mm diameter glass fiber filter (GFF) (with an identical back-up filter) to collect P-phase organic compounds. The data obtained with the backup filter were used to correct for the adsorption of G-phase SOCs to the front filter as described for quartz filters by Hart and Pankow (1994). (On average, the mass of a compound of interest found on the backup QFF was ~15% of that on the front QFF; no compound dependence was observed in this number.) Following the filters, two parallel trains were used to collect G-phase compounds. One train employed two sequential adsorption/thermal desorption (ATD) cartridges containing ~1 g each of Tenax-GC to collect the more volatile compounds. The

Table 4.1. Sampling Data for Collection of Ambient and Smog Chamber Aerosols.

Event	Date	Sampling period (min)	Temperature (°C)	TSP ($\mu g/m^3$)
Smog ambient (low-vol)	08/01/96	235	37	114
Smog ambient (low-vol)	08/14/96	240	37	106
Smog ambient (high-vol)	08/12/96	240	37	104
Gasoline SOA - chamber	08/02/96	30	31	540
Gasoline SOA - chamber	08/07/96	65	31	394
DOP - chamber	08/05/96	60	36	210
DOP - chamber	08/14/96	60	36	460
$(NH_4)_2SO_{4(s)}$ - chamber	08/09/96	90	32	109

second train employed two sequential 198 cm^3 polyurethane foam (PUF) plugs to collect the less volatile compounds. The GFFs were pre-cleaned by baking at 370 °C overnight, then held at room temperature in a desiccator containing indicating silica gel prior to sampling. The PUF plugs were Soxhlet-extracted with methylene chloride for 24 h before use. Each ATD cartridge was cleaned by pumping one liter of 1:1 hexane:acetone through the cartridge at 2 mL/min, purged with ultra-pure helium at 50 °C for 20 min to remove the solvents, then conditioned at 300 °C for 2 h with a 1 mL/min flow of ultra-pure helium. During sampling, the flow rates were: filters, 70.8; Tenax-GC train, 0.324; and PUF train, 70.8 L/min, respectively. The face velocity for the filters was 18.5 cm/s.

The TSP was measured for each experiment by collecting particles with a 47 mm Teflon-coated GFF (tc-GFF) at a flow rate of 30 L/min for 20 min. Before use, each tc-GFF was Soxhlet-extracted with methylene chloride for 12 h and air dried at room temperature, then kept in a petri dish prior to sampling. The tc-GFFs were weighed both before and after sampling. In each case, prior to weighing, the tc-GFFs were conditioned for 1 h at 23 °C and 40 % RH.

Complete aerosol number and size distribution measurements were recorded for every smog chamber experiment with a one-minute sampling frequency using a TSI (St. Paul, MN) Model 3071 cylindrical scanning electrical mobility spectrometer (SEMS) equipped with a TSI Model 3025 condensation nuclei counter. This equipment was housed in an enclosed cart maintained at 25 °C and located directly adjacent to the chamber. The SEMS system was operated with sheath and excess flows of 2.5 L/min, and inlet and classified aerosol flows of 0.25 L/min to allow for the measurement of aerosol size distributions in the 30-850 nm range. The aerosol size distribution data were used to provide independent measures of the TSP values.

4.3.2 Ambient Aerosol Sampling

Low-volume sampling was performed on the roof of Keck Laboratory during two separate smog episodes. The same equipment and filter type employed to sample the smog chamber were used. The sampling period for both episodes was 12 pm to 4 pm. The average RH for the two days was 42%. Other sampling information is given in Table 4.1. The GFFs were weighed before and after sampling as with the tc-GFFs in the chamber experiments.

A single high-volume aerosol sample for carbon analysis and specific surface area measurement was taken at the same location from 12 pm to 4 pm during a third smog episode. An 8 × 10 inch quartz fiber filter (QFF) was used to collect particles at a flow rate of 1.4 m^3/min. The QFF was pre-cleaned by baking overnight at 370 °C, then held at room temperature in a desiccator containing indicating silica gel until used. After sampling, a portion of the QFF was analyzed for inorganic carbon (IC), elemental carbon (EC), and organic carbon (OC) by Sunset Laboratory (Forest Grove, OR). Total carbon (TC) was taken to be the sum IC + EC + OC. Results for carbon analysis are given in Table 4.2. Another portion of the QFF was sent to Micromeritics (Norcross, GA) for specific surface area measurements. The remaining QFF was used for elemental analyses in our lab (see Chapter Five for details).

Table 4.2 Elemental Carbon (EC), Organic carbon (OC), and Total Carbon Content for Los Angles Ambient Smog Aerosol[a]

	EC (ug/cm^2)	OC (ug/cm^2)	TC (ug/cm^2)	OC/TC (%)	OC/EC
Blank QFF	-0.07 ± 0.20	0.22 ± 0.21	0.15 ± 0.31		
Sample QFF	2.14 ± 0.31	14.28 ± 0.91	16.42 ± 1.12	87	6.7

[a]obtained by Sunset Laboratory (Forest Grove, OR)

4.3.3 Analytical Procedures

After sampling, each ATD cartridge was capped, sealed in a screw cap culture tube, and kept at -25 °C until analyzed. Each ATD cartridge was analyzed by thermal desorption with capillary GC/MS as described elsewhere (Rounds *et al.*, 1993). Immediately after sampling, each PUF plug and each GFF was spiked with surrogate standard compounds (acenaphthene-d_{10}, phenanthrene-d_{10}, and chrysene-d_{12}), then Soxhlet-extracted overnight with 400 and 250 mL, respectively, of methylene chloride. PUF and GFF blanks were also extracted for each experiment. The extracts were concentrated down to ~30 mL by rotary evaporation, then kept at -25 °C until analyzed. Prior to GC/MS analysis, each extract was blown down to ~100 µL with N_2, weighed, and then spiked with internal standard compounds (naphthalene-d_8, anthracene-d_{10}, and perylene-d_{12}). Each extract was analyzed using GC/MS with a splitless injection of 1 µL. A 30-m, 0.32-mm-i.d., 0.25-µm film thickness DB-5 capillary column (J&W Scientific, Folsom) was used. The GC temperature program used was: hold at 50 °C for 2 min, 50-100 °C at 25 °C/min, 100-300 °C at 10 °C/min, then hold at 300 °C for 2 min. On average, recoveries for acenaphthene-d_{10}, phenanthrene-d_{10}, and chrysene-d_{12} were 93.3 ± 6.1, 93.7 ± 3.8, and 96.4 ± 5.4, respectively.

4.4 Results and Discussion

4.4.1 Adsorptive Partitioning to $(NH_4)_2SO_{4(s)}$ Aerosol

If adsorption is the dominant partitioning mechanism, a surface-area-normalized constant $K_{p,s}$ can be defined as (Storey *et al.*, 1995)

$$K_{p,s}\ (\mathrm{m}^3/\mathrm{m}^2) = \frac{K_p}{a_{TSP}\,10^{-6}\mathrm{g}/\mu\mathrm{g}} \tag{4-5}$$

where a_{TSP} (m^2/g) is the specific surface area of the adsorbing solid. In this case, equation (4-3) can be re-written as

$$\log K_{p,s} = m_{r,s} \log p_L^\circ + b_{r,s} \tag{4-6}$$

where $m_{r,s} = m_r$ and $b_{r,s} = b_r - \log(a_{TSP}/10^6)$.

Table 4.3 gives the log K_p values for the PAHs and *n*-alkanes for sorption to $(NH_4)_2SO_{4(s)}$ aerosol. Table 4.4 provides the corresponding m_r and b_r values. Log $K_{p,s}$ values were calculated by normalizing the measured K_p values with a_{TSP} according to equation (4-5), and are listed in Table 4.3. The value of a_{TSP} was estimated to be 17.5 m^2/g by assuming that the $(NH_4)_2SO_{4(s)}$ particles were spherical with a density of 1.77 g/cm^3.

It is well known that the partitioning of organic compounds to inorganic surfaces is RH-dependent (Goss, 1992; Storey *et al.*, 1995), and that the sorption becomes stronger as the RH decreases. Since the partitioning experiments performed in the chamber with $(NH_4)_2SO_{4(s)}$ were conducted at the relatively low RH of 10%, and since the ambient smog *n*-alkane data were collected at RH = 42%, extrapolations of the $(NH_4)_2SO_{4(s)}$ log $K_{p,s}$ values to RH = 42% were necessary to permit a comparison of the two data sets. Because of the presence of sorbed water on inorganic surfaces even at relatively low RH values, the adsorption of non-polar organic gases has been found to be fundamentally similar for a range of inorganic surfaces including quartz, silica, and clay (Goss, 1994). We will therefore assume that adsorption to $(NH_4)_2SO_{4(s)}$ particle surfaces is similar to adsorption to quartz surfaces. Storey *et al.* (1995) have provided a detailed examination of the RH-dependence of the adsorption of a range of PAHs and *n*-alkanes to a quartz surface. The needed compound-specific extrapolations were therefore based on the 30% to 70% RH data of Storey *et al.* (1995). It was assumed that: 1) only $b_{r,s}$ is a function of RH; and 2) the change

Table 4. 3 Measured Log K_p and Log $K_{p,s}$ values for $(NH_4)_2SO_{4(s)}$ and Ambient Smog Aerosols

Compound	log p_L^o (torr)[a]	log K_p ($m^3/\mu g$)	log $K_{p,s}$ (10% RH)	log $K_{p,s}$ (42% RH)
		$(NH_4)_2SO_{4(s)}$ - Chamber (32 °C and 10% RH)		
Heptadecane C_{17}	-3.07	-4.48	0.28	-0.13
Octadecane C_{18}	-3.57	-4.06	0.70	0.28
Nonadecane C_{19}	-4.06	-4.04	0.72	0.31
Eicosane C_{20}	-4.55	-3.58	1.18	0.76
Heneicosane C_{21}	-5.04	-2.76	2.00	1.59
Docosane C_{22}	-5.53	-2.30	2.46	2.04
Tetracosane C_{24}	-6.51	-1.23	3.53	3.11
Fluorene	-1.91	-5.48	-0.72	-1.53
Phenanthrene	-2.74	-4.46	0.30	-0.51
Anthracene	-2.76	-4.52	0.24	-0.56
Fluoranthene	-3.87	-3.31	1.45	0.65
Pyrene	-4.05	-3.27	1.49	0.68
		Ambient Smog[b]- Ambient (37 °C and 42% RH)		
Octadecane C_{18}	-3.31	-5.07		0.63
Eicosane C_{20}	-4.23	-4.36		1.34
Heneicosane C_{21}	-4.71	-4.01		1.69
Docosane C_{22}	-5.18	-3.55		2.15
Tetracosane C_{24}	-6.13	-2.11		3.59

[a] log p_L^o values are temperature corrected.

[b] log K_p values are the averages for the 08/01/96 and 08/14/96 experiments.

Table 4.4 Summary of Slopes (m_r) and Intercepts (b_r) for Log K_p vs. Log p_L^o Correlation Lines

Aerosol Type	m_r	b_r
	PAHs	
$(NH_4)_2SO_{4(s)}$ (t = 32 °C and RH = 10%)	-1.04	-7.41
DOP (t = 36 °C and RH = 10%)	-1.09	-7.02
Gasoline SOA (t = 31 °C and RH = 10%)	-1.05	-7.24
ETS[a] (t = 20 °C and RH = 60%)	-1.02	-6.90
	***n*-Alkanes**	
$(NH_4)_2SO_{4(s)}$ (t = 32 °C and RH = 10%)	-0.96	-7.66
DOP (t = 36 °C and and RH = 10%)	-0.98	-7.15
Gasoline SOA (t = 31 °C and RH = 10%)	-1.09	-8.37
Ambient Smog (t = 37 °C and RH = 42%)	-1.03	-8.68
ETS[a] (t = 20 °C and RH = 60%)	-0.89	-7.44

[a] data are from Liang and Pankow (1996).

in $b_{r,s}$ with RH for $(NH_4)_2SO_{4(s)}$ is similar to that for quartz. The extrapolated compound-dependent increases in log $K_{p,s}$ for quartz between RH = 42% and RH = 10% were therefore subtracted from the values for $(NH_4)_2SO_{4(s)}$ obtained in this study. The extrapolated log $K_{p,s}$ values are given in Table 4.3 and plotted in Figure 4.1. The a_{TSP}-normalized ambient smog *n*-alkane data are also plotted in Figure 4.1. Sheffield and Pankow (1994) have reported that $a_{TSP} = 2.1$ m^2/g for UPM collected during the summer in Portland, OR. Corn *et al.* (1971) reported that $a_{TSP} = 1.9$ m^2/g for UPM collected during the summer in Pittsburgh, PA. These values are consistent with measurements made in this study. The value of a_{TSP} for the ambient smog sample in this study was taken to be 2.0 m^2/g.

Normalizing ambient smog aerosol log K_p values by an estimate of a_{TSP} allows one to test whether adsorption is an important partitioning mechanism for UPM. As seen in Figure 4.1, the calculated log $K_{p,s}$ values for the *n*-alkanes sorbing to the ambient smog samples at RH = 42% are much larger than those for sorption to $(NH_4)_2SO_{4(s)}$ aerosol as extrapolated to RH = 42%. (A similar comparison for the PAHs is not possible because the PAH concentrations were too low to be quantified accurately with the methods used.) Considering that the inorganic portion of the midday smog aerosol was probably well represented by $(NH_4)_2SO_{4(s)}$, it seems that adsorption to inorganic surfaces probably cannot account for the sorption of the *n*-alkanes observed in the ambient samples. This suggests that adsorption is not the operative mechanism controlling the partitioning of SOCs to ambient smog aerosol, and that the log $K_{p,s}$ values calculated for the *n*-alkanes sorbing to ambient smog are not physically meaningful quantities.

4.4.2 Absorptive Partitioning to Organic Aerosols

When absorption into a liquid (or at least amorphous) organic matter (om) phase is the dominant sorption mechanism, an om-phase-normalized constant $K_{p,om}$ can be defined as (Odum *et al.*, 1996; Pankow, in press)

$$K_{p,om} = \frac{K_p}{f_{om}} \qquad \textbf{(4-7)}$$

where f_{om} is the weight fraction of the TSP that comprises the om phase. In this case,

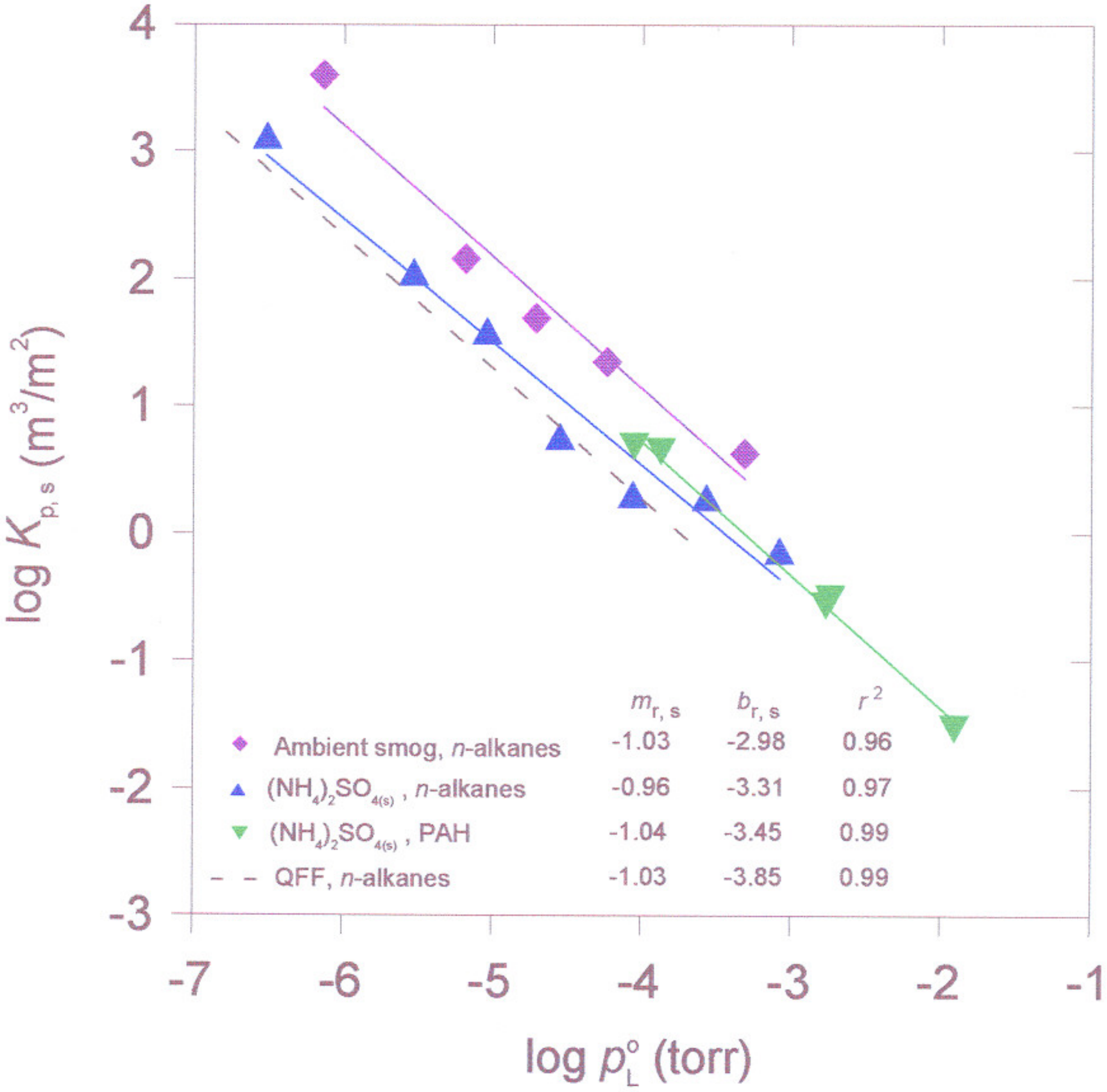

Figure 4.1 Comparison of log $K_{p,s}$ vs. log p_L° correlation among different types of aerosols at RH = 42%. QFF (quartz fiber filter) data are from Storey *et al.* (*1995*).

equation (4-3) can be re-written as

$$\log K_{\mathrm{p,om}} = m_{\mathrm{r,om}} \log p_{\mathrm{L}}^{\circ} + b_{\mathrm{r,om}} \tag{4-8}$$

where $m_{r,om} = m_r$ and $b_{r,om} = b_r - \log f_{om}$. Based on theory developed by Pankow (1994), it can be shown that (Pankow, in press)

$$K_{\mathrm{p,om}} = \frac{760\ RT}{M_{\mathrm{om}}\ \zeta\ p_{\mathrm{L}}^{\circ}\ 10^{6}} \tag{4-9}$$

where M_{om} is the number-average molecular weight of the om phase, ζ is the mole-fraction-scale activity coefficient of the compound of interest in that phase, and R is the gas constant (8.206×10^{-5} m^3 atm mol^{-1} K^{-1}).

The measured log K_p values for the liquid DOP aerosol and the amorphous SOA generated from the photooxidation of whole gasoline are given in Table 4.5. The corresponding log K_p vs. log p_L° correlation parameters are given in Table 4.4. The log $K_{p,om}$ vs. log p_L° plots are given in Figure 4.2 and Figure 4.3. Also given are the regression lines for the partitioning of PAHs and *n*-alkanes to environmental tobacco smoke (ETS) as determined by Liang and Pankow (1996). For the DOP, SOA, and ETS aerosols, f_{om} was taken to be 1.0, yielding $K_p = K_{p,om}$. For the ambient smog samples, the carbon analyses revealed that IC in those samples was essentially zero so that TC = OC + EC. On average, TC constituted 21% of the TSP, with 87% of the TC being organic (OC/EC = 6.7) (see Table 4.2). When all the aerosol is secondary in nature, Izumi and Fukuyama (1990) have found that the mass of the om phase is 2.0 times the mass of total OC mass alone assuming the density of om is 1.0 g/cm^3. On the other hand, when most of the primary organic aerosol in LA in the summertime is coming from diesel exhaust and meat cooking (1996), then most of the carbon is heavy alkanes and aldehydes. For these kinds of aerosol, the mass of the om phase is 1.2 times the mass of total OC alone (1982). In this context, allowing for the presence of other elements in the organic matrix (*e.g.* hydrogen and oxygen, including that in the water in the om phase), the mass of the om phase in Los Angeles aerosol was taken to be 1.6 times the mass of the total OC mass alone since 53-58% of the total OC was estimated to be secondary in nature for our ambient smog samples (see text below). These considerations lead to the estimate $f_{om} = 0.29$ for the ambient smog samples. This value was

Table 4.5 Measured Log K_p and Log $K_{p,s}$ values for the Chamber-Generated Organic Aerosols.

Compound	log p_L^o (torr)[a]	log K_p ($m^3/\mu g$)
	DOP[b] - Chamber (36 °C and 10% RH)	
Hexadecane C_{16}	-2.45	-4.81
Heptadecane C_{17}	-2.93	-4.32
Heneicosane C_{21}	-4.86	-2.34
Docosane C_{22}	-5.34	-1.58
Tetracosane C_{24}	-6.30	-1.24
Fluorene	-1.80	-4.95
Phenanthrene	-2.62	-4.23
Anthracene	-2.65	-4.31
Fluoranthene	-3.74	-2.82
Pyrene	-3.92	-2.80
	Gasoline SOA[c] - Chamber (31 °C and 10%RH)	
Hexadecane C_{16}	-2.63	-5.53
Heptadecane C_{17}	-3.12	-4.79
Octadecane C_{18}	-3.62	-4.36
Nonadecane C_{19}	-4.11	-3.71
Eicosane C_{20}	-4.61	-3.70
Heneicosane C_{21}	-5.10	-2.59
Docosane C_{22}	-5.60	-2.72
Tetracosane C_{24}	-6.58	-1.06
Pentacosane C_{25}	-7.08	-0.44
Naphthalene	-0.21	-6.28
Acenaphthene	-1.58	-6.10
Fluorene	-1.95	-5.58
Phenanthrene	-2.78	-4.57
Anthracene	-2.80	-4.01
Fluoranthene	-3.92	-3.30
Pyrene	-4.10	-3.15
Chrysene	-5.34	-1.07

[a] log p_L^o values are temperature corrected.

[b] log K_p values are the averages for the 08/05/96 and 08/14/96 experiments.

[c] log K_p values are the averages for the 08/02/96 and 08/07/96 experiments.

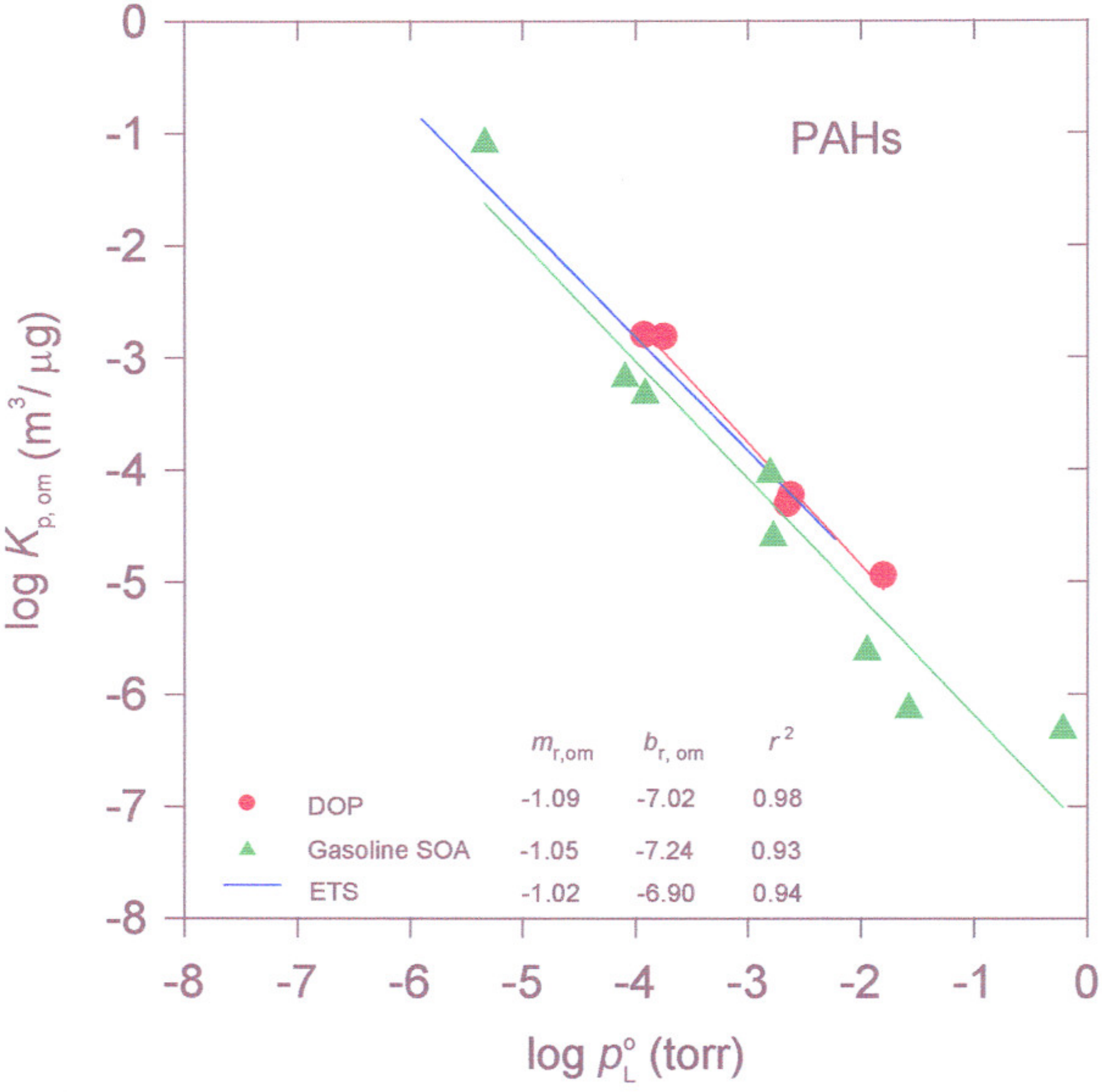

Figure 4.2 **Comparison of log $K_{p,om}$ vs. log p°_L correlation for PAHs among different types of organic aerosols. ETS data are from Liang and Pankow (1996).**

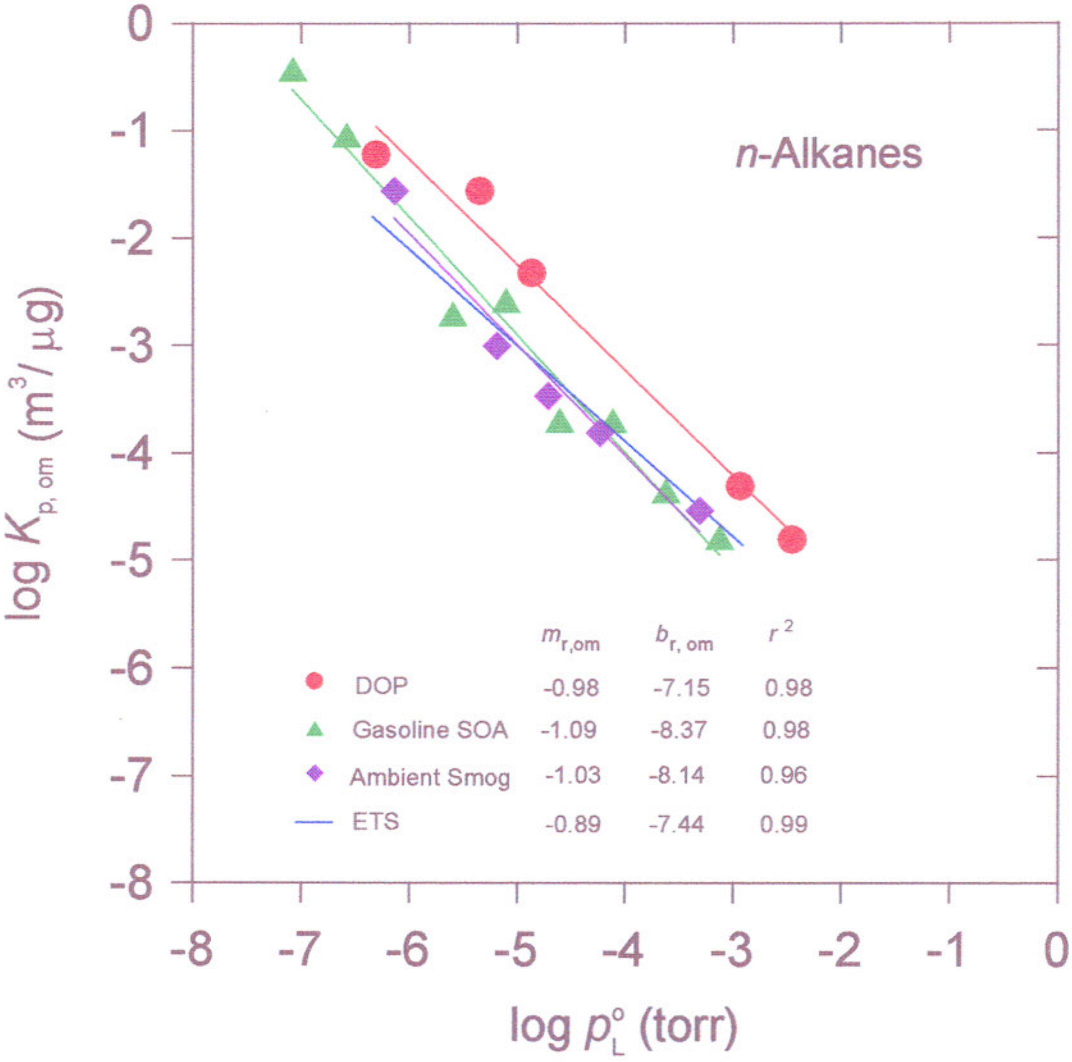

Figure 4.3 Comparison of log $K_{p, om}$ vs. log p°_{L} correlation for *n*-alkanes among different types of organic aerosols. ETS data are from Liang and Pankow (1996). The f_{om} values for the DOP, gasoline SOA, ambinet smog, and ETS aerosols were taken to be 1.0, 1.0, 0.29, and 1.0, respectively.

used with equation (4-8) and the assumption that the partitioning to the ambient smog was absorptive in nature to calculate log $K_{p,om}$ values for the ambient smog samples. The results are plotted in Figure 4.3.

The slopes and intercepts for the three regression lines in Figure 4.2 were compared using the "analysis of covariance" method described by Snedecor and Cochran (1986). The slopes of the three regression lines in Figure 4.2 are all close to -1 and not significantly different (95% confidence level). This indicates that within each of the three organic aerosols phases, ζ remained approximately constant for the range of PAHs of interest for a given RH. Analysis of covariance (Snedecor and Cochran, 1989) was used to determine whether the regression lines in Figure 4.2 could be regarded as the same statistically. The analysis of covariance is a technique that combines the features of analysis of variance and regression. It is accomplished by comparing adjusted means among different experiments. The standard model used for these adjustments assumes that the slopes and the deviation mean squares are homogeneous in different classes. Results for the three regression lines in Figure 4.2 are given in Table 4.6. The intercepts of the three regression lines in Figure 4.2 are moreover not significantly different (95% confidence level), indicating that the factor $M_{om}\zeta$ is approximately the same for the three organic aerosols considered. The partitioning of the *n*-alkanes to the organic aerosols is considered in Figure 4.3. On average, the partitioning of the *n*-alkanes to the organic aerosols was weaker than that of the PAHs. The partitioning of the *n*-alkanes was found to be similar for the gasoline SOA, ambient smog, and ETS aerosols. Within this group, the slopes of log $K_{p,om}$ vs. log p_L^o regression lines are all close to -1 and the intercepts are not significantly different (95% confidence level). (See Table 4.7 for the results of these analyses of covariance.) The sorption of the *n*-alkanes to the DOP aerosol, however, was much stronger than to the other three aerosols. Since it is very likely that M_{DOP} was larger than the M_{om} values for the other aerosols, the increase of partitioning is probably due to significantly lower ζ values for the *n*-alkanes in the DOP aerosol as compared to the other aerosol phases.

During summer smog episodes in the South Coast Air Basin, a significant fraction of the ambient organic aerosol is often of secondary origin (Gartrell and Friedlander, 1975;

Table 4.6 Comparison of Regression Lines for PAHs Partitioning to Three Types Organic aerosols.

	n	n-1	$\sum x^2$	$\sum xy^2$	$\sum y^2$	β	Deviation from regression		
							n-2	SS	MS
Within									
DOP	5	4	3.09	3.71	-3.36	-1.08	3	0.06	0.02
ETS	11	10	15.03	16.62	-15.36	-1.02	9	0.93	0.10
Gasoline	8	7	18.27	21.71	-19.22	-1.05	6	1.48	0.24
Alternative hypothesis							18	2.48	0.14
Pool (W)	24	21	36.39	42.04	-42.74	-1.04	20	2.50	0.12
Between (B)		2	6.48	9.04	-2.72		2	0.001	0.007
W+B	24	23	42.87	51.09	-45.47	-1.06	22	2.86	0.13
							2	0.37	0.18

Comparison of slopes: $F = 0.007/0.14 = 0.05$ ($F_{2,18} = 3.55$) not significantdifferent

Comparison of intercepts: $F = 0.18/0.12 = 1.50$ ($F_{2,20} = 3.49$) not significantdifferent

n = number of data points   β = regression coefficient

$$\sum x^2 = \sum_j^n x_j^2 - \frac{(\sum_j^n x_j^2)^2}{n} \qquad SS = \sum y_i^2 - \beta \sum xy \qquad MS = \frac{SS}{n-2}$$

$$\sum y^2 = \sum_j^n y_j^2 - \frac{(\sum_j^n y_j^2)^2}{n} \qquad \sum xy = \sum_j^n x_j y_j - \frac{(\sum_j^n x_j)(\sum_j^n y_j)}{n}$$

Table 4.7 Comparison of Regression Lines for *n*-Alkanes Partitioning to Three Types Organic aerosols[a].

	n	n-1	$\sum x^2$	$\sum xy^2$	$\sum y^2$	β	Deviation from regression		
							n-2	SS	MS
Within									
ETS	13	12	13.27	10.59	-11.80	-0.89	11	0.11	0.01
Gasoline	9	8	15.25	18.63	-16.70	-1.09	7	0.50	0.07
LA ambient	5	4	4.45	4.91	-4.58	-1.03	3	0.18	0.06
Alternative hypothesis							21	0.79	0.04
Pool (W)	27	24	32.98	34.13	-33.08	-1.00	23	0.94	0.04
Between (B)		2	-0.09	-0.21	-0.17		2	0.15	0.08
W+B	27	26	32.88	33.92	-33.26	-1.01	25	1.13	0.05
							2	0.19	0.09

Comparison of slopes: $F = 0.08/0.04 = 2.00$ ($F_{2,21} = 3.47$) not significant
Comparison of intercepts: $F = 0.09/0.04 = 2.25$ ($F_{2,23} = 3.42$) not significant
[a] see Table 4.6 for definitions of the variables.

Grosjean and Friedlander, 1975; Larson *et al.*, 1989; Turpin and Huntzicker, 1991; Pandis *et al.*, 1992; Turpin and Huntzicker, 1995) . Using the data from Claremont, CA, Turpin and Huntzicker (Turpin and Huntzicker, 1995) have provided a method to estimate the secondary OC content based on the total OC (= OC_{pri} + OC_{sec}), and a derived correlation between OC_{pri} and EC. Assuming that the OC_{pri}/EC ratio for Pasadena was similar to that observed by Turpin and Huntzicker (Turpin and Huntzicker, 1995) in Claremont, we estimated that 53-58% of total OC was secondary in origin. Considering that such a significant fraction of the om-phase of the Pasadena UPM is secondary in nature and that the anthropogenic volatile organic gas profile in the South Coast Air Basin is very similar to that of whole gasoline vapor (Harley *et al.*, 1994), it does seem likely that the SOA generated in the basin was similar to the SOA that was generated from whole gasoline in the smog chamber as suggested by Figure 4.3. Furthermore, the similarity between the sorption properties of the ambient smog aerosol and that of SOA generated from gasoline indicates that it may be valid to extrapolate SOA yield data from smog chamber studies (Odum *et al.*, 1996) to predict the extent of SOA formation during summer midday smog episodes.

O'Brien *et al.* (1975) have reported that mono- and dicarboxylic acids make up an appreciable portion (22% and 10%, respectively) of the organic content of particulate material found under photochemical smog conditions in Los Angeles area. Schuetzle *et al.* (1975) have found high concentrations of organic alcohols and difunctional organic compounds in SOA. Based on the significant organic content of the ambient smog samples examined here, it is likely that the polarity of the om-phase of the ambient smog aerosol and the SOA generated from gasoline is much higher than that of DOP. Moreover, because of the presence of the two long alkane chains in DOP molecules, DOP aerosol are likely to be more hospitable to n-alkanes, the ζ values for the *n*-alkanes in DOP are expected to be closer to 1.0 as well as lower than in the other aerosol phases.

The overall spread in the log K_p vs. log p_L^o correlation lines in Figure 4.3 is greater than that in Figure 4.2. This result may be the consequence of a greater sensitivity in the absorptive uptake of *n*-alkanes to changes in the polarity of the om-phase than is the case for the PAHs. It would be useful to know all of the M_{om} values for the organic aerosols studies here so that this hypothesis could be tested directly by calculating the average ζ values for the PAHs and *n*-alkanes for each different aerosol type. (Methods for estimating ζ value in liquid mixture of known composition are also available (Fredenslund *et al.*, 1975; Gmehling, 1986; Fredenslund and Sorensen; 1994)). Unfortunately, the only M_{om} value which is known with some certainty at the present time is M_{DOP}, though it may be possible to estimate the molecular weight properties of diesel particle (Rogge *et al.*, 1993), smoke aerosol (bin Abas *et al.*, 1995), atmospheric fine particle (Hildemann *et al.*, 1993; Fraser *et al.*, 1996), and secondary aerosol (O'Brien *et al.*, 1975; Schuetzle *et al.*, 1975). For DOP, we note that the solubility of DOP in water is only 3 mg/L at 25 °C (Wolfe *et al.,* 1980). Since the mutual solubilities of water and organic compounds are well correlated (Pankow, 1991), it can be concluded that the solubility of water in DOP will also be fairly low. Because the RH in the chamber experiments was only ~10%, it is very reasonable to assume that M_{DOP} was very close to the molecular weight of pure DOP, namely 390 g/mol. When log $p_{\mathrm{L}}^{\mathrm{o}} = -3$, the regression parameters in Table 4.3 for DOP give log $K_{\mathrm{p,om}} = -3.75$ and -4.21 for the PAHs and the *n*-alkanes, respectively. These values yield $\zeta = 0.28$ and 0.8, respectively, for these two compound classes at that log $p_{\mathrm{L}}^{\mathrm{o}}$ value. These results are consistent with literature values for ζ in DOP. In particular, the ζ values for benzene and octane in DOP have been reported to be 0.57 (60 °C) and 1.4 (120 °C) (Tiegs *et al.*, 1986).

While it is instructive as well as useful to have a detailed understanding of the individual values of ζ and M_{om} for a given compound or class of compounds sorbing to a given organic aerosol, there will be many circumstances for which knowledge of the product of $M_{\mathrm{om}}\zeta$ alone will be sufficient. In this context, we note the sorption properties of ETS and the SOA generated from gasoline were very similar, both for the PAHs and *n*-alkanes. This suggests that ETS may be a useful surrogate phase for SOA. It may therefore be possible to use ETS and the methods of Liang and Pankow (1996) to estimate the log $K_{\mathrm{p,om}}$ values for other classes of compounds (*e.g.* organic alcohols and carboxylic acids) in SOA. Similarly, DOP aerosol may be a useful surrogate for ambient organic aerosol which consists mainly of moderately-non-polar organic compounds of primary emission origin (*e.g.,* diesel aerosol which is about 50% organic carbon on average (Japar *et al.*, 1984)).

In summary, we conclude that the G/P partitioning of SOCs to UPM containing a significant fraction of secondary organic carbon will be dominated by absorptive partitioning. This finding is consistent with the conclusions of Liang and Pankow (1996) for UPM. This suggests that G/P partitioning in urban environments is correctly described by equations (4-7) to (4-9), and supports the absorptive model for SOA formation proposed by Odum *et al.* (1996).

4.5 Acknowledgements

This work was supported in part by a grant from the U.S. Environmental Protection Agency's Office of Exploratory Research (U.S. EPA/OER) under Grant R822312-01-0. This work was also supported in part by the U.S. Environmental Protection Agency Center on Airborne Organics under grant R-819714-01-0, National Science Foundation grant ATM-9307603, the Coordinating Research Council, and the Chevron Corporation. We gratefully acknowledge the technical assistance of Timothy P.W. Jungkamp, Robert J. Griffin, Lorne M. Isabelle, and Wentai Luo in the design, sampling preparation, and analysis phases of the experimental work. We also appreciate Martha J. Shearer and Paul G. Tratnyek for their helpful suggestions on the statistical analysis of the data. Finally, the authors would like to thank Donna Reed for assisting with many details associated with the shipment of the sampling equipment.

4.6 Glossary

A	gas-phase concentration of a compound (ng/m^3)
a_{TSP}	specific surface area of suspended particles (m^2/g)
APM	atmospheric particulate material
b_{r}	intercept in a plot of log K_{p} vs. log $p_{\mathrm{L}}^{\mathrm{o}}$
$b_{\mathrm{r,om}}$	intercept in a plot of log $K_{\mathrm{p,om}}$ vs. log $p_{\mathrm{L}}^{\mathrm{o}}$
$b_{\mathrm{r,s}}$	intercept in a plot of log $K_{\mathrm{p,s}}$ vs. log $p_{\mathrm{L}}^{\mathrm{o}}$
DOP	dioctyl phthalate
EC	elemental carbon (µg/cm^2)

ETS	environmental tobacco smoke
F	particulate-phase concentration of compound (ng/m^3)
f_{om}	weight fraction of the TSP that comprises the om phase
GFF	glass fiber filter
IC	inorganic carbon
K_{p}	gas/particle partitioning coefficient (m^3/µg)
$K_{\mathrm{p,om}}$	om-phase-normalized gas/particle partitioning constant (m^3/µg)
$K_{\mathrm{p,s}}$	surface-area-normalized gas/particle partitioning constant (m^3/m^2)
M_{DOP}	number-average molecular weight of the DOP phase (g/mol)
M_{om}	number-average molecular weight of the om phase (g/mol)
m_{r}	slope in a plot of log K_{p} vs. log $p_{\mathrm{L}}^{\mathrm{o}}$
$m_{\mathrm{r,om}}$	slope in a plot of log $K_{\mathrm{p,om}}$ vs. log $p_{\mathrm{L}}^{\mathrm{o}}$
$m_{\mathrm{r,s}}$	slope in a plot of log $K_{\mathrm{p,s}}$ vs. log $p_{\mathrm{L}}^{\mathrm{o}}$
OC	organic carbon (µg/cm^2)
$\mathrm{OC_{pri}}$	primary organic carbon
$\mathrm{OC_{sec}}$	secondary organic carbon
om	organic matter
$p_{\mathrm{L}}^{\mathrm{o}}$	vapor pressure of pure subcooled liquid (torr)
ppbV	part per billion (10^9) by volume
QFF	quartz fiber filter
R	gas constant ($= 8.206 \times 10^{-5}$ m^3 atm mol^{-1} K^{-1})
RH	relative humidity
SOA	secondary organic aerosol
SOCs	semi-volatile organic compounds
T	temperature (K)
TC	total carbon (µg/cm^2)
tc-GFF	Teflon-coated glass fiber filter
TSP	concentration of total suspended particulate material (µg/m^3)
UPM	urban particulate material

ζ mole-fraction-scale activity coefficient of a compound in organic matter phase

4.7 References

bin Abas M. R., Simoneit B. R. R., Elias V., Cabral J. A., and Cardoso J. N. (1995) Composition of higher molecular weight organic matter in smoke aerosol form biomass combustion in Amazonia. *Chemosphere* **30**, 995-1015.

Corn M., Montgomery T. L., and Esmen N. A. (1971) Suspended particulate matter: seasonal variation in specific surface areas and densities. *Environ. Sci. Technol.* **5**, 155-158.

Countess R. J., Wolff G. T., and Cadle S. H. (1980) The Denver winter aerosol: A comprehensive chemical characterization. *J. Air. Pollut. Control Assoc.* **30**, 1194-1200.

Fraser M. P., Grosjean D. , Grosjean, E., Rasmussen R. A., and Cass, G. R. (1996) Air quality model evaluation data for organics. 1. Bulk chemical composition and gas/particle distribution factor. *Environ. Sci. Technol.* **30**, 1731-1743.

Fredenslund A., Jones R. L., and Prausnitz (1975) Group-contribution estimation of activity coefficients in nonideal liquid mixtures. *AICHE* **21**, 1086-1099.

Fredenslund A. and Sorensen J. M. (1994) Group contribution estimation methods. in *Models For Thermodynamic and Phase Equilibria Calculations*. Sandler S. I. Ed., Marcel Dekker, Inc: New York, 287-361.

Gartrell G. Jr. and Friedlander S. K. (1975) Relating particulate pollution to sources: the 1972 California aerosol characterization study. *Atmos. Environ.* **9**, 279-299.

Gmehling J. (1986) Group contribution methods for the estimation of activity coefficients. *Fluid Phase Equilibria* **30**, 119-134.

Goss K. U. (1992) Effects of temperature and relative humidity on the sorption of organic vapors on quartz sand. *Environ. Sci. Technol.* **26**, 2287-2294.

Goss K. U. (1994) Adsorption of organic vapors on polar mineral surfaces and on a bulk water surface: Development of an empirical predictive model. *Environ. Sci. Technol.* **28**, 640-645.

Gray H. A., Cass G. R., Huntzicker J. J., Heyedrahl E. K., and Rau J. A. (1984) Elemental and organic carbon particle concentration: A long-term perspective. *Sci. Tot. Environ.* **36**, 17-25.

Grosjean D. and Friedlander S. K. (1975) Gas-particle distribution factor for organic and other pollutants in the Los Angeles atmosphere. *J. Air Pollut. Control Ass.* **25**, 1038-1044.

Kamens R., Odum J. R., and Fan Z. (1995) Some observations on times to equilibrium for semivolatile polycyclic aromatic hydrocarbons. *Environ. Sci. Technol.* **29**, 43-50.

Harley R. A., Hannigan M. P. and Cass G. R. (1992) Respeciation of organic gas emissions and the detection of excess unburned gasoline in the atmosphere. *Environ. Sci. Technol.* **26**, 2395-2408.

Hart K. M. and Pankow J. F. (1994) High-volume air sampler for particle and gas sampling. 2. use of backup filter to correct for the adsorption of gas-phase polycyclic aromatic hydrocarbons to the front filter. *Environ. Sci. Technol.* **28**, 655-661.

Hildemann L. M., Markowski G. R., and Cass G. R. (1991) Chemical composition of emission from urban sources of fine aerosol. *Environ. Sci. Technol.* **25**, 744-759.

Hochhauser A. M., Benson J. D., Burns V. R., Gorse, R. A., Koehl W. J., Painter L. J.,Ribbon, B. H., Reuter R. M. and Rutherford J. A. (1991) Effects of gasoline sulfur level on mass exhaust emissions - Auto/oil air quality improvement research program. *SAE technical paper no. 912322*, Society of Automotive Engineers, Warren, PA.

Izumi K. and Fukuyama T. (1990) Photochemical aerosol formation from aromatic hydrocarbons in the presence of NO_x. *Atmos. Environ.* **24A**, 1433-1441.

Japar S. M., Szkariat A. C., Gorse R. A. Jr, Heyerdahl E. K., Johnson R. L., Rau J. A., and Huntzicker J. J. (1984) Comparison of solvent extraction and thermal-optical carbon analysis methods: Application to diesel vehicle exhaust aerosol. *Environ. Sci. Technol.* **28**, 231-234.

Junge C. E. (1977) Basic consideration about trace constituents in the atmosphere as related to the fate of global pollutants, in Fate of Pollutant in the Air and Water Environment, Part I, Suffet I. H. Ed; Wiley: New York; 7-26

Larson S. M., Cass G. R., and Gray H. A. (1989) Atmospheric carbon particles and the Los Angeles visibility problem. *Aerosol Sci. Technol.* **10**, 118-130.

Liang C. and Pankow J. F. (1996) Gas/particle partitioning of organic compounds to environmental tobacco smoke: Partition coefficient measurements by desorption and comparison to urban particulate material. *Environ. Sci. Technol.* **30**, 2800-2805. (See also Errata *Environ. Sci. Technol.* **1996**, *30*, 3650)

O'Brien R. J., Crabtree J. H., Holmes J. R/, Hoggan M. C., and Bockian A. H. (1975) Formation of photochemical aerosol from hydrocarbons. *Environ. Sci. Technol.* **9**, 577-582.

Odum J. R., Hoffmann T., Bowman F., Collins D., Flagan R. C., and Seinfeld J. H. (1996) Gas/particle partitioning and secondary organic aerosol yields. *Environ. Sci. Technol.* **30**, 2580-2585.

Pandis S. N., Paulson S. E., Seinfeld J. H., and Glagan R. C. (1991) Aerosol formation in the photooxidation of isprene and β-pinene. *Atmos. Environ.* **25A**, 997-1008.

Pandis S. N., Harley R. A., Cass G. R., and Seinfeld, J. H. (1992) Secondary organic aerosol formation and transport. *Atmos. Environ.* **26A**, 2269-2282.

Pankow J. F. (1987) Review and comparative analysis of the theories on partitioning between the gas and aerosol particulate phases in the atmosphere. *Atmos. Environ.* **21**, 2275-2283.

Pankow J. F. (1991) Common y-intercept and single compound regression of gas-particle partitioning data vs 1/T. *Atmos. Environ.* **25A**, 2229-2239.

Pankow J. F. (1991) *Aquatic Chemistry Concepts*; Lewis Publishers: Chelsea, MI, 335-338.

Pankow J. F. (1992) Application of common y-intercept regression parameters for log K_p vs 1/T for predicting gas-particle partitioning in the urban environment. *Atmos. Environ.* **26A**, 2489-2497.

Pankow J. F. (1994) An absorption model of gas/particle partitioning of organic compounds in the atmosphere. *Atmos. Environ.* **28**, 185-188.

Pankow J. F. In *Gas and Particle Partitioning Measurements of Atmospheric Organic Compound*; Lane D.A. Ed; Gordon and Breach:Newark, in press.

Rogge W. F., Hildemann L. M., Mazurek M. A., and Cass G. R. (1993) Sources of fine organic aerosol. 2. Noncatalyst and catalyst-equipped automobiles and heavy-duty diesel trucks. *Environ. Sci. Technol.* **27**, 636-651.

Rounds S.A., Tiffany B. A., and Pankow J. F. (1993) Description of gas/particle sorption kinetics with an intraparticle diffusion model: Desorption experiments. *Environ. Sci. Technol.* **27**, 366-377.

Schauer J. J., Rogge W. F., Hildemann L. M., Mazurek M. A., and Cass G. R. (1996) Source apportionment of airborne particulate matter using organic compounds as tracers.

Atmos. Environ. **30**, 3837-3855.

Schuetzle D., Cronn D., and Crittenden A. L. (1975) Molecular composition of secondary aerosol and its possible origin. *Environ. Sci. Technol.* **9**, 838-845.

Shah J. J., Johnson R. L., Heyerdahl E. K., and Huntzicker J. J. (1986) Carbonaceous aerosol at urban and rural sites in the United State. *J. Air Pollut. Control Assoc.* **36**, 254-257.

Sheffield A. E. and Pankow J. F. (1994) Specific surface area of urban atmospheric particulate matter in Portland, Oregon. *Environ. Sci. Technol.* **28**, 1759-1766.

Snedecor G. W. and Cochran W. G. (1989) *Statistical Methods*. Iowa State University press: Ames, IA.

Storey J. M. E., Luo W., Isabelle L. M., and Pankow J. F. (1995) Gas/solid partitioning of semivolatile organic compounds to model atmospheric solid surfaces as a function of relative humidity. Part 1. Clean Quartz. *Environ. Sci. Technol.* **29**, 2420-2428.

Tiegs D., Gmehling J., Medina A., Soares M., Bastos J., Alessi P., and Kikic I. (1986) *Activity Coefficients at Infinite Dilution*; **Vol. IX**, Part 1 & Part 2; DECHEMA: Germany.

Turpin B. C. and Huntzicker J. J. (1991) Secondary formation of organic aerosol in the Los Angeles basin: A descriptive analysis of organic and elemental carbon concentrations. *Atmos. Environ.* **25A**, 207-215.

Turpin B. J. and Huntzicker J. J. (1995) Identification of secondary organic aerosol episodes and quantitation of primary and secondary organic aerosol concentrations during SCAQS. *Atmos. Environ.* **29**, 3527-3544.

Wang S. C., Paulson S. E., Grosjean D., Flagan R. C., and Seinfeld J. H. (1992) Aerosol formation and growth in atmospheric organic/NO_x system - Part I. Outdoor smog chamber studies of C_7- and C_8-hydrocarbons. *Atmos. Environ.* **26A**, 403-420.

Wolfe N. L., Steen W. C., and Burns L. A. (1980) Phthalate ester hydrolysis: linear free energy relationships. *Chemosphere* **9**, 403-408.

Yamasaki H., Kuwata K., and Miyamoto K. (1982) Effect of temperature on aspects of airborne polycyclic aromatic hydrocarbons. *Environ. Sci. Technol.* **16**, 189-194.

CHAPTER 5

PHYSICOCHEMICAL PARAMETERS FOR ENVIRONMENTAL TOBACCO SMOKE PARTICLES AND LOS ANGELES AMBIENT SMOG AEROSOLS

5.1 Introduction

As discussed in Chapters Three and Four, absorptive partitioning is considered to be the dominant mechanism for G/P partitioning of semivolatile organic compounds (SOCs) to: 1) urban particulate material (UPM) containing a significant fraction of secondary organic carbon; and 2) any organic aerosol (such as environmental tobacco smoke (ETS) particles and secondary organic aerosol generated from whole gasoline vapor). Based on Pankow's absorption theory (1994), the number-average molecular weight (MW_{om}) of the organic matter (om) phase is one of the most important parameters affecting absorption (*e.g.* decreasing MW_{om} favors absorption). In this context, it is instructive as well as useful to have a detailed understanding of MW_{om} for any given organic aerosol. Unfortunately, no reported MW_{om} values are found in the literature.

MW_{om} was measured for a sample of ETS particles using vapor pressure osmometry (VPO) by a contract laboratory. The values of MW_{om} for the ETS particles were then compared with those derived from the gas/particle (G/P) partitioning coefficient of water to the ETS particles. Measurements of MW_{om} were also attempted for the Los Angeles UPM by VPO. But in this case, the measured MW_{om} for a range of standard solutions sent to the contract laboratory did not match the true MW_{om} values, so we have difficulties to interpret this set of reported data. Therefore this chapter will only focus on MW_{om} for the ETS sample, and no further discussion on MW_{om} is given for the LA UPM.

In order to further understand the nature of the ETS particles and the Los Angeles UPM, elemental compositions for these two aerosols were measured to provide insights of the polarity and the degree of oxidation of the two aerosol phases.

5.2 Experimental Section

5.2.1 MW_{om} for ETS Particles

5.2.1.1 ETS Particle Collection and Sample Preparation

ETS particles were collected in a local business place used earlier (Pankow *et al.*, 1993; Liang and Pankow, 1996) with an 8 inch × 10 inch QFF for 4 h using the same method as described in the Experimental Section in Chapter Three. The QFF was weighed both before and after the sampling. Pre-equilibration overnight at 66% RH and room temperature took place in each case before weighing. Two 47-mm diameter filter sections were cut from the QFF for measurements of partitioning coefficients of water to ETS particles (Section 5.2.1.3). The balance of the QFF was Soxhlet-extracted overnight with 400 mL methylene chloride. The extract was concentrated to ~5 mL with a three-ball Synder column, and was stored at -25 °C before further treatments.

5.2.1.2 Water Removal

A significant amount of water was found in the ETS om phase (~15% by weight). This amount of water has a large effect on the value of MW_{om}. Since the water content in the om phase varies with the conditions under which the samples are collected (*e.g.* relative humidity) and the polarity of the om phase, it is desirable to obtain a MW_{om} value in the absence of the effects of variable amounts of water. This can be accomplished by removing water from ETS filter extracts before any measurements of MW_{om}. A new variable, $MW_{om,dry}$ (g/mol), is therefore defined as the number-average molecular weight of the dry ETS om phase.

A schematic diagram of the apparatus used to remove water from ETS extracts is shown in Figure 5.1. Nitrogen gas was pre-cleaned by passing through a hydrocarbon trap containing activated carbon and molecular sieve 13X (baked at 204 °C for 12 h before use). This gas was then purged into 300 mL of methylene chloride solvent at 25 °C. The methylene chloride was dried with molecular sieve 13X for 24 h before use. After allowing

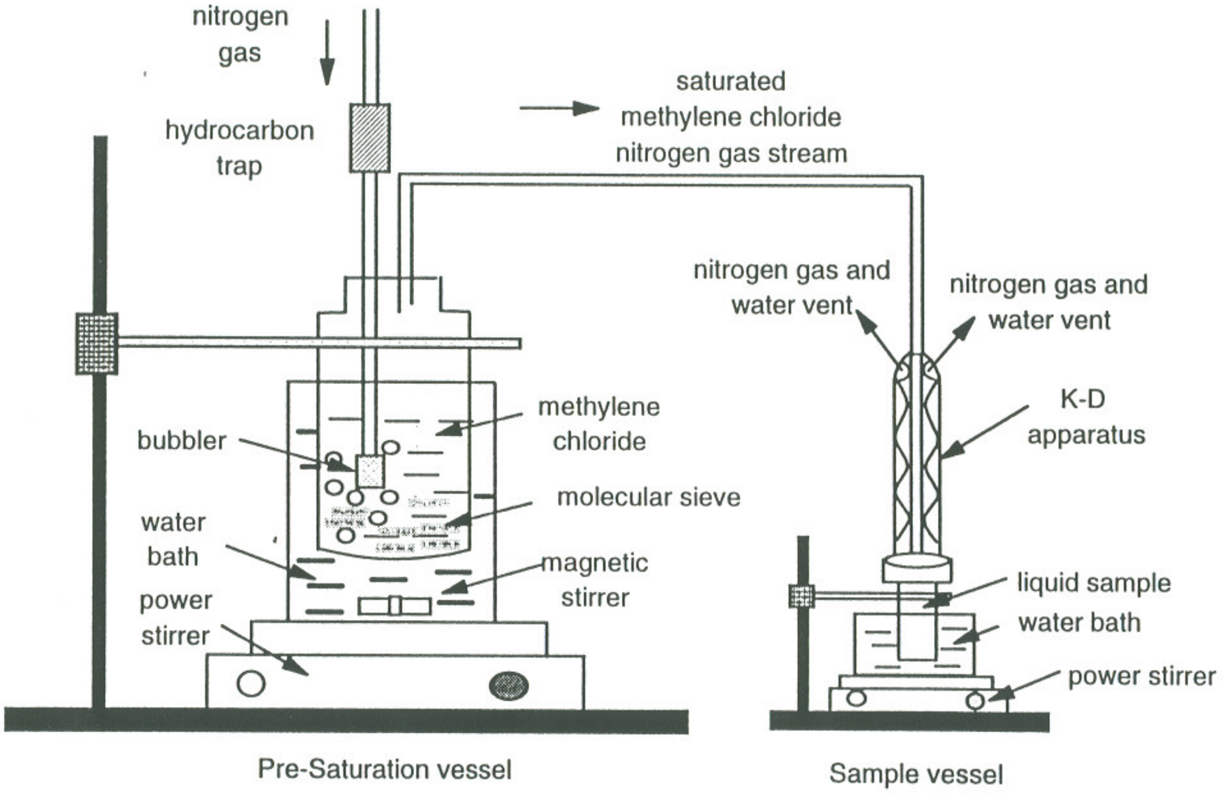

Figure 5.1 Schematic diagram of apparatus used to remove water from filter extracts.

one hour to establish equilibrium with the methylene chloride, the methylene-chloride-saturated dry N_2 gas was then bubbled into an ETS extract in a glass vial (25 °C) via a Kuderna-Danish (K-D) apparatus. Water in the extract was thereby stripped from the extract.

The efficiency of this method was first tested by removing water from a water-saturated methylene chloride solution. This solution was prepared by repeatedly shaking methylene chloride and water and allowing the two phases to separate in a separatory funnel. 5 mL of the methylene chloride from the organic layer was then placed into a pre-weighed glass vial for water removal. The flow rate of the methylene-chloride-saturated N_2 gas through the system was measured periodically with a bubble flowrate meter, and averaged 1 mL/min. Aliquots (100 μL) were taken from the test solution with a syringe at 10-minute intervals over a span of 120 min. These aliquots were analyzed by infrared (IR) absorption spectroscopy to obtain information on the disappearance of water as a function of purging time. Figure 5.2 presents the IR spectra for all of the aliquots in the region of the water stretch. A separate experiment was carried out to determine the mass of solvent lost due to the application of the method. No aliquots were removed from the methylene chloride in this case. The sample glass vial was weighed immediately both before and after the experiment. The weight difference was negligible at only 0.6% (0.038 g) of the original mass (6.633 g) of the mixture.

The method was then applied to remove water from the 3.382-mL ETS extract described in section 5.2.1.1. The measured flow rate through the system averaged 1.06 mL/min. By defining C_o as the initial water concentration in the extract and C/C_o as the fraction of the remaining water, respectively, and by assuming C/C_o was 10^{-3}, the needed purging time to reach the desired C/C_o was estimated to be 68 min according to equation (5-3). This ETS extract was therefore purged for 70 min for water removal. Another 0.5-mL ETS extract obtained by other researchers in our lab was also subject to purging for 10 min (estimated with equation (5-3)) for water removal. The resulting two "dry" ETS extracts along with three standard solutions were then sent to Huffman Laboratory Inc. (Golden, Colorado) for molecular weight measurements by VPO. Detailed information on the standard solutions and the results from the Huffman Lab are given in Table 5.1.

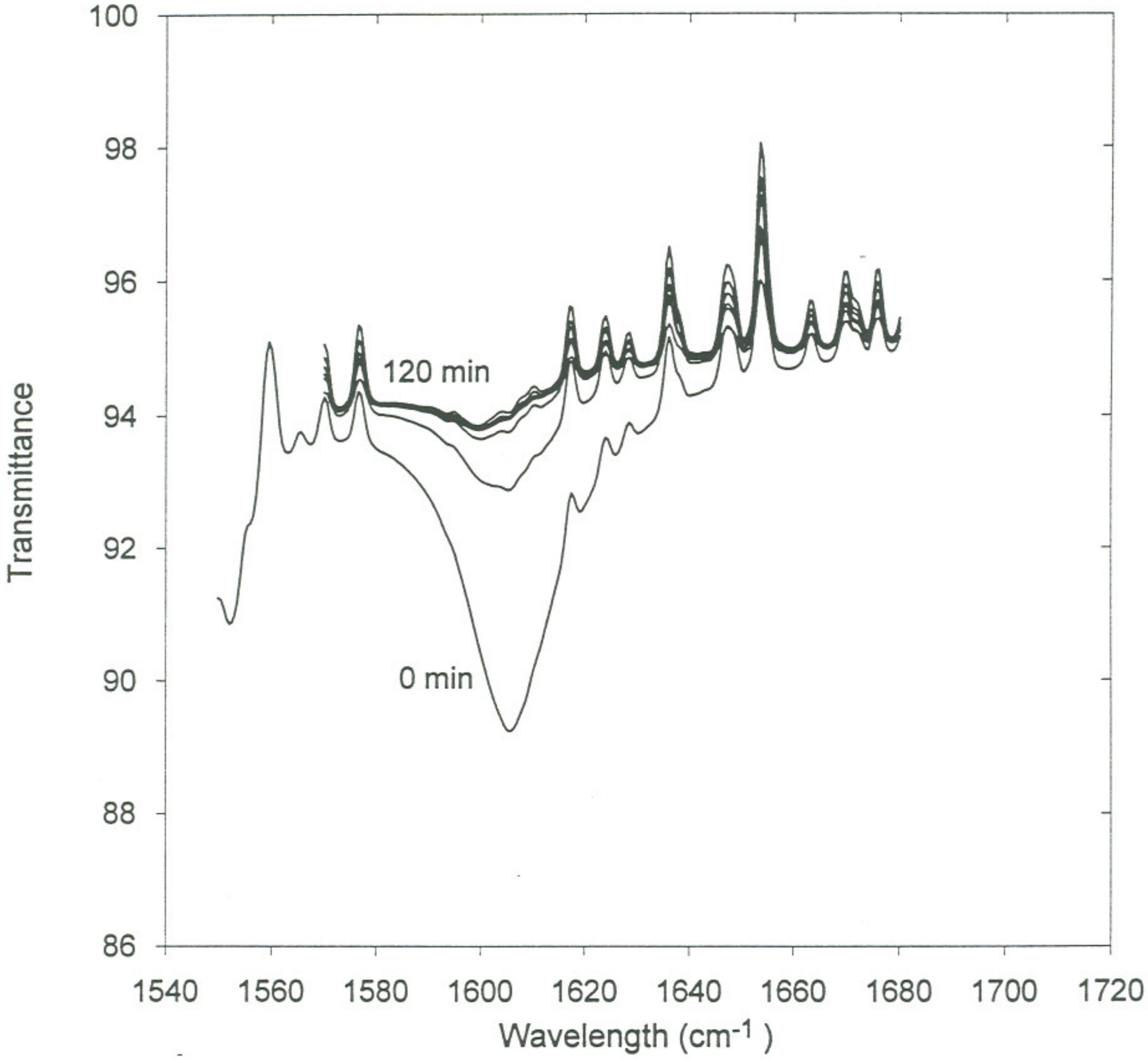

Figure 5.2 Infrared spectra of methylene chloride as a function of time during water removal.

Table 5.1 Mean Molecular Weight (MW_{om}) Obtained by Vapor Pressure Osmometry (VPO) and as Derived from the G/P Partitioning Coefficient of Water Sorbed to the ETS Particles

Name	Composition	Method	Experimental MW_{om}	True MW_{om}	Ratio of Measured/True Values
Standard 1	acridine, benzo[a]anthracene, fluoranthene, and hexadecane	VPO	191	203	0.94
Standard 2	acridine, benzo[a]anthracene, hexadecane, 2,3,5-trimethylphenol, phenanthrenequinone, and phenoxyacetic acid	VPO	176	179	0.98
Standard 3	hexadecane	VPO	226	198	1.14
Sample 1	ETS filter extract	VPO	220		
Sample 2	ETS filter extract	VPO	231		
Sample 3	ETS particles	derived from $K_{p,w}$	242		
Sample 4	ETS particles	derived from $K_{p,w}$	289		

5.2.1.3 G/P Partitioning Coefficient of Water (log $K_{p,w}$) Sorbed to ETS Particles

Measurements of log $K_{p,w}$ provide an indirect way to obtain information on $MW_{om,dry}$ (see text below). Before starting any $K_{p,w}$ experiments, a blank QFF was equilibrated in a RH-controlled chamber (RH=66% at room temperature). It was weighed every 12 h to determine the minimum time needed for the filter to reach equilibrium with the chamber atmosphere. No weight changes were observed for the filter after equilibrating for 48 h, so a period of 48 h was considered to be the minimum time for equilibration for later $K_{p,w}$ experiments.

One of the 47-mm diameter QFFs described in Section 5.2.1.1 was used for $K_{p,w}$ measurements. After drying in a desiccator containing indicating silica gel for 48 h at room temperature, the filter was weighed to obtain the mass of dry ETS particles. The QFF was then equilibrated inside different RH-controlled chambers for 48 h each in sequence, and weighed after each equilibration. Saturated potassium acetate, calcium chloride hexahydrate, and sodium bisulfate monohydrate solutions were used to achieve RH = 27.8, 32.3, and 53.6% at room temperature, respectively. The information on water uptake by the ETS particles for these three equilibrations is given in Table 5.2. Another 47-mm diameter filter was used to determine volatilization loss during storage. It was found that only 2.68% of the mass of the ETS particles was lost during the first two days when the filter was stored in a RH controlled chamber (RH = 66% at room temperature), and another 0.95% of the mass was lost during the next 15 days of storage.

5.2.2 Carbon/Hydrogen/Nitrogen/Sulfur/Oxygen (CHNSO) Analyses

5.2.2.1. ETS Particles

5.2.2.1.1 Material Preparation

ETS particles were collected with an 8 inch × 10 inch QFF for 4 h using the same procedure as described in the Experimental Section in Chapter Three. The sample filter was weighed both before and after sampling following conditioning in a constant humidity chamber with RH = 66% at room temperature. A pre-baked blank QFF was placed into a different constant humidity chamber (RH=66%) before analysis. Since both the sample and

Table 5.2 Values of the Experimental log $K_{p,w}$ and the Derived Mean Molecular Weight for Dry ETS Organic Phase ($MW_{om,dry}$) and Activity Coefficient for Water (ζ_w) in the ETS Organic Phase

Saturated solution	RH (%)	Water Uptake			log $K_{p,w}$	$MW_{om,dry}$	ζ_w
		Blank Filter (BF) (mg)	ETS Particles + BF (mg)	ETS Particles (mg)			
Potassium acetate ($KC_2H_3O_2$)	27.8	0.58	0.73	0.15	-8.33	242	1.78
Calcium chloride hexahydrate ($CaCl_2 \cdot 6H_2O$)	32.3	0.74	0.92	0.18	-8.31	289	0.94
sodium bisulfate monohydrate ($NaHSO_4 \cdot H_2O$)	53.6	1.21	1.61	0.4	-8.17		

blank QFFs were conditioned at the same RH, blank subtractions can correct for not only the background levels of elements of interest, but also the amounts of hydrogen and oxygen on the sample QFF due to water adsorption.

Tin capsules were used for the CHNS analyses. They were washed with acetone, distilled water, and alcohol, then dried at 110 °C for 1 h to ensure complete dryness. Silver capsules were used for the oxygen analyses. They were first washed with acetone, water, and alcohol, then dried under ultra-pure hydrogen at room temperature. They were then heated to 400 °C for 30 min under ultra-pure hydrogen to reduce any oxidation product Ag_2O to Ag, and then cooled under ultra-pure hydrogen. All the clean capsules were kept in pre-cleaned glass jars sealed with Teflon liners.

5.2.2.1.2 Procedure

All of the analyses were carried out using a Carlo Erba Nitrogen Analyzer 1500 Series 2 (Fisons, Danvers, MA). Three empty capsules (tin or silver) were crimped and placed into the cell wells of the auto sampler in the analyzer as equipment blanks. Several 5.7 mm-diameter filter punches were taken from both the blank and the sample QFFs. All the blank and sample filter punches as well as standard compounds (sulfanilam and benzoic acid for the CHNS and O analyses, respectively) were placed into pre-weighed clean capsules individually. The capsules were then crimped, weighed, and placed into the cell wells of the auto sampler for analyses. The capsules were placed in the cell wells in the following order: 1) equipment blanks, 2) standard compounds, 3) blank QFF punches, and 4) sample QFF punches.

A schematic diagram for the CHNS apparatus is shown in Figure 5.3. The system employs a flash combustion in oxygen (Kirsten, 1983; Pella, 1990a; Pella, 1990b). The gaseous combustion products are separated by GC and measured with a thermal conductivity detector (TCD). Each automatic analytical cycle was begun with injection of oxygen into helium carrier gas stream by means of an oxygen valve. The flow rates for He and O_2 were 100 and 80 mL/min, respectively. After 13 seconds, the sampler dropped a sample into a combustion tube, where the sample was burned at 1020 °C. The resulting gas mixture,

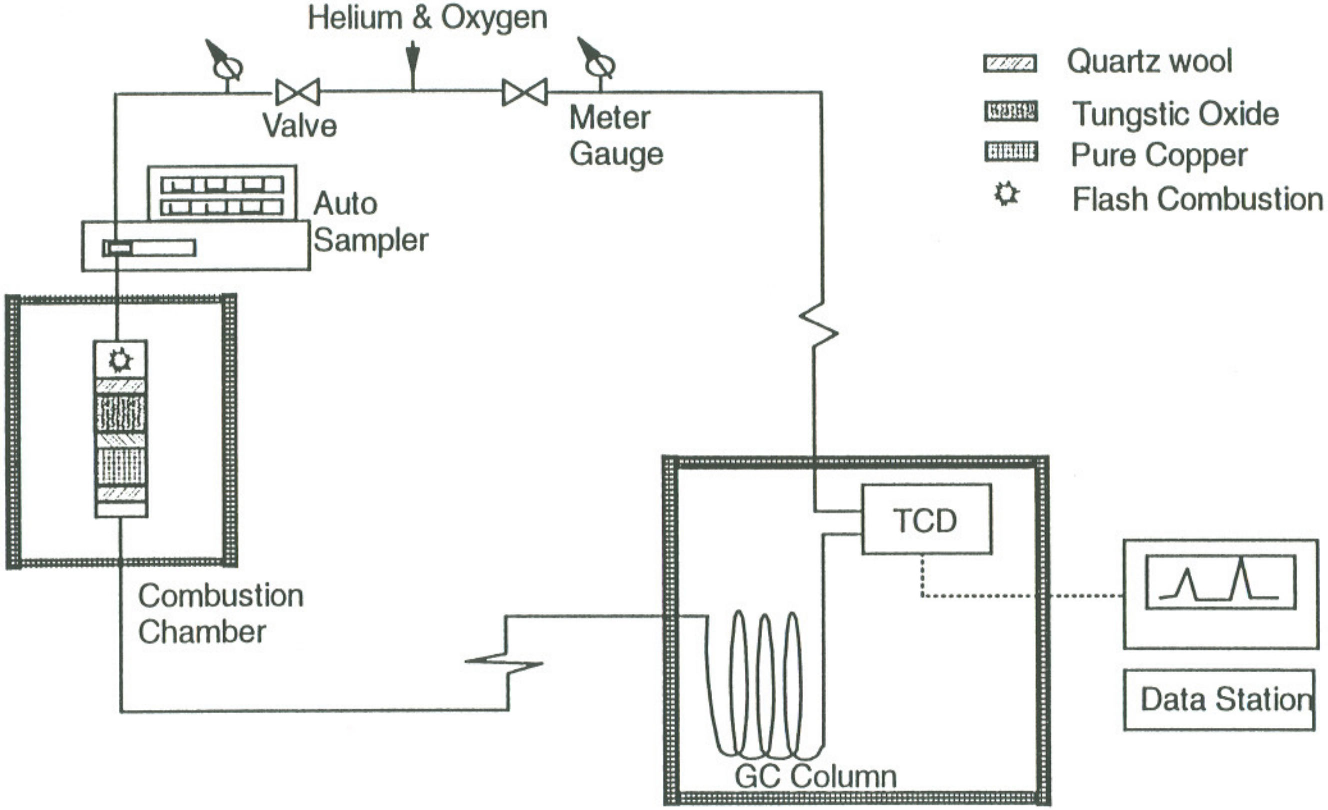

Figure 5.3 Schematic diagram of the CHNS analysis apparatus.

which contained carbon dioxide, water, nitrogen, nitrogen oxides, and combustion products of other elements from the sample, passed through a layer of tungstic oxide (used as an oxidation catalyst), where complete oxidation was achieved. The gas mixture then entered a reduction tube, which contained pure copper at 650°C. The copper retained the excess oxygen, and chemically reduced the nitrogen oxides to elemental nitrogen and SO_3 to SO_2. The remaining gas mixture (N_2, CO_2, H_2O, and SO_2) then passed into a GC column where its individual components were separated. Detection was by means of a TCD. Each sample run lasted 10 min.

A schematic diagram for the oxygen apparatus is shown in Figure 5.4. Oxygen analyses were performed by converting organic oxygen to carbon monoxide. Unlike the protocol in CHNS analyses, O_2 was not introduced into the system. Instead, the sample was pyrolyzed over nickelized carbon at 1070 °C . The flow rate of the He carrier gas was 100 mL/min. During the pyrolysis, a gas mixture containing carbon monoxide, volatile nickel compounds, hydrogen, nitrogen, methane, and other acidic gases was formed. The mixture was then passed through a scrubber containing sodium hydroxide and anhydrous magnesium perchlorate granules, where interfering substances were retained. The carbon monoxide finally reached a GC column packed with molecular sieve where separation and detection occurred in the same manner as in the CHNS analyses. Each sample run lasted about 13 min.

5.2.2.2 LA Ambient Smog Aerosol

A single high-volume aerosol sample was taken with an 8 inch × 10 inch QFF on the roof of Keck Laboratory at the Caltech campus from 12 pm to 4 pm on Aug 12, 1996 during a smog episode (see the Experimental Section in Chapter Four for the sampling procedures and Table 4.1 for the sampling condition). Several 5.7 mm-diameter filter punches were taken from the 8 inch × 10 inch sample QFF and were subject to the CHNS and O analyses using the same methods as described in Sections 5.2.2.1.1 and 5.2.2.1.2.

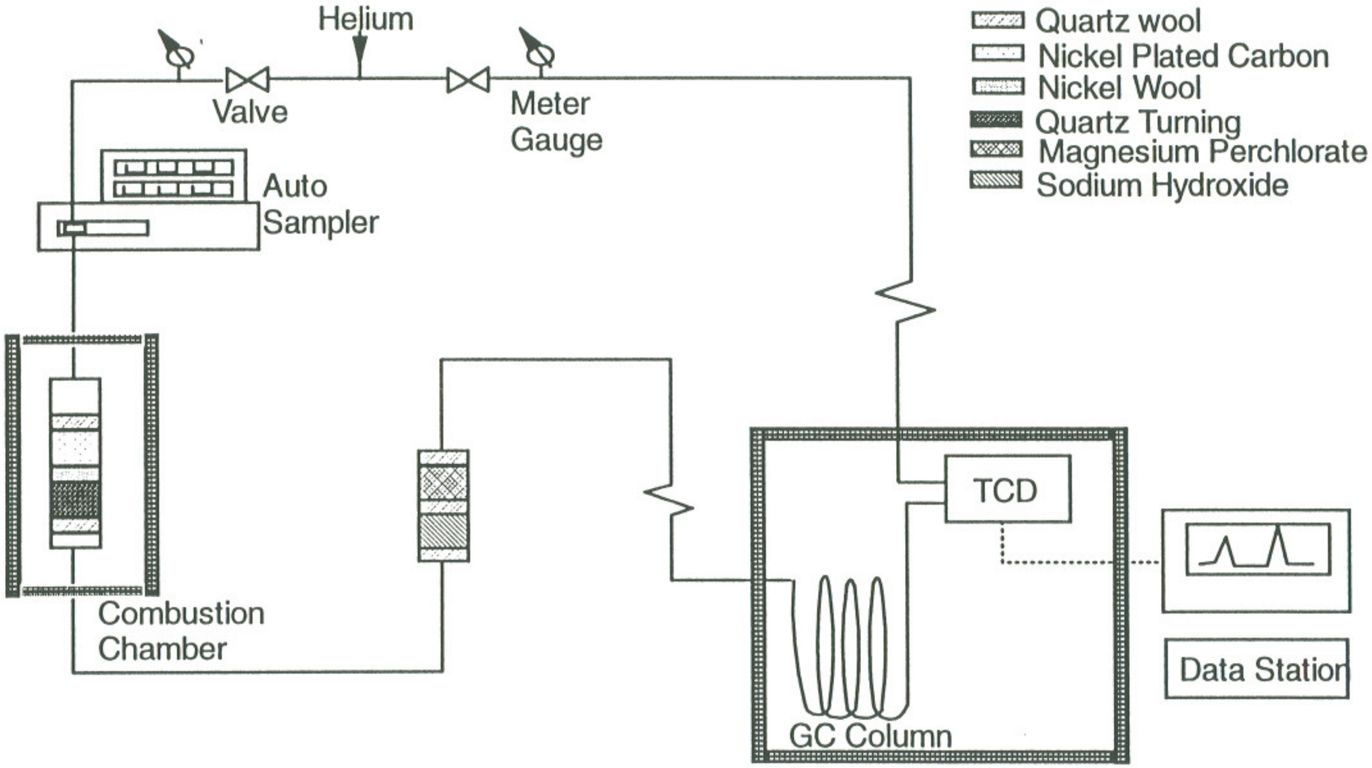

Figure 5.4 Schematic diagram of the oxygen analysis apparatus.

5.3 Results and Discussion

5.3.1 MW_{om} for ETS

5.3.1.1 Water Removal from Extracts

For any given desired fraction (C/C_o) of remaining water in a methylene chloride filter extract, the minimum time (T_{min}) for vaporizing that amount of water from the extract depends on the value of the Henry's law constant (H_w) for water dissolved in the solvent. H_w is defined as

$$H_w = \frac{P}{C} \tag{5-1}$$

where P (atm) is the partial vapor pressure of water in equilibrium with the water concentration C (mol/m^3) in methylene chloride at a temperature T (K). At 293 K, the water solubility in methylene chloride is 0.24% (w/w) (176.8 mol/m^3), and the saturated water vapor pressure is 0.02 atm. H_w and the dimensionless Henry's law constant (H_w/RT) are therefore estimated to be 1.305×10^{-4} atm m^3/mol and 5.4×10^{-3}, respectively. The total volume (V_g, mL) of saturated methylene chloride gas needed to achieve a desired C/C_0 in the extract is given by (Pankow, 1986)

$$V_g = -\frac{\ln\frac{C}{C_0}}{\frac{H_w}{RT}} V_s \tag{5-2}$$

where V_s and C_o are the volume (mL) and the initial water concentration of the extract, respectively, and C/C_0 is the fraction of the remaining water. For a case of vaporizing water from a water-saturated methylene chloride solution and assuming C/C_0 to be 10^{-3}, T_{min} is calculated according to

$$T_{min} = \frac{V_g}{f} = \frac{\ln\frac{C}{C_o}}{\frac{H_w}{RT}} \frac{V_s}{f} \tag{5-3}$$

where f is the flow rate of N_2 gas stream. Since f = 1 mL/min and V_s = 5 mL for the efficiency experiment, T_{min} was calculated to be 107 min using equations (5-2) and (5-3). The IR spectra in Figure 5.2 confirm that most of the water was removed from the test solution after 110 min of purging.

For the ETS filter extracts, however, it was impossible to use IR spectra to confirm the absence of water in the extracts after water removal because many compounds in the extracts contain -OH functional groups (see Section 1.2.2.3). Considering the success of removing almost all the water from the water-saturated methylene chloride solution in the efficiency test, it is reasonable to believe that most of the water was removed from the ETS extracts before the MW_{om} measurements were carried out.

Two factors are critical for the success of water removal with the method used here. Firstly, f should be kept low enough (*e.g.* a few mL/min) to permit equilibrium between N_2 and the methylene chloride solvent in the pre-saturation vessel. Secondly, temperatures for the pre-saturation vessel and the sample vial should be the same. If the temperature is higher for the pre-saturation vessel, methylene chloride could condense in the transfer line between the two and in the sample vial. Condensation can reduce the flow rate through the system, and even stop the procedure. On the other hand, if the temperature is higher for the sample vial, there would be methylene chloride solvent evaporation from the filter extract. Solvent loss from the extract could cause precipitation of some ETS components. If the precipitation is irreversible, some components could be removed from the extract, and could further affect the accuracy of the $MW_{\mathrm{om,dry}}$ measurements.

5.3.1.2 VPO and $MW_{\mathrm{om,dry}}$

VPO is a widely used tool for measurement of mean molecular weight. It is an application of Raoult's Law (Burge, 1977; Honeychuck *et al.*, 1993). At a constant temperature, the vapor pressure of a liquid is lowered if a second substance is dissolved in it. At sufficiently low concentrations, the decrease in the vapor pressure is proportional to the molar concentration of the solute. Therefore, measurement of the vapor pressure change as a function of the weight concentration of the solute can be used to determine the molecular weight of the solute. In practice, it is difficult to measure changes in vapor pressure directly. On the other hand, since it is relatively simple to measure changes of temperature (ΔT) with sufficient accuracy (10^{-5} °C) (Eurge, 1977), and since change in vapor pressure is directly proportional to changes in temperature, measurements of ΔT are preferable. Therefore, in the experimental procedure, the temperature difference caused by balancing the vapor pressures of the solution and pure solvent in a solvent-saturated atmosphere is determined. A plot of $\Delta T/C$ *vs.* C gives an intercept of $K \cdot MW_{\mathrm{om,dry}}$, with the intercept yielding a value of $MW_{\mathrm{om,dry}}$ according to

$$MW_{\mathrm{om,dry}} = \frac{K}{(\Delta T/C)_o} \tag{5-4}$$

where K is an experimentally-determined instrument constant, C is the concentration of the solute in grams of solute per kilogram of solution, and $(\Delta T/C)_o$ is the intercept. Several four-point molecular weight measurements were obtained for the ETS extracts along with three standard solutions at the Hoffmann Laboratory, Inc. The reported results are given in Table 5.1.

5.3.1.3. $K_{\mathrm{p,w}}$ and $MW_{\mathrm{om,dry}}$

Based on equation (3-1), $K_{\mathrm{p,w}}$ (µg/m^3) for water is defined as

$$K_{\mathrm{p,w}} = \frac{F/\mathrm{TSP}}{A} \tag{5-5}$$

Assuming water vapor behaves as an ideal gas, A can be calculated according to the Ideal Gas Law as

$$A(\mu\mathrm{g/m}^3) = \frac{18 \times 10^6 P_{\mathrm{sat}} RH}{RT} \tag{5-6}$$

where P_{sat} is the saturated partial pressure for water at temperature T, R is the gas constant (8.206×10^{-5} m^3·atm/mol·K), and RH is a specified relative humidity. By defining W (mg) as the mass of water taken up by the ETS particles at a given RH and m (mg) as the mass of the dry ETS particles on the filter, $K_{\mathrm{p,w}}$ (m^3/µg) can be estimated by

$$K_{\mathrm{p,w}} = \frac{(W/m)RT}{18 \times 10^6 P_{\mathrm{sat}} RH} \tag{5-7}$$

Based on the conclusion of Chapter Three that absorption is the dominant mechanism for compounds sorbing to the ETS particles, $K_{\mathrm{p,w}}$ can also be estimated by the absorption theory as described in equation (3-12)

$$K_{p,w} = \frac{f_{om} 760 RT}{MW_{om} \zeta p^{\circ}_{L} \times 10^{6}} \tag{5-8}$$

Since the ETS om phase consists of the original dry ETS particles and the uptaken water, MW_{om} is calculated by

$$MW_{om} = \frac{18\times 10^{-3}(m + W)}{18n + 10^{-3} W} \tag{5-9}$$

where n ($=10^{-3}m/MW_{om,\,dry}$) is the number of moles of m (mg) of the dry ETS particles. By combining equations (5-7), (5-8), and (5-9), $K_{p,w}$ can be re-written as

$$K_{p,w} = \frac{f_{om}\ 760\ RT}{\frac{18\times 10^{-3}(m + W)}{18n\ +\ 10^{-3} W}\ \zeta\ p^{\circ}_{L,w}\ 10^{6}} \tag{5-10}$$

Once all the variables in equation (5-7) are measured, $K_{p,w}$ can be calculated for any specific RH. Since there are two unknowns in equation (5-10), namely n and ζ, at least two $K_{p,w}$ are needed in order to obtain the values for n and ζ. With the obtained values of n, $MW_{om,\,dry}$ can be calculated directly. The resulting values of $MW_{om,dry}$ derived from the values of $K_{p,w}$ under three different RH are listed in Table 5.1. The assumption is that ζ does not change under the RH chosen here. To achieve this, $K_{p,w}$ should be measured within a relatively narrow RH region, hence the RH values of 27.8% and 32.3% were chosen for this study. The RH of 53.6% was chosen because it was similar to the 52% RH measured at the time of the original sampling. Since 53.6% RH is much higher than the other two RH used here, ζ may have been different, and so use of the value of log $K_{p,w}$ at 53.6% RH with one of the log $K_{p,w}$ at the other two RH may not derive accurate values for ζ_{w} and $MW_{om,dry}$. As shown in Table 5.1, the derived $MW_{om,dry}$ by using log $K_{p,w}$ at 53.6% is higher than other measured values since the log $K_{p,w}$ at 53.6% RH is higher than those at 27.8% and 32.3% RH. By excluding $MW_{om,dry}$ of 289, the average $MW_{om,dry}$ was estimated to be 231 ± 11.

As shown in Table 5.2, the activity coefficient for water in ETS om phase (ζ_{w}) is very close to 1.0. The polarity of the ETS om phase is therefore expected to be very similar to that of water surfaces. The partitioning coefficient for water sorbed to water surfaces (log $K_{p,ww}$) at room temperature was calculated to be -7.34. Since the average value for $MW_{om,\,dry}$ is 231 g/mol and since the molecular weight of water is 18 g/mol, log $K_{p,ww}$ was estimated to be 1.1 log units larger than log $K_{p,w}$ based on equation (5-8) by taking ζ_w to be 1.0. Indeed, this estimation is consistent with the measured values with log $K_{p,ww}$ being 0.98 log units larger than log $K_{p,w}$ (= -8.32). This agreement provides further evidence that partitioning of compounds to the ETS om phase can be adequately described by the absorption model.

The results in Table 5.1 indicate that the values of $MW_{om,\,dry}$ obtained by VPO and derived by the values of $K_{p,w}$ are in good agreement. Although the $K_{p,w}$ measurements provide an alternative way to determine $MW_{om,\,dry}$, this method might be subject to some errors. Firstly, volatile compound loss during the experiments can cause errors in weight measurements. However, the total mass loss was only 3.62% for a period of 15 days storage. Assuming all the loss was from very light compounds with average molecular weight of 100, the value of $MW_{om,\,dry}$ was estimated to be 218, which was 6% different from the measured value of 231 obtained in this study. Therefore, errors due to volatilization are unlikely to cause very large errors in the final values of $MW_{om,\,dry}$. Note that the VPO method could also be subject to volatilization loss during filter extract preparation and the water removal process. Secondly, the RH in the chamber containing the balance is not necessarily the same as that in the RH-controlled chamber containing the filter, so that there might be water uptake or loss during weighing. Therefore, in order to minimize the RH changes, the filter was taken out of the RH-controlled chamber immediately before weighing. Since it took less than 2 min to get a reading, it is unlikely that significant water uptake or loss occurred in such a short period of time. Thirdly, equilibrium between the ETS particles and the water in the chamber is controlled by diffusion of the water molecules, and there is no obvious way to determine whether equilibrium was in fact reached in the measurements. The minimum equilibration time (48 h) obtained by using a blank QFF is not necessarily applicable to the sample QFF. Since the sample QFF was covered by the liquid ETS particles, it might require longer time for the particles deep within the filter to reach equilibrium with the surrounding water molecules. However, since longer times are required for the ETS particles to establish equilibrium with the surrounding environment associated with a higher RH, 48 h (obtained for RH = 66%) is considered to be long enough in this study since the three events for the $K_{p,w}$ measurements were carried out under lower RH. Regardless of some defects, using the values of $K_{p,w}$ to derive the values of $MW_{om,dry}$ provides reasonable agreement with those obtained by the VPO method.

5.3.2 Elemental Composition of ETS Particles

Five sulfanilam ($C_6H_8N_2O_2S$) standard runs (STD S1-S5) and three benzoic acid ($C_7H_6O_2$) standard runs (STD B1-B3) were carried out for the CHNS and O analyses, respectively. The results are given in Table 5.3. The data for the standard runs were used to ensure the accuracy of the system and to generate calibration curves for the corresponding elements. Peak area integrations for both the blank and the ETS QFF punches are given in Table 5.4. The elemental compositions of the ETS particles were calculated by subtracting the average of the background levels obtained for the blank QFF punches. The resulting values (SMP S1-S5 for the CHNS analyses and SMP B1-B4 for the O analyses) are given in Table 5.5. All the sample runs are replicates taken from the same ETS QFF rather than different samples.

The data in Table 5.5 show that carbon, hydrogen, nitrogen, and oxygen account for 71%, 9%, 5%, and 17% (w/w), respectively, in the ETS particle matrix, with only trace amount of sulfur present. The relatively high percentage of oxygen in the ETS matrix and the large amount of water (15% by weight) present in the ETS matrix indicate that the ETS matrix is quite polar, which is consistent with the results discussed above based on ζ_w. Infrared absorption spectroscopy data for an ETS extract indicate that there are vibration stretchings in the alcohol and acid regions (see Figure 5.5). Indeed, Dube and Green (1982) have found a large quantity of oxygen-containing organic compounds in the mainstream smoke particulate phase (w/w): carboxylic acids, 13%; aldehydes and ketones, 11%;

Table 5.3 Elemental Composition of Standard Compounds for the ETS Particle CHNOS Analyses

Name	Sulfanilam				Benzoic acid
	C (%) 41.84	H (%) 4.68	N (%) 16.27	S (%) 18.62	O (%) 26.20
STD S1	41.83	4.86	16.28	18.62	
STD S2	42.08	5.00	16.36	18.65	
STD S3	43.17	5.09	16.68	19.48	
STD S4	41.96	4.87	16.52	18.99	
STD S5	39.87	4.42	17.41	18.07	
STD B1					25.67
STD B2					26.15
STD B3					26.18
Average	41.78 ± 1.19	4.85 ± 0.26	16.65 ± 0.45	18.76 ± 0.52	26.00 ± 0.29

Table 5.4 Peak Area Integrations for the Blank and the ETS Sample QFF Punches

C		N		H		S		O	
Blank	Sample	Blank	Sample	Blank	Sample	Blank	Sample	Blank	Sample
7934	526705	610	15908	18471	208725	0	105	62114	157013
8373	540706	621	16133	19689	215205	0	167	65372	156847
8447	546905	661	16514	19951	216345	0	244	70387	161022
9141	568319	724	16643	20366	225478	0	296		170162
	569873		17121		233954				

Table 5.5 Elemental Composition of the ETS Particles

Name	C (%)	H (%)	N (%)	S (%)	O (%)
SMP S-1	67.72	8.82	5.19	0.058	
SMP S-2	69.55	9.13	5.27	0.059	
SMP S-3	70.36	9.18	5.40	0.060	
SMP S-4	73.16	9.61	5.54	0.062	
SMP S-5	73.36	10.00	5.60		
SMP B-1					16.24
SMP B-2					16.27
SMP B-3					16.99
SMP B-4					18.64
Average	70.83	9.35	5.38	0.06	17.03
Standard deviation	2.42	0.46	0.16	0.002	1.12
Total	**102.6 ± 2.7%**				

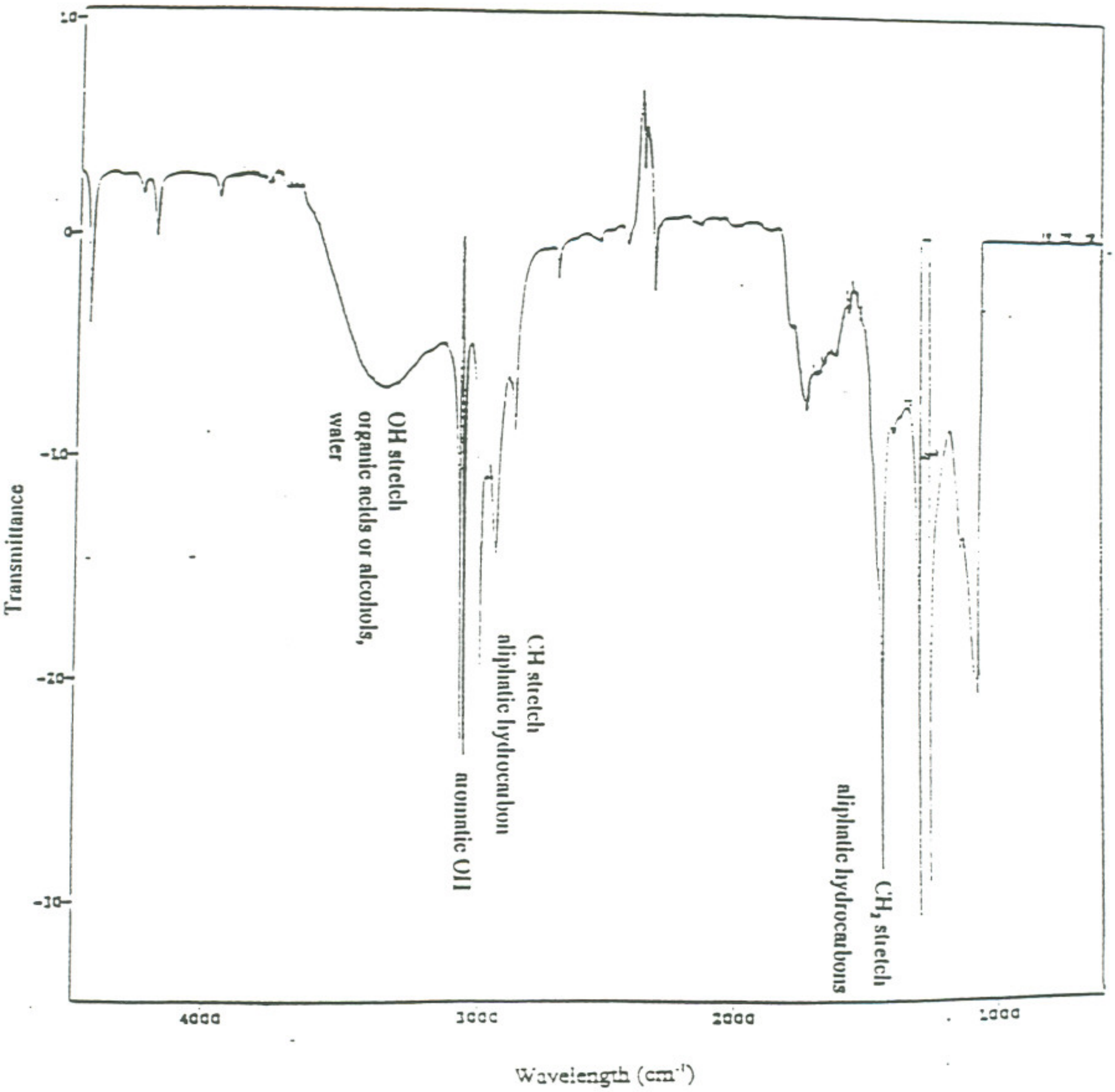

Figure 5.5 Infrared absorption spectrum of ETS filter extract.

alcohols, 8%; phenols, 3.5%; esters, 3.5%; water, 16%. Similarly, Rogge *et al.* (1994) have conducted extensive studies by GC/MS to identify the marker compounds present in the cigarette smoke particle from exhaled mainstream plus sidestream smoke. Out of all the identified compounds from the extractable and elutable organic mass, they found that the major portion (w/w) was made up of nitrogen-heterocyclic compounds (35.6%), phytosterols (10.7%), phenolic compounds (8.2%), *n*-alkanols (6.6%), and carboxylic acids (19%).

5.3.3 Elemental Composition of LA Smog Ambient Aerosol

Three sulfanilam ($C_6H_8N_2O_2S$) standard runs (STD S1-S3) and three benzoic acid ($C_7H_6O_2$) standard runs (STD B1-B3) were carried out for the CHNS and the O analyses, respectively. The results are given in Table 5.6. The data for the standard runs were used to ensure accuracy of the system and to generate calibration curves for the corresponding elements as described in Section 5.3.2. Peak area integrations for both the blank QFF and the LA ambient smog aerosol QFF punches are given in Table 5.7. The elemental compositions of the LA ambient smog aerosol were calculated by subtracting the average of the background levels obtained for the blank QFF punches. The resulting values (SMP S1-S8 for the CHNS analyses and SMP B1-B6 for the O analyses) are given in Table 5.8. All the sample runs are replicates taken from the same QFF rather than different samples.

Inorganic carbon (IC), elemental carbon (EC), and organic carbon (OC) analyses for the same LA ambient smog aerosol by the Sunset Laboratory (Forest Grove, OR) indicated that total carbon (TC) is 16.42 $\mu g/cm^2$ with OC/TC being 0.87 (see Table 4.2). Because the area for the 8 inch × 10 inch QFF covered by the particles was 432.9 cm^2, the amount of TC on the QFF was calculated to be 7.1 mg. As the TSP level during the smog aerosol sampling was 104 $\mu g/m^3$ (see Table 4.1), the mass of the total particles collected on the QFF in 240 min with a 1.4 m^3/min flow rate was estimated to be 34.9 mg. Therefore TC/TSP was 0.20, which was in excellent agreement with the TC/TSP of 0.21 obtained from the CHNS analyses. Since OC/TC was 0.87, a value of 0.19 was obtained for OC/TSP.

Forrest *et al.* (1980) investigated the possibility of NH_4NO_3 losses during sampling

Table 5.6 Elemental Composition of the Standard Compounds for the the LA Ambient Smog Aerosol CHNSO Analyses

Name	Sulfanilam				Benzoic acid
	C (%)	H (%)	N (%)	S (%)	O (%)
	41.84	4.68	16.27	18.62	26.20
STD S1	42.72	5.02	16.65	18.90	
STD S2	42.12	4.95	16.54	18.72	
STD S3	41.83	4.75	16.20	18.61	
STD B1					25.49
STD B2					26.14
STD B3					26.37
Average	42.22 ± 0.37	4.91 ± 0.11	16.46 ± 0.19	18.74 ± 0.12	26.00 ± 0.37

Table 5.7 Peak Area Integrations for the Blank and LA Ambient Smog Aerosol QFF Punches

C		N		H		S		O	
Blank	Sample	Blank	Sample	Blank	Sample	Blank	Sample	Blank	Sample
8664	37395	4929	4961	55188	56217	0	532	69299	101861
8746	38899	4973	5030	53606	66741	0	864	69664	99958
7202	39338	5505	5113	51856	58728	0	0	66663	106010
7255	36467	5163	5040	55213	55486	0	0	68143	106034
7773	37787	5099	4965	56559	58355	0	0	65672	101908
9720	38036	5327	4758	53121	70465	0	1019		103175
7659	37202	5556	5044	56258	68272	0	859		
7054	35957	5429	4668	51772	62239	0	914		

Table 5.8 Elemental Composition of the LA Ambient Smog Aerosol

Name	C (%)	H (%)	N (%)	S (%)	O (%)
SMP S-1	21.03	0.507	-0.43	0.83	
SMP S-2	22.10	3.150	-0.30	1.34	
SMP S-3	22.42	1.138	-0.15	0	
SMP S-4	20.36	0.324	-0.28	0	
SMP S-5	21.31	1.044	-0.42	0	
SMP S-6	21.49	4.085	-0.81	1.59	
SMP S-7	20.89	3.534	-0.28	1.34	
SMP S-8	20.00	2.019	-0.98	1.42	
SMP B-1					41.70
SMP B-2					39.37
SMP B-3					46.80
SMP B-4					46.83
SMP B-5					41.76
SMP B-6					43.32
Average	21.20	1.98	-0.46	1.30	43.30
Standard deviation	0.82	1.45	0.29	0.28	3.00
Total	**67.3 ± 3.5%**				

by spiking a standard NH_4NO_3 solution onto a QFF under various RH. They have found that up to 72% of the NH_4NO_3 was lost through volatilization from the QFF. The losses were the greatest at relatively low RH (< 60%). Appel *et al.* (1980 and 1981) performed ambient aerosol sampling in the Los Angeles Basin and observed nitrate loss from their Teflon filters. The losses were the largest (more than 50%) for the midday samples, which were sampled at relatively high temperatures and relatively low RH.

Since no special measurements were taken to determine nitrate loss during our ambient smog aerosol sampling, it is impossible to correct for any nitrate losses, so that the N data obtained by the CHNS analyses may be unreliable for the actual aerosol at the time of sampling. As the peak areas for both the blank and sample QFF punches for N in Table 5.7 are shown to be basically the same, the detected N are considered to be from the background rather than from the ambient smog aerosol.

In order to estimate the inorganic oxygen levels in the LA ambient smog aerosol, masses for nitrate, sulfate, and the crustal material were taken from the samples obtained under similar conditions in the Los Angeles air basin (Larson and Cass, 1989). The resulting data are shown in Table 5.9. By combining contributions from both the fine suspended particulate matter and the coarse particulate matter, the inorganic oxygen accounted for 28% of the TSP. The organic oxygen (OO) was estimated by the difference between the total oxygen and inorganic oxygen, and was concluded to be 15 % of the TSP. The relatively high percentage of OO present is most likely due to gas-phase photochemical reactions (photooxidation) (Pandis *et al.*, 1991; Turpin *et al.*, 1991; Pandis *et al.*, 1992; Turpin and Huntzicker, 1995) resulting in a large amount of secondary organic alcohols, organic acids, and difunctional compounds in the LA ambient smog aerosol (Schuetzle *et al.*, 1975; Forstner *et al.*, 1997).

Since most of the ammonium salts are likely to be lost during sampling and handling, and because the CHNS and O analyses were carried out for the dry filter punches, the hydrogen detected on the filter punches was assumed to be organic. The organic hydrogen (OH) was calculated to be 1.98% of the TSP. The sum of OC + OO + OH is 36% of TSP, therefore om ($\approx$ OC + OO + OH) is taken to be 1.9 times OC.

Table 5.9 Inorganic Oxygen-Containing Compounds in the Pasadena Aerosol[a]

fine suspended particulate matter, av % by mass in TSP		**oxygen (% by mass)**
sulfate	18.0	7.84
nitrate	3.4	1.72
crustal material	8.1[b]	2.25
fine mass, $\mu g/m^3$	55.6	
coarse suspended particulate matter, av % by mass		
sulfate	3.5	1.01
nitrate	21.4	7.14
crustal material		
Al_2O_3	7.8	1.58
SiO_2	27.3	6.28
Fe_2O_3	3.3	0.43
remaining	7.5[c]	0.03
coarse mass, $\mu g/m^3$	38.9	
	total (%)	**28.28**

[a] adapted from the data of Larson & Cass (1989)

[b] average oxygen level was taken to be 47% (w/w) in crustal material (Mason and Moore, 1982)

[c] average oxygen level was taken to be 1% (w/w) for the remaining crustal material (Mason and Moore, 1982)

When an aerosol consists of mainly primary organic carbon, the mass of the om has been taken to be 1.2 times the mass of the OC measured (Countess *et al.*, 1980; Gray *et al.*, 1986; Schauer *et al.*, 1997). On the other hand, when an aerosol is mainly secondary in nature, the mass of om has been taken to be 2.0 times the mass of OC (Izumi and Fukuyama, 1990). As the LA smog aerosol collected in this study contained 53% - 58% of secondary OC, the mass of om was estimated to be 1.6 to 1.7 times the mass of OC, which is in good agreement with the factor of 1.9 based on the elemental compositions of the LA smog aerosol considering the uncertainty of adapting data from other studies and the experimental errors.

5.4 Summary

A simple approach was developed for water removal from filter extracts before any MW_{om} measurements. The values of $MW_{\mathrm{om,dry}}$ for the ETS om phase were obtained by VPO and were derived from the values of $K_{\mathrm{p,w}}$. The resulting values by these two methods were in good agreement, and averaged 231.

The CHNSO analyses were carried out for both the ETS particles and the LA ambient smog aerosol. The ETS om phase contained 70% C, 9% H, 5% N, and 17% O, which indicates that the ETS om phase is somewhat polar. The LA ambient smog aerosol consisted of 19% OC, 15% OO, and 2% OH in the TSP, which indicates the mass of om was equal to 1.9 times the mass of OC. The multiplication factor of 1.9 obtained from this study is compatible with the factor of 1.6-1.7 estimated from other studies.

CHAPTER 6

COMPARATIVE ANALYSIS OF THE THEORIES ON PARTITIONING BETWEEN THE GAS AND AEROSOL PARTICULATE PHASES IN THE ATMOSPHERE

6.1 Introduction

Gas/particle (G/P) partitioning studies of semi-volatile organic compounds (SOCs) to different types of aerosol have been carried out extensively since the last decade in both the field and the laboratory. Pankow (1994a) has proposed that in any given situation both *ad*sorption and *ab*sorption may be operative. When atmospheric particulate material is mainly mineral material of continental origin, simply physical adsorption will dominate the sorption process. However, since urban particulate material (UPM) generally contains a significant amount of amorphous, organic carbon (Gray *et al.*, 1984; Shah *et al.*, 1986), it seems likely that absorptive partitioning must be playing at least some role in urban air, and also in air affected by urban sources (Pankow, 1994b; Liang *et al.*, 1997).

The purpose of this chapter is to provide direction in determining the controlling mechanisms for the G/P partitioning of SOCs to UPM. This is accomplished by comparing the literature data on PAHs and *n*-alkanes sorbing to UPM in different regions of the world with those presented in Chapters Three and Four.

6.2 Approach

Reported data on G/P partitioning of polycyclic aromatic hydrocarbons (PAHs) and *n*-alkanes to UPM were compiled for the following regions: 1) Denver, CO (Foreman and Bidleman, 1990); 2) Columbia, SC (Foreman and Bidleman, 1987); 3) Portland, OR (Ligocki and Pankow, 1989); 4) Portland, OR (Hart, 1989); 5) Osaka, Japan (Yamasaki *et al.*, 1982). Other available data on sorption to UPM were not included in this study when: 1) event-to-event variations in regression parameters were large (*e.g.* urban Chicago data (Cotham and Bidleman, 1995)) ; 2) corrections were not made for gas adsorption artifacts (*e.g.* Oregon Coast data (Ligocki and Pankow, 1989)); and 3) needed information was not available. The Denver study (Foreman and Bidleman, 1990) is one of the few cases that the authors reported the G/P partitioning of both PAHs and *n*-alkanes to UPM, and was included even though no gas adsorption artifacts were corrected for this data set.

As shown in equation (3-2) or equation (4-3), within a given compound class (*e.g.* PAHs and *n*-alkanes), the partitioning coefficient (log K_p) tends to be linearly correlated with subcooled liquid vapor pressure (log p_L^o). Regression coefficients m_r and b_r for log K_p *vs.* log p_L^o for PAHs and *n*-alkanes sorbing to UPM in all the regions considered here are given in Table 1. The values of m_r and b_r were either obtained directly from the literature, or derived from the raw data when they were not reported.

6.3 Results

6.3.1. Adsorptive Partitioning

When adsorption is the dominant partitioning mechanism, a surface-area-normalized constant $K_{p,s}$ can be defined as described by equation (4-3). In this case, knowledge of specific surface area of the sorbing solid (a_{TSP}) is essential. The values of specific surface area in summer and winter time were taken to be 2.0 (Corn *et al.*, 1971; Sheffield and Pankow, 1994; Liang *et al.*, 1997) and 3.05 (Corn *et al*, 1971), respectively. The corresponding regression parameters $m_{r,s}$ and $b_{r,s}$ were then calculated by equation (4-6). The results are given in Table 1. The log $K_{p,s}$ vs. log p_L^o plots are given for PAHs and *n*-alkanes in Figure 6.1 and Figure 6.2, respectively. The a_{TSP}-normalized log K_p values for PAHs and *n*-alkanes sorbed to $(NH_4)_2SO_{4(s)}$ aerosol and QFF data (all extrapolated to RH = 42%) as discussed in Chapter Four are also plotted in Figures 6.1 and 6.2.

It is well known that the partitioning of organic compounds to inorganic surfaces is RH-dependent (Goss, 1992; Storey *et al.*, 1995), and that the sorption becomes weaker as the

Table 6.1 Regression Coefficients ($m_{r,s}$ and $b_{r,s}$) of log $K_{p,s}$ vs. log p^{o}_{L} for PAHs and *n*-Alkanes sorbing to UPM, $(NH_4)_2SO_{4(s)}$, and QFF

Aerosol type	Compound	Date	m_r	b_r	TSP[a] ($\mu g/m^3$)	a_{TSP} (m^2/g)	$m_{r,s}$	$b_{r,s}$	Reference
UPM, Denver	PAHs	07/85 to 01/86	-0.76	-6.71	27 to 157	3.05[b]	-0.76	-1.19	Foreman and Bidleman, 1990
UPM, Columbia (Lab work)	PAHs	10/84 to 08/85	-1.30	-9.15	46.6 to 59.4	2.00[c]	-1.30	-3.45	Foreman and Bidleman, 1987
UPM, Portland	PAHs	1984 to 1985	-0.84	-6.54	30[d]	3.05	-0.84	-1.02	Ligocki and Pankow, 1989
UPM, Portland	PAHs	02/88 to 12/88	-0.94	-6.80	51	2	-0.94	-1.10	Hart, 1989
UPM, Osaka	PAHs	1977 to 1978	-0.98	-7.87	61 to 272	2.53[e]	-0.98	-2.27	Yamasaki *et al.*, 1982
$(NH_4)_2SO_{4(s)}$ (42% RH)	PAHs	08/96	-1.04	-7.41	109	17.5	-1.04	-3.45	Liang *et al.*, 1997
QFF (42% RH)	PAHs					1.65	-1.18	-4.59	Liang *et al.*, 1997
QFF (70% RH)	PAHs					1.65	-1.18	-5.07	Storey *et al.*, 1995
UPM, Los Angeles	*n*-alkanes	08/96	-1.03	-8.68	108	2	-1.03	-2.98	Liang *et al.*, 1997

Table 6.1 Cont'd

Aerosol type	Compound	Date	m_r	b_r	TSP[a] (μg/m^3)	a_{TSP} (m^2/g)	$m_{r,s}$	$b_{r,s}$	Reference
UPM, Denver	*n*-alkanes	07/85 to 01/86	-0.86	-7.29	27 to 157	3.05	-0.86	-1.77	Foreman and Bidleman, 1990
UPM, Portland	*n*-alkanes	02/88 to 12/88	-1.00	-8.06	51	2.53	-1.00	-2.45	Hart, 1989
$(NH_4)_2SO_{4(s)}$ (42% RH)	*n*-alkanes	08/96	-0.96	-7.66	109	17.5	-0.96	-3.31	Liang *et al.*, 1997
QFF (42% RH)	*n*-alkanes					1.65	-1.03	-3.85	Liang *et al.*, 1997
QFF (70% RH)	*n*-alkanes					1.65	-1.01	-3.94	Storey *et al.*, 1995

[a] measured values unless specified otherwise

[b] value for the winter UPM in Pittsburgh, PA (Corn *et al.*, 1971)

[c] average value for the summer UPM in Pittsburgh, PA (Corn *et al.*, 1971) and the summer UPM in Portland, OR (Sheffield and Pankow, 1994)

[d] mean TSP level for Portland, OR (Oregon Department of Environmental Quality, 1985 and 1986)

[e] average value for the summer UPM in Portland, OR (Sheffield and Pankow, 1994) and the winter UPM in Pittsburgh, PA (Corn *et al.*, 1971)

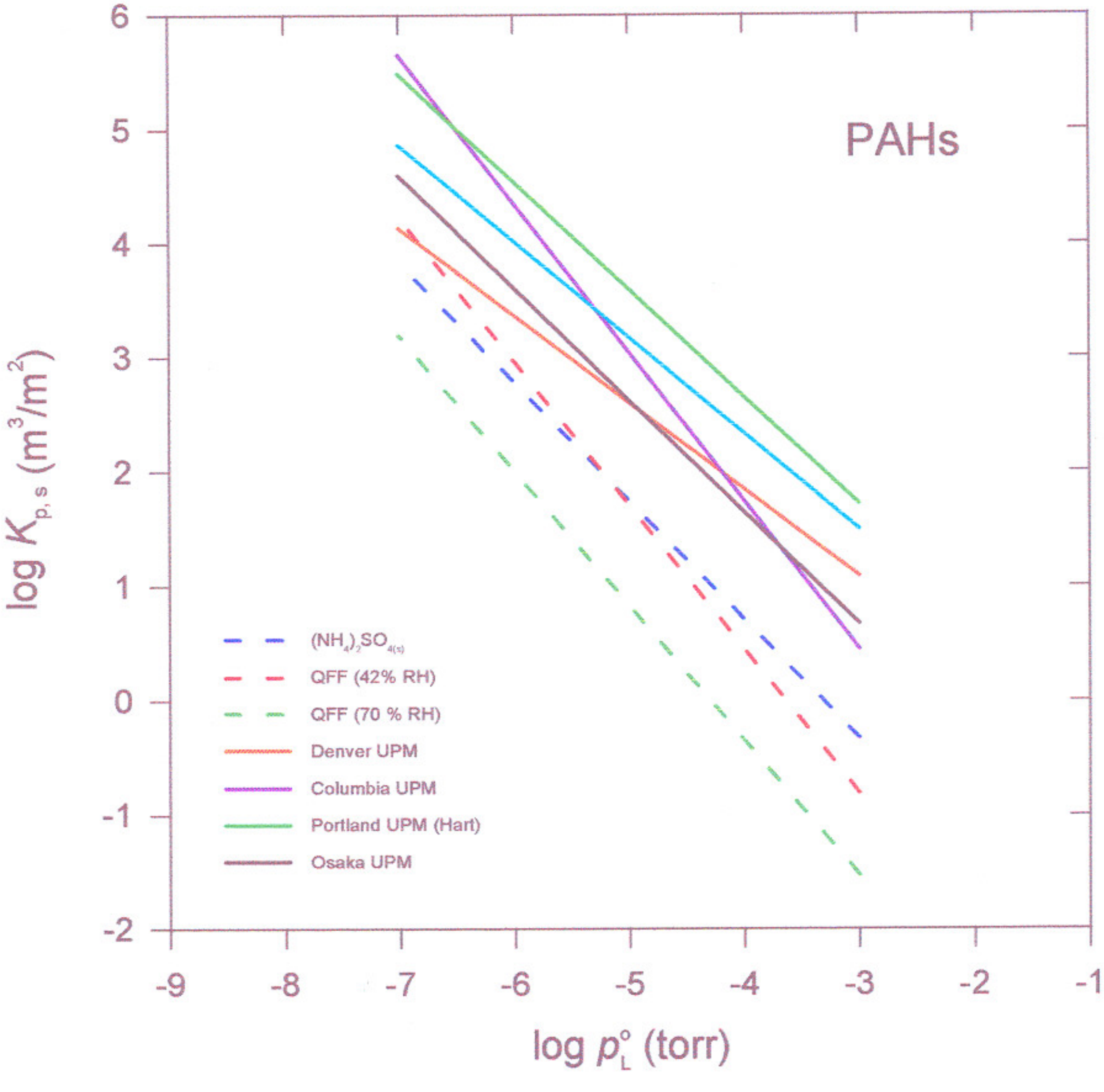

Figure 6.1 Comparison of log $K_{p,s}$ vs. log p_L° correlation for PAHs to UPM collected in different regions, QFF (quartz fiber filter), and $(NH_4)_2SO_{4(s)}$.

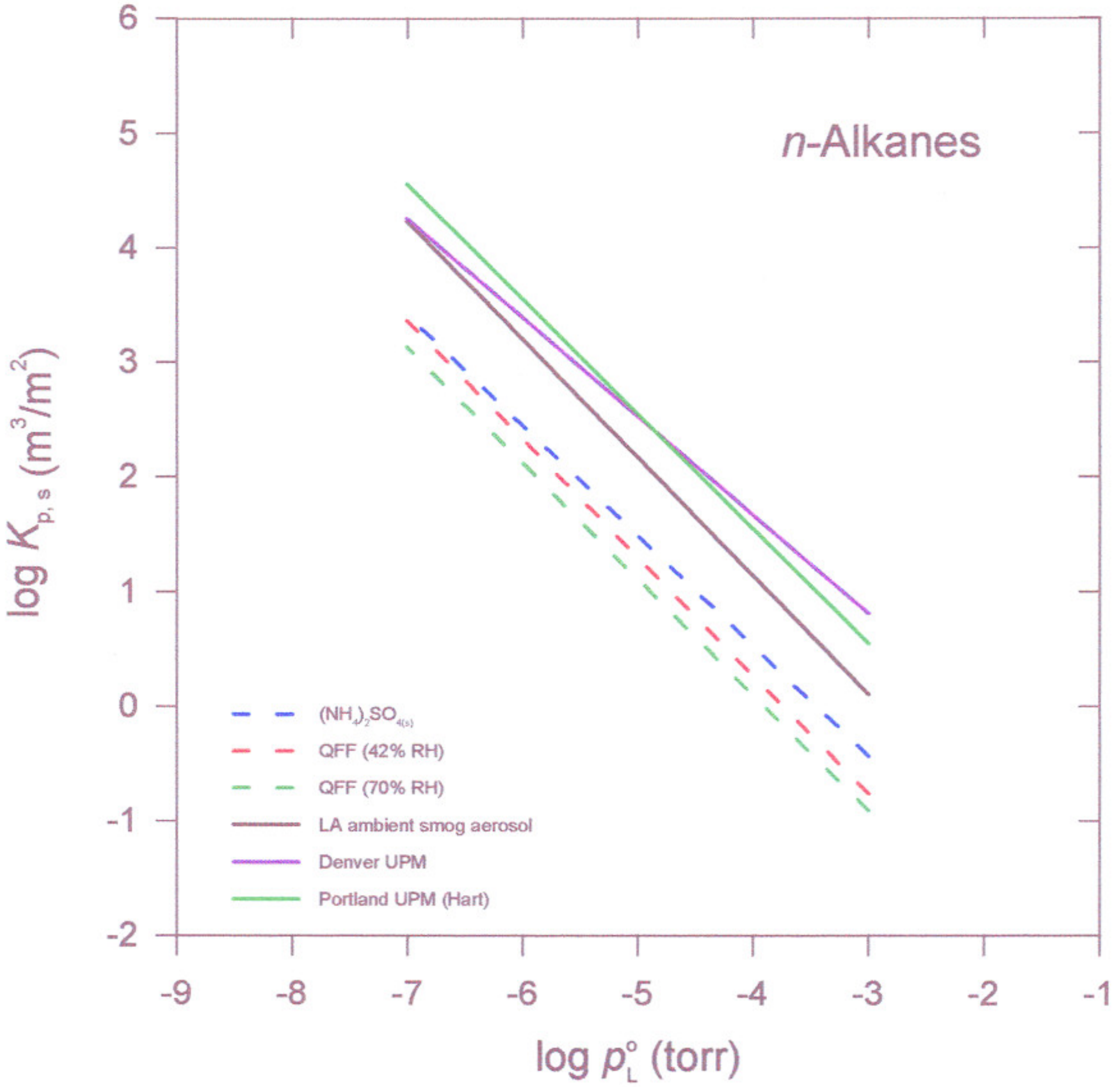

Figure 6.2 Comparison of log $K_{p,s}$ vs. log p_L^o correlation for n-alkanes to UPM collected in different regions, QFF (quartz fiber filter), and $(NH_4)_2SO_{4(s)}$.

RH increases. The 24-hr mean RH in Osaka, Japan from 1977 to 1978 has been estimated to be 72 % (Yamasaki *et al.*, 1982; Storey, 1993). The RH for Portland were compiled from the reported data for Portland International Airport measured by National Weather Service in 1988, and the average annual RH was calculated to be 74%. This average RH number was also considered applicable to the Portland UPM sampling in 1984-1985 of Ligocki and Pankow (1989). No RH data were available for the Denver and Columbia sampling events. Since the sampling carried out in these two regions was over a period of more than 6 months (see Table 1), the average RH is likely to fall between 40 to 70% RH. LA ambient smog sampling was carried out at 42% RH (Liang *et al.*, 1997).

Normalizing measured log K_p values by an estimate of a_{TSP} allows one to test whether adsorption is an important partitioning mechanism for UPM. As seen in Figure 6.1, the calculated log $K_{p,s}$ values for sorption to Portland UPM and Osaka UPM are much larger (4 log units and 3 log units, respectively) than those for sorption to QFF at RH = 70%. The calculated log $K_{p,s}$ values for sorption to both Denver and Columbia UPM are much larger than those to $(NH_4)_2SO_{4(s)}$ aerosol and QFF as extrapolated to RH = 42% and QFF at RH = 70%.

The partitioning of the *n*-alkanes to the UPM in different regions is considered in Figure 6.2. On average, the partitioning of the *n*-alkanes to the UPM considered here is weaker than that of the PAHs. The calculated log $K_{p,s}$ values for the *n*-alkanes sorbing to the LA ambient smog samples at RH = 42% are much larger than those for sorption to $(NH_4)_2SO_{4(s)}$ aerosol as extrapolated to RH = 42% as discussed in Chapter Four. As for the sorption of *n*-alkanes to Denver and Portland UPM, the partitioning is much larger than that for both $(NH_4)_2SO_{4(s)}$ aerosol and QFF as extrapolated to RH = 42% and QFF at RH =70% (about 1.5 to 2 log units).

The discussions above suggest that adsorption is not the operative mechanism controlling the partitioning of PAHs and *n*-alkanes to UPM considered here, and that the log $K_{p,s}$ values calculated for the PAHs and *n*-alkanes sorbing to the UPM are not physically meaningful quantities.

6.3.2 Absorptive Partitioning

When absorption into a liquid (or at least amorphous) organic matter (om) phase is the dominant sorption mechanism, an om-phase-normalized constant $K_{\mathrm{p,om}}$ can be defined as equation (4-7). In this case, the weight fraction of the TSP that comprises the om phase (f_{om}) is very important. Since there is no direct method to measure f_{om} at this stage, f_{om} is estimated from the fraction of OC in the om phase (OC/TSP). For most of the regions studied here, the values of OC/TSP were taken directly from the reported carbon analyses data. When no OC/TSP data were available, the reported annual average data (Shah *et al.*, 1986) obtained for the same region were used.

As discussed in Chapter Four, when all the aerosol is secondary in nature, the mass of the om phase is typically 2.0 times the mass of total OC mass alone. When most of the aerosol is mainly primary in nature, the mass of the om phase is 1.2 times the mass of total OC alone. Keeping these guidelines in mind, the values for f_{om} in different regions were estimated based on the major sources of the aerosol and the time of the year when the sampling events occurred. The results are given in Table 2.

The corresponding regression parameters $m_{\mathrm{r,om}}$ and $b_{\mathrm{r,om}}$ are calculated according to equation (4-8). The results are given in Table 2. The log $K_{\mathrm{p,om}}$ vs. log p_L^o plots are given for PAHs and *n*-alkanes in Figure 6.3 and Figure 6.4, respectively. The log $K_{\mathrm{p,om}}$ vs. log p_L^o plots for PAHs and *n*-alkanes sorbing to ETS (Liang and Pankow, 1996), gasoline SOA (Liang *et al.*, 1997), and diesel combustion particles (Kamens *et al.*, 1995) are also considered and plotted in Figures 6.3 and 6.4, respectively.

As discussed in Chapter Three, for any given compound, using equation (3-13) to normalize the K_{p} values for two different samples of absorbing atmospheric particulate material will yield similar $K_{\mathrm{p,om}}$ values insofar as the samples are characterized by: 1) similar MW_{om} values; and 2) similar ζ values for the compound of interest (Pankow, 1997). It seems possible that both assumptions might be approximately valid for the ETS material, gasoline SOA, diesel combustion aerosol, and organic material found in UPM considered here.

For PAHs, the regression lines shown in Figure 6.3 for UPM collected in different regions lie very close to those for ETS and gasoline SOA. Subject to the validity of the

Table 6.2 Regression Coefficients ($m_{r,om}$ and $b_{r,om}$) of log $K_{p,om}$ vs. log p_L^o for PAHs and *n*-Alkanes sorbing to UPM, ETS, and Chamber-Generated Aerosol.

Aerosol type	Compound	Date	m_r	b_r	TSP[a] (μg/m^3)	TC/ TSP	OC/ TC	OC/ TSP	f_{om}	$m_{r,om}$	$b_{r,om}$	Reference
SOA from Gasoline* (Chamber)	PAHs	08/96	-1.05	-7.24	394 to 540				1.00	-1.05	-7.24	Liang *et al.*, 1997
ETS, Portland	PAHs	05/95	-1.02	-6.90	454.8				1.00	-1.02	-6.90	Liang and Pankow, 1996
Diesel combustion particles (Chamber)	PAHs		-0.97	7.52					0.2 to 0.4[b]	-0.97	-6.82 to -7.12	Kamens *et al.*, 1995
UPM, Denver	PAHs	07/85 to 01/86	-0.76	-6.71	27 to 157	0.11[c]	0.65[c]	0.07	0.09[d]	-0.76	-5.70	Foreman and Bidleman, 1990
UPM, Columbia* (Lab work)	PAHs	10/84 to 08/85	-1.30	-9.15	46.6 to 59.4	0.12 to 0.19	0.59[c]	0.09	0.11[d]	-1.30	-8.19	Foreman and Bidleman, 1987

Table 6.2 Cont'd

Aerosol type	Compound	Date	m_r	b_r	TSP (μg/m^3)	TC/ TSP	OC/ TC	OC/ TSP	f_{om}	$m_{r,om}$	$b_{r,om}$	Reference
UPM, Portland*	PAHs	1984 to 1985	-0.84	-6.54	30[e]	0.33		0.2 to 0.3[f]	0.24 to 0.36[d]	-0.84	-5.92 to -6.10	Ligocki and Pankow, 1989
UPM, Portland*	PAHs	02/88 to 12/88	-0.94	-6.80	51			0.24[f]	0.29[d]	-0.94	-6.26	Hart, 1989
UPM, Osaka	PAHs	1977 to 1978	-0.98	-7.87					0.1[g]	-0.98	-6.87	Yamasaki *et al.*, 1982
UPM, Los Angeles*	*n*-alkanes	08/96	-1.03	-8.68	108	0.21	0.87	0.2	0.29[h]	-1.03	-8.14	Liang *et al.*, 1997
SOA from Gasoline*	*n*-alkanes	08/96	-1.09	-8.37	394 to 540				1.00	-1.09	-8.37	Liang *et al.*, 1997
ETS, Portland	*n*-alkanes	05/95	-0.86	-7.44	454.8				1.00	-0.89	-7.44	Liang and Pankow, 1996

Table 6.2 Cont'd

Aerosol type	Compound	Date	m_r	b_r	TSP (μg/m^3)	TC/ TSP	OC/ TC	OC/ TSP	f_{om}	$m_{r,om}$	$b_{r,om}$	Reference
UPM, Denver	*n*-alkanes	07/85 to 01/86	-0.86	-7.29	27 to 157	0.11[c]	0.65[c]	0.1	0.09[d]	-0.86	-6.22	Foreman and Bidleman, 1990
UPM, Portland*	*n*-alkanes	02/88 to 12/88	-1.00	-8.06	51			0.24[f]	0.29[d]	-1.00	-7.51	Hart, 1989

* gas adsorption correction was included

[a] measured values except specified otherwise

[b] personal communication with Jay R. Odum (1997)

[c] adapted from Shah *et al.*, 1986

[d] mass of om phase is estimated to be 1.2 times of mass of OC alone (Countess *et al.*, 1980)

[e] mean TSP level in Portland (Oregon Department of Environmental Quality, 1985, 1986)

[f] sample event average

[g] from Liang and Pankow, 1996

[h] mass of om phase is estimated to be 1.2 times of mass of OC alone (Liang *et al.*, 1997)

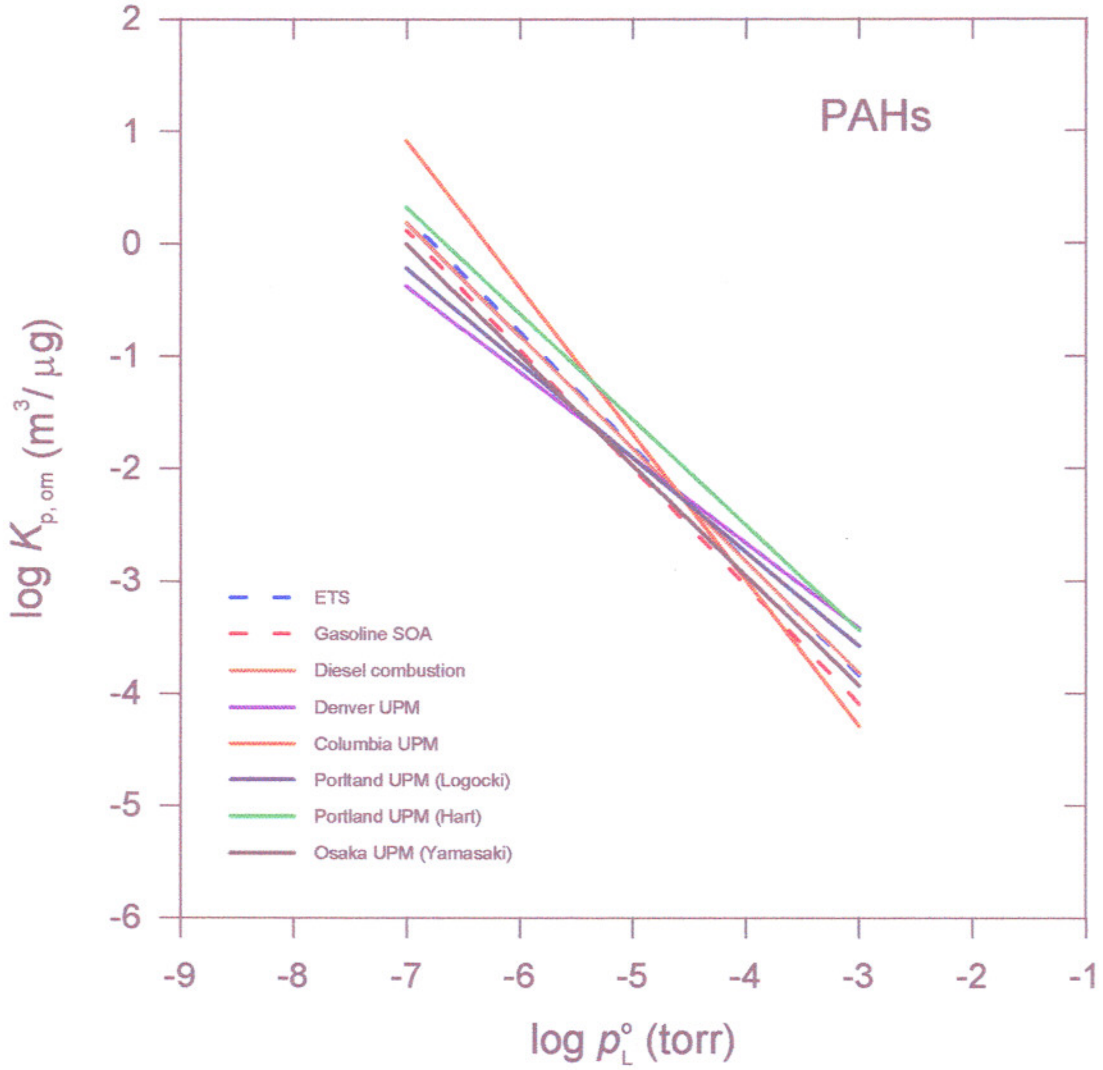

Figure 6.3 Comparison of log $K_{p,om}$ vs. log p°_L correlation for PAHs to UPM collected in different regions, diesel combustion aerosol, environmental tobacco smoke (ETS), and gasoline secondary organic aerosol (SOA).

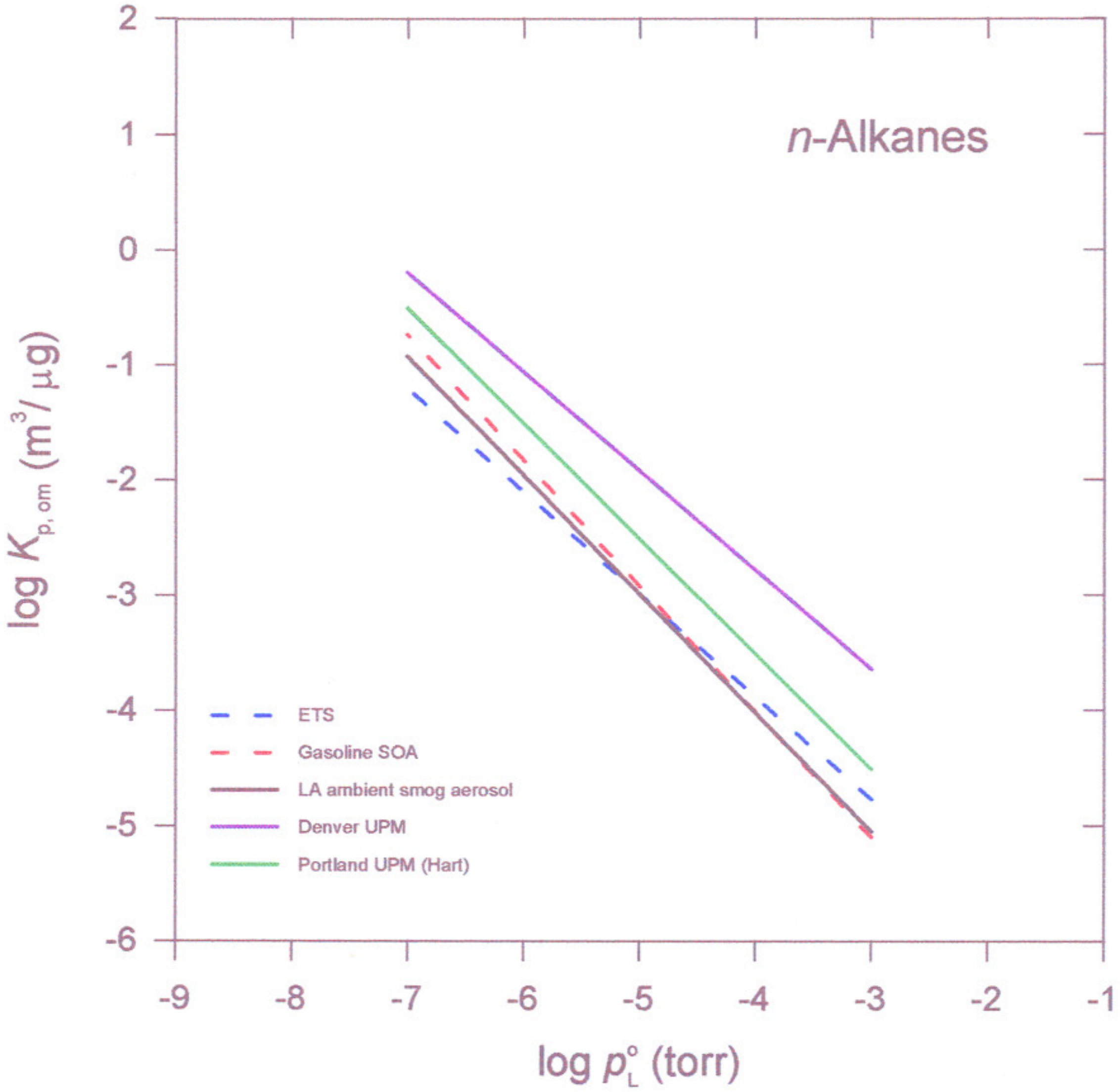

Figure 6.4 Comparison of log $K_{p,om}$ vs. log p°_L correlation for *n*-alkanes to UPM collected in different regions, environmental tobacco smoke (ETS), and gasoline secondary organic aerosol (SOA).

assumptions discussed above regarding MW_{om} and ζ, as well as the accuracy of the values of f_{om}, very good agreement is observed among the ETS, gasoline SOA, and UPM lines in this figure. Since the dominant controlling mechanism for SOCs sorbed to ETS and gasoline SOA is concluded to be absorption (Liang and Pankow, 1996; Liang *et al.*, 1997), the agreement is supportive of the hypothesis that absorptive partitioning is the dominant mechanism for PAHs partitioning to UPM. The f_{om}-normalized log K_p values for diesel combustion aerosol are very close to those for gasoline SOA, which suggests that equations (4-7) and (4-8) can correctly describe the G/P partitioning of PAHs to both primary and secondary aerosol.

As seen in Figure 6.4, sorption of *n*-alkanes to LA UPM is very similar to that to ETS and gasoline SOA as shown in Chapter Four. On the other hand, sorption to Denver UPM is much larger than that to ETS and gasoline SOA. As we discussed earlier, no gas adsorption artifact corrections were carried for this data set, which might cause some errors in the reported values of log K_p. Differences in the values of log K_p before and after gas adsorption corrections for both PAHs (Ligocki and Pankow, 1989; Hart, 1989) and *n*-alkanes (Hart, 1989) are studied here to provide information on the errors on log K_p contributed from gas adsorption. The results for PAHs are given in Figures 6.5 and 6.6, and the results for *n*-alkanes are given in Figure 6.7.

The results in Figures 6.5 and 6.6 show that the difference between the corrected and uncorrected log $K_{p,om}$ values for PAHs is indistinguishable, therefore, gas adsorption corrections are fairly small for PAHs. Hart and Pankow (1994) have reported that the values of K_p for PAHs could be overestimated by an average factor of 1.2-1.6, which gives the values of log K_p being overestimated by only 0.08-0.2. If the regression line for Denver UPM in Figure 6.3 is lowered by 0.08 to 0.2 log unit, the conclusions we made for PAHs in Figure 6.3 remain unchanged. On the other hand, as shown in Figure 6.7, the corrected log $K_{p,om}$ values for *n*-alkanes is about 1.0 log unit lower than those without gas adsorption correction. The reason for the different behavior between PAHs and *n*-alkanes might be due to the stronger adsorption of *n*-alkanes on the filters than adsorption of PAHs. For three-ring and four-ring PAHs, 14% and 10% of that on the front filter were found on the backup filter,

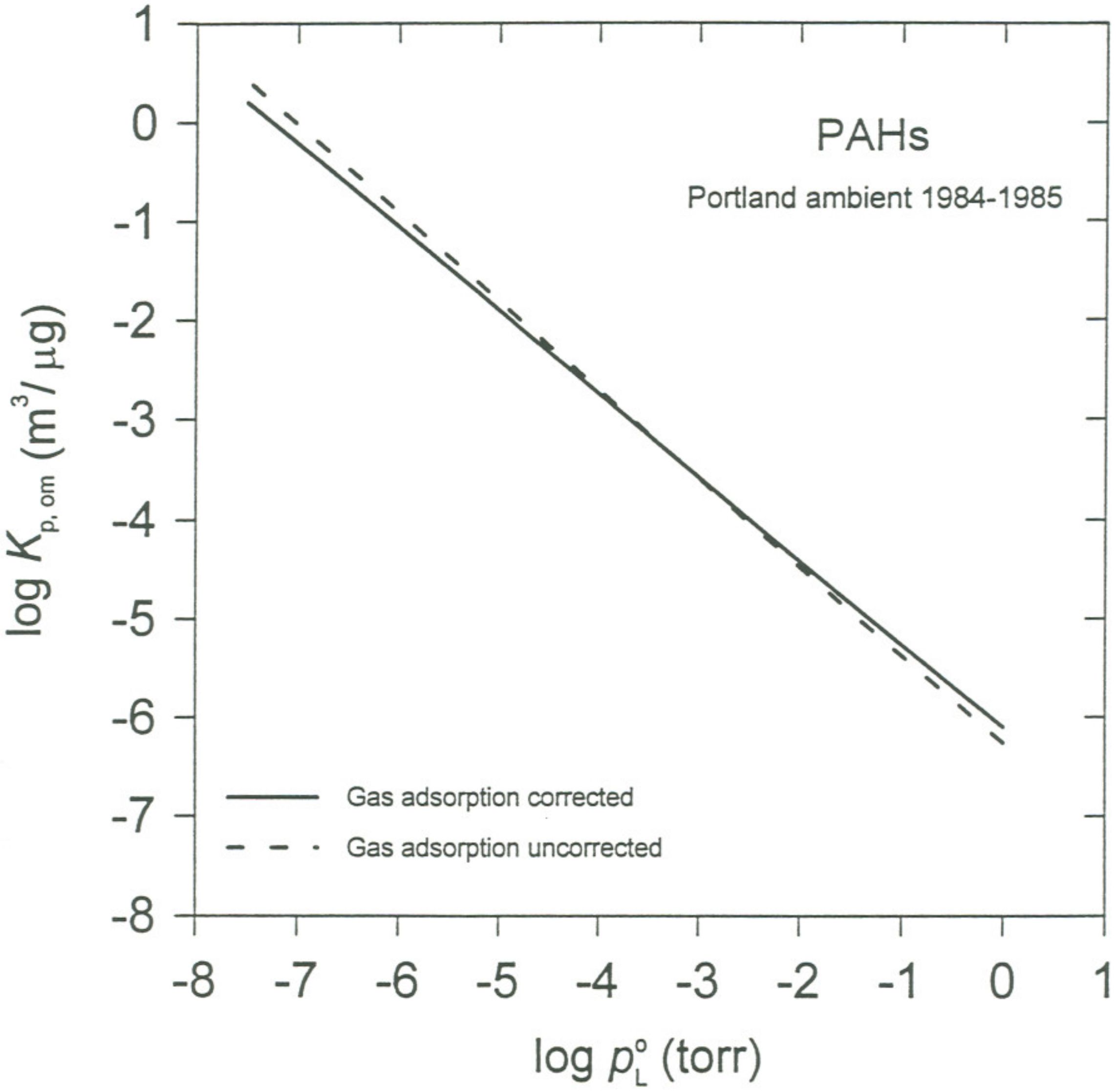

Figure 6.5 Comparison of $K_{p,om}$ vs. log p_L^o correlations for PAHs with and without gas adsorption corrections for Portland UPM collected in 1984 to 1985.

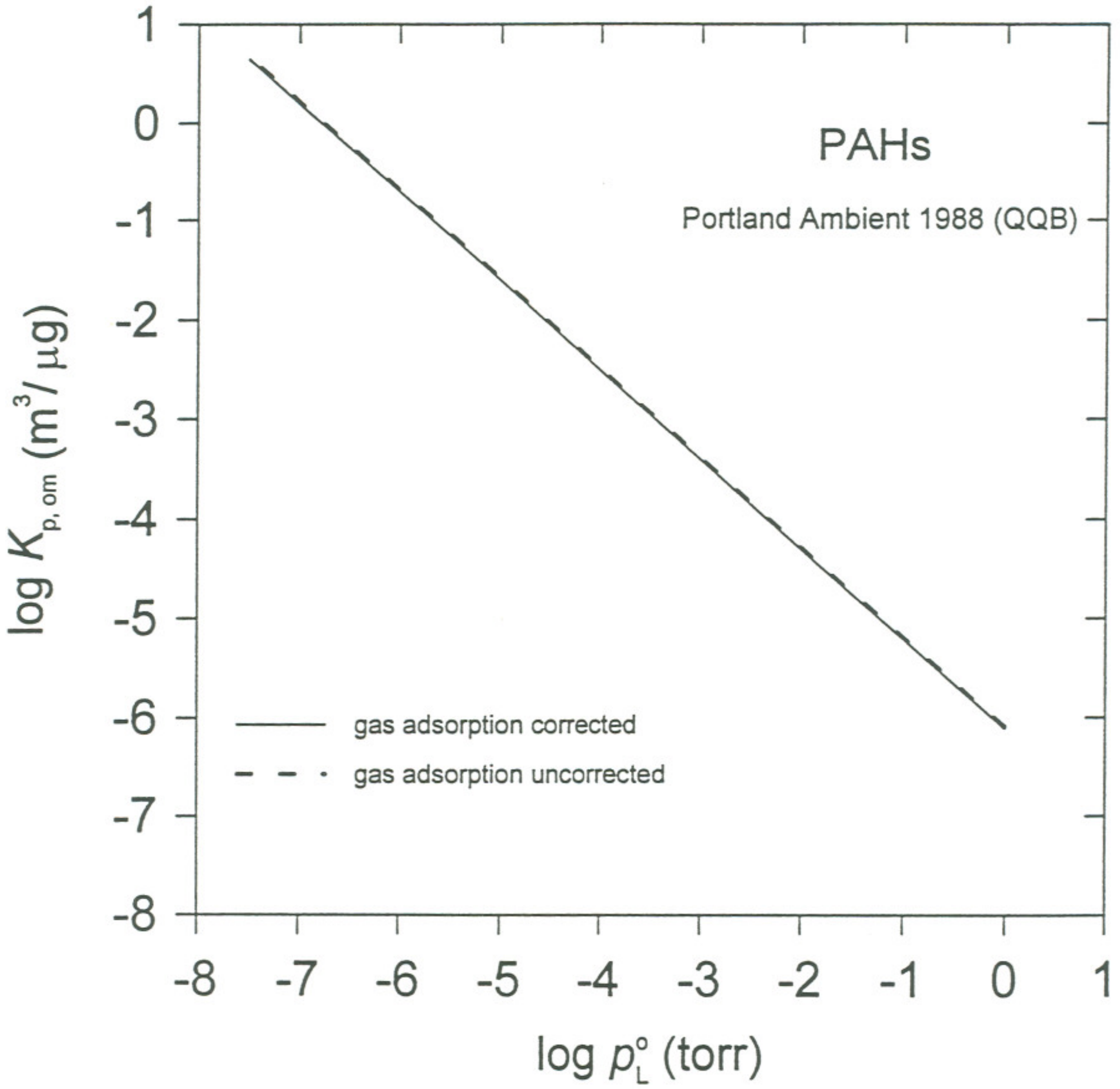

Figure 6.6 Comparison of $K_{p,om}$ vs. log p_L^o correlations for PAHs with and without gas adsorption corrections for Portland UPM collected in 1988.

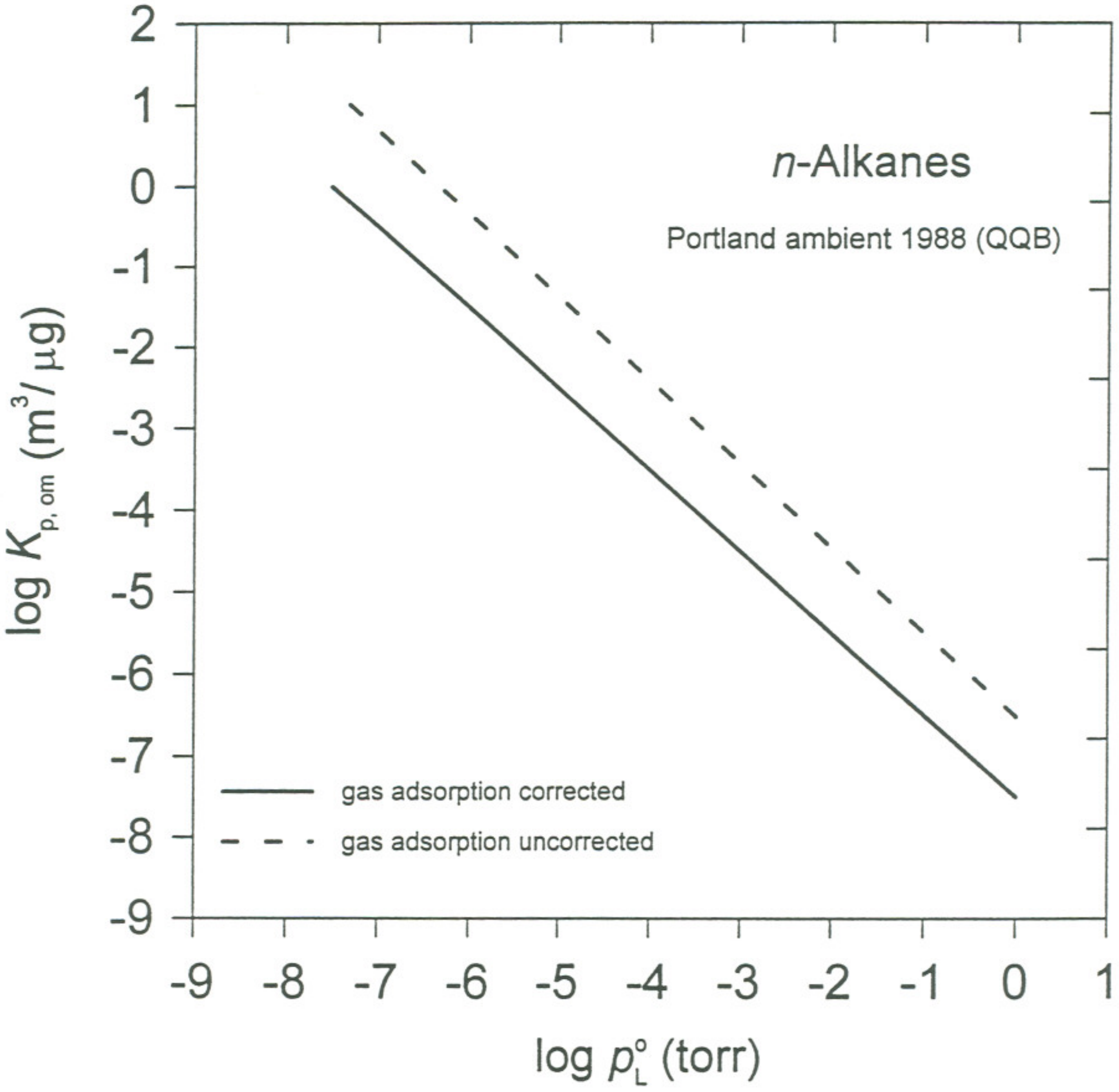

Figure 6.7 **Comparison of $K_{p,om}$ vs. log p_L^o correlations for *n*-alkanes with and without gas adsorption corrections for Portland UPM collected in 1988.**

respectively (Cotham and Bidleman, 1995), whereas for eicosane, 71% of the front filter mass was found on the backup filter (Ligocki and Pankow, 1989). Therefore, the *n*-alkanes require significant gas adsorption corrections. Assuming that the magnitude of gas adsorption for *n*-alkanes during the Denver sampling was the same as that for Portland, the regression line for Denver UPM in Figure 6.4 was shifted downward by the same distance as the difference between the corrected and uncorrected values as shown in Figure 6.7. The corrected Denver UPM data are then plotted in Figure 6.8. After the gas adsorption correction, the sorption of *n*-alkanes to the Denver UPM is very similar to that to ETS, gasoline SOA, and LA UPM. The regression line for Portland UPM is about 0.5 log unit above the other regression lines in Figure 6.8, which is much smaller than the distance (1.5 to 2.0 log unit) of the same regression line above the regression line for QFF at RH = 70% in Figure 6.2. This indicates that absorption is a more dominant mechanism than adsorption for *n*-alkanes sorbed to Portland UPM. Therefore, we conclude that absorptive partitioning is the dominant mechanism for *n*-alkanes partitioning to UPM studied here.

6.4 Conclusions

Comparison of the literature data on sorption of PAHs and *n*-alkanes to UPM with those presented in Chapter Three and Four gives fairly strong evidence that absorption is the dominant mechanism for partitioning of both PAHs and *n*-alkanes to the UPM considered here. Since the selected UPM data were obtained in different regions in the world and different seasons, these data could be more or less representative. Therefore, the conclusions obtained here for sorption of PAHs and *n*-alkanes to UPM in the selected regions may be applicable to UPM in other regions with the similar characteristics.

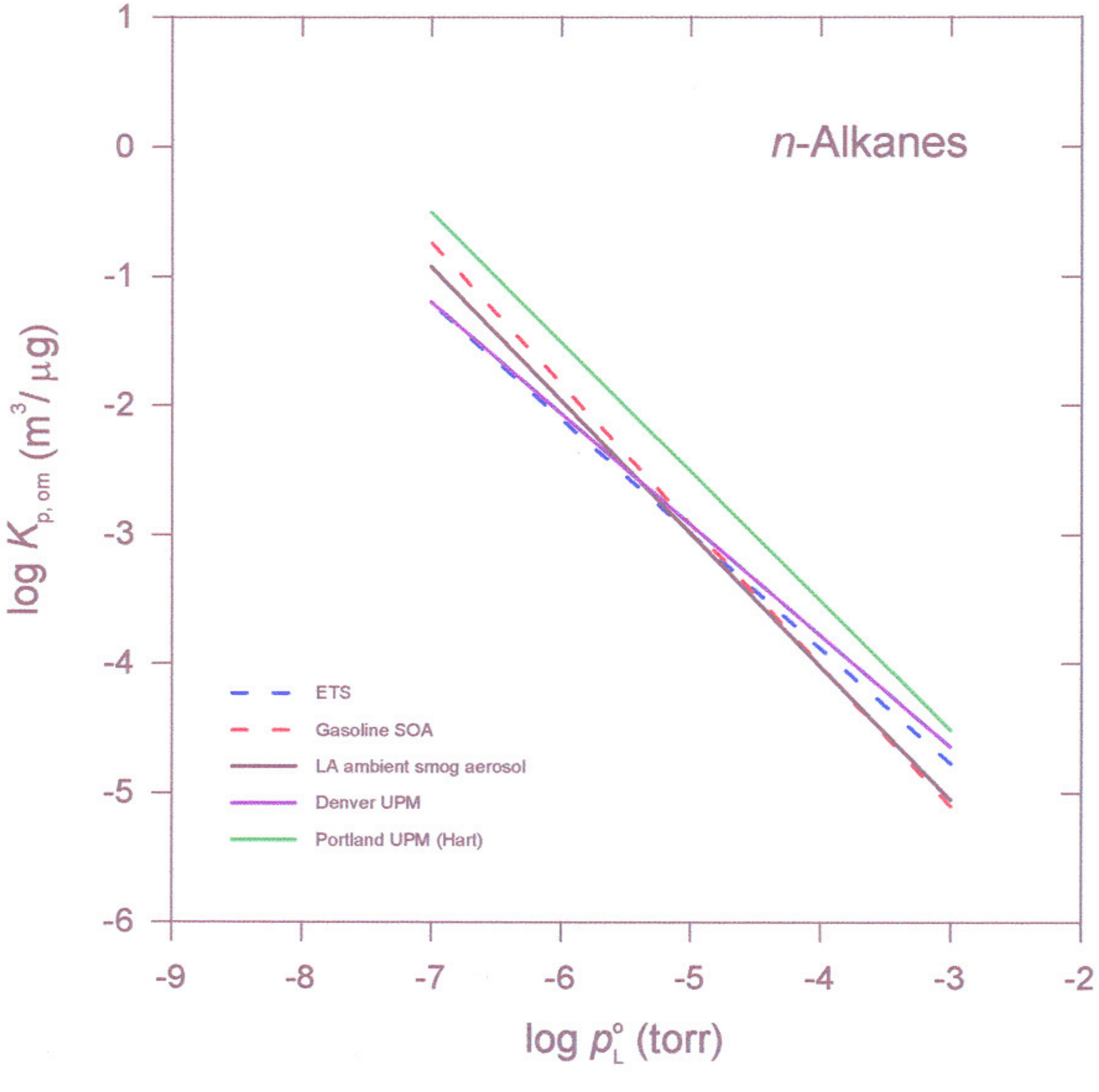

Figure 6.8 Comparison of log $K_{p,om}$ vs. log p_L° correlation for *n*-alkanes to UPM collected in different regions, environmental tobacco smoke (ETS), and gasoline secondary organic aerosol (SOA) after gas adsorption corrections.

CHAPTER 7

SUMMARY

An overview of current gas/particle (G/P) partitioning theory has been presented with emphasis on recent research into the partitioning behavior of semivolatile organic compounds (SOCs) to model inorganic aerosol, model organic aerosol, and urban particulate material (UPM). By normalizing the measured partitioning coefficients (log K_p) with the corresponding specific surface area of the adsorbing solid (a_{TSP}, m^2/g) , the G/P partitioning of PAHs and *n*-alkanes to UPM collected in Columbia, Denver, Los Angles, Portland, and Osaka was much stronger than the partitioning to quartz and $(NH_4)_2SO_{4(s)}$ surfaces. This phenomenon indicates that *ad*sorption is not the operative mechanism controlling the partitioning of PAHs and *n*-alkanes to UPM considered here. On the other hand, by normalizing log K_p with the weight fraction of the TSP that comprises the organic matter (om) phase (f_{om}) , very similar behavior of the G/P partitioning of PAHs and *n*-alkanes to UPM was observed as compared to the partitioning to environmental tobacco smoke (ETS), secondary organic aerosol (SOA) generated from whole gasoline vapor, organic aerosol comprised of dioctyl phthalate, and diesel combustion particles. This finding provides further evidences that *ab*sorption is the dominant mechanism controlling the G/P partitioning of PAHs and *n*-alkanes to UPM considered here.

When absorption is the dominant mechanism for sorption, number-average mean molecular weight of the om phase (MW_{om}) is a very important parameter. Since the presence of water has a large effect on the final value of MW_{om} and since the water content in the om phase varies with the conditions under which the samples are collected (*e.g.* relative humidity) and the polarity of the om phase, it is desirable to obtain a MW_{om} value in the absence of the effects of variable amounts of water. An experimental apparatus was therefore designed to accomplish this requirement. Considering the success of removing almost all the water from the water-saturated methylene chloride solution in the efficiency test, it is reasonable to believe that this approach was efficient enough to remove most of the water from the ETS extracts before the MW_{om} measurements were carried out. MW_{om} were measured by vapor pressure osmometry and as derived from the log K_p value of water sorbed to the ETS particles. These two methods provided good agreement with average values of MW_{om} to be 231.

The elemental analyses (CHNS and O analyses) of ETS particles reveal that the ETS matrix is comprised of 71% of carbon, 9% of hydrogen, 5% of nitrogen, and 17% oxygen (w/w), with only trace amounts of sulfur present. The relatively high percentage of oxygen in the ETS matrix and the large amount of water (15% by weight) present in the ETS matrix indicate that the ETS matrix is quite polar, which is consistent with the derived activity coefficient of water (ζ_w) in ETS matrix being very closed to 1.0. Infrared adsorption spectroscopy data provide further evidence on the presence of large quantities of oxygen-containing compounds in the ETS matrix.

Elemental analyses were also carried out for the Los Angeles ambient smog aerosol samples. Carbon and oxygen accounted for 21 and 43% of the TSP, respectively. Independent carbon analyses gave TC/TSP being 0.20, which was in excellent agreement with the TC/TSP of 0.21 obtained from the CHNS analyses. Since no special measurements were taken to determine nitrate loss during our ambient smog aerosol sampling, it is impossible to correct for any nitrate losses, so that the N data obtained by the CHNS analyses may be unreliable for the actual aerosol at the time of sampling, and was therefore discarded. By incorporating these data with the reported chemical composition data obtained under similar sampling conditions (Larson and Cass, 1989), the mass of om was estimated to be 1.9 times of the mass of organic carbon (OC) alone. The multiple factor of 1.9 is agreeable with the suggested value of 1.6 in the literature.

In light of the results of this study, the following five areas of future work can be suggested: 1) development of an activity coefficient prediction model for complex mixtures using the UNFAC (universal function group activity coefficient) approach; 2) mean molecular weight measurements for UPM; 3) determination of how the partitioning of inorganics and organics affect each other since water in aerosols might affect the partitioning of organics; 4) identification and determination of the relative importance of compounds that are actually contributing significantly to the aerosol mass, including the dependence on air parcel history, etc.; and 5) design of better apparatus for accurate G/P partitioning measurements.

CHAPTER 8

REFERENCES

Adams J., Menzies K., and Levins P. (1977) Selection and evaluation of sorbent resins for the collection of organic compounds. *US Environmental Protection Agency Report (EPA-600-7-77-0445)*, Springfield, VA.

Ando M., Tamura K., and Katagiri K. (1991) Study on suspended particulate matter and polycyclic aromatic hydrocarbons in indoor and outdoor air. *Int. Arch Occup. Environ. Health* **63**, 297-301.

Appel B. R., Wall S. M., Tokiwa Y., and Halk M. (1980) Simultaneous nitric acid, particulate nitrate and acidity measurements in ambient air. *Atmos. Environ.* **14**, 549-554.

Appel B. R., Tokiwa, Y., and Halk M. (1981) Sampling of nitrates in ambient air. *Atmos. Environ.* **15**, 283-289.

Arey J., Zielinska B., Atkinson R., and Winer A. M. (1987) Polycyclic aromatic hydrocarbons and nitroarene concentration in ambient air during a wintertime high NO2 episode in the Los Angeles Basin. *Environ. Sci. Technol.* **21**, 1437-1444.

Armitage A. K. and Turner D. M. (1970) Absorption of nicotine in cigarette smoke through the oral mucosa. *Nature*, **226**, 1231-1232.

Baker J. E. and Eisenreich S. J. (1990) Concentrations and fluxes of polycyclic aromatic hydrocarbons and polychlorinated biphenyls across the air-water interface of Lake Superior. *Environ. Sci. Technol.* **24**, 342-352.

Baker R. R. (1980) Mechanisms of smoke formation and delivery. *Recent. Adv. Tob. Sci.* **6**, 184-224.

Baker R. R. and Proctor C. J. (1990) The origins and properties of environmental tobacco smoke. *Environ. Int.* **16**, 231-245.

Ball W. P. and Roberts P. V. (1991) Long-ferm sorption of halogenated chemical by aquifer materials. Part 2. Intraparticle diffusion. *Environ. Sci. Technol.* **25**, 1237-1249.

Benner C. L., Bayona J. M., Cake F. M., Tang H., Lewis l., Crawford J., Lamb J. D., Lee M. L., Lewis E. A., Hansen L. D., and Eatough D. J. (1989) Chemical composition of environmental tobacco smoke. Part 2. Particulate-phase compounds. *Environ. Sci. Technol.* **23**, 688-699.

Berglund B., Berglund U., and Lindvall T. (1986) Assessment of discomfort and irritation from the indoor air. In *Proc. IAQ-86. American Society of Heating, Refrigerating and air Conditioning Engineers; Atlanta, GA*, 138-149.

Bertsch W., Chang R. C., and Zlatkis A. (1974) The determination of organic volatiles in air pollution studies: Characterization of profiles. *J. Chromatogr.* **301**, 448-453.

Betz W. R. and Firth M. C. (1988) Utilization of carbon-based adsorbents for monitoring adsorbates in various sampling modes of operation. *Proceedings, 1988 EPA/APCA International Symposium on Measurement of Toxic and Related Air Pollution, Research Triangle Park, NC*, 670-678.

Bidleman T. F. and Olney C. E. (1974) High volume collection of atmospheric PCB. *Bull. Environ. Contam. Toxicol.* **11**, 442-447.

Bidleman T. F., Billings W. N., and Foreman W. T. (1986) Vapor-particle partitioning of semi-volatile organic compounds: estimates from field collections. *Environ. Sci. Technol.* **20**, 1038-1043.

Bidleman T. F. (1988) Atmospheric processes. *Environ. Sci. Technol.* **22**, 316-367.

bin Abas M. R., Simoneit B. R. R., Elias V., Cabral J. A., and Cardoso J. N. (1995) Composition of higher molecular weight organic matter in smoke aerosol form biomass combustion in Amazonia. *Chemosphere* **30**, 995-1015.

Bjorseth A. *Handbook of Polycyclic Aromatic Hydrocarbons.* Marcel Dekker: New York, 1983.

Black A., Pritchared J. N., and Walsh M. (1987) An exposure system to assess the human uptake of airborne pollutants by radio-tracer. *J. Aerosol Sci.* **18**, 757-760.

Boulik T., Fried V., and Hala E. (1984) *The Vapor Pressure of Pure Substances: Selected Values of the Temperature Dependence of the Vapor Pressure of Some Pure Substances in the Normal and Low Pressure Region*, 2nd Ed; Elsevier Scientific Pub. Co.: New York.

Braubar N. (1995) Direct effects of nicotine on the brain: evidence for chemical addition. *Arch. Environ. Health* **50**, 263-266.

Brumley W. C., Brownrigg C. M., and Brilis G. M. (1991) Characterization of nitrogen-containing aromatic compounds in soil and sediment by capillary gas chromatography-mass spectrometry after fractionation. *J. Chromatogr.* **558**, 223-233.

Brunnemann K. D. and Hoffmann D. (1974) The pH of tobacco smoke. *Food Cosmet. Toxicol.* **12**, 115-124.

Burge D. E. (1977) Molecular weight determination by osmometry. *Am. Lab.* **9**, 41-51.

Cake F. M., Eatough D. J., Lewis E. A., Tang H., Hammond S. K., Leaderer B. P., Koutrakis P., Spengler J. D., Fasana A., McCarthy J., Ogden M. W., and Lewtas J. (1990) An intercomparison of sampling techniques for nicotine in indoor environments. *Environ. Sci. Technol.* **24**, 1196-1203.

Cautreels W. and Van Cauwenberghe, K. (1978) Experiments on the distribution of organic pollutants between airborne particulate matter and their corresponding gas phase. *Atmos. Environ.* **12**, 1133-1141.

Chuang J. C., Mack G. A., Kuhlman M. R., and Wilson N. K. (1991) Polycyclic aromatic hydrocarbons and their derivatives in indoor and outdoor air in an eight-home study. *Atmos. Environ.* **25B**, 369-380.

Cohen M. A., Ryan P. B., Yanagisawa Y., and Hammond S. K. (1990) The validation of a passive sampler for indoor and outdoor concentrations of volatile organic compounds. *J. Air Waste Manage.* **40**, 993-997.

Connaughton D. F., Stedingen J. R., Lion L. W., and Shuler M. L. (1993) Description of time-varying desorption kinetics: Release of naphthalene from contaminant soil. *Environ. Sci. Technol.* **27**, 2397-2403.

Conner J. M., Oldaker G. B., and Murphy J. J. (1990) Method of assessing the contribution of environmental tobacco smoke to respirable suspended particles in indoor environments. *Environ. Technol.* **11**, 189-196.

Corn M., Montgomery T. L., and Esmen N. A. (1971) Suspended particulate matter: seasonal variation in specific surface areas and densities. *Environ. Sci. Technol.* **5**, 155-158.

Cotham W. E. and Bidleman T. F. (1995) Polycyclic aromatic hydrocarbons and polychlorinated biphenyls in air at an urban and rural site near Lake Michigan. *Environ. Sci. Technol.* **29**, 2782-2789.

Cotham W. E. (1990) *Chemical and Physical Processes Affecting the Transport and Fate* *of Semivolatile Contaminants in the Environment*. Ph.D. Thesis, University of South Carolina, Columbia, SC.

Countess R. J., Wolff G. T., and Cadle S. H. (1980) The Denver winter aerosol: A comprehensive chemical characterization. *J. Air. Pollut. Control Assoc.* **30**, 1194-1200.

Coutant R. W., Lewis R. G., and Mulik J. D. (1986) Modification and evaluation of a thermally desorbable passive sampler for volatile organic compounds in air. *Anal. Chem.* **58**, 445-448.

Coutant R. W., Brown L., Chuang J. C., Riggin R. M., and Lewis, R. G. (1988) Phase distribution and artifact formation in ambient air sampling for polynuclear hydrocarbons. *Atmos. Environ.* **22**, 403-409.

Coutant R. W., Callahan P. J., Kumlman M. R., and Lewis R. G. (1989) Design and performance of a high-volume compound annular denuder. *Atmos. Environ.* **23**, 2205-2211.

Crank J. (1975) *The Mathematics of Diffusion.* 2nd Ed. Clarendon: Oxford.

Das A., Frenkel M., Gadalla N. A. M., Kudchadker S., Marsh K. N., Rodger A. S., and Wilhoit R. Ċ. (1993) Thermodynamic and thermophysical properties of organic nitrogen compounds. Part II. 1- and 2-butanamine, 2-methyl-1-propanamine, 2-methyl-2-propanamine, pyrrole, 1-, 2-, and 3-methylpyrrole, pyridine, 2-, 3-, and 4-methylpyridine, pyrrolidine, piperidine, indole, quinoline, isoquinoline, acridine, carbazole, phenanthridine, 1-and 2-naphthalenamine, and 9-methylcarbazole *J. Phys. Chem. Ref. Data* **22**, 659-782.

Dravnieks A., Krotoszynski B. K. Whitefield J., O'Donnel A., and Burgwald T. (1971) High speed collection of organic vapors from the atmosphere. *Environ. Sci. Technol.* **12**, 1220-1222.

Dube M. F. and Green C. R. (1982) Methods of collection of smoke for analytical purposes. *Recent Adv. Tob. Sci.* **8**, 42-102.

Eagle S. and Scott J. W. (1950) Liquid-phase adsorption equilibrium and kinetics. *Ind. Eng. Chem.* **42**, 1287-1294.

Eatough D. J., Benner C. L., Bayona J. M., Richard G., Lamb J. D., Lee M. L., Lewis E. A., and Hansen L. D. (1989) Chemical composition of environmental tobacco smoke. 1. Gas-phase acids and bases. *Environ. Sci. Technol.* **23**, 679-687.

Eudy L. W., Throne F. A., Heavor D. L., Green C. R., and Ingebrethsen B. J. (1985) Studies on the vapor-phase distribution of environmental nicotine by selected trapping and detection methods. Presented at 39th Tobacco Chemists Research Conference: Montreal.

Evan W. H. , Thomas N. C. , Boardman M. C., and Nash, S. J. (1993) Relationship of polycyclic aromatic hydrocarbon yield with particulate matter (water and nicotine free) yield in mainstream and sidestream cigarette smoke. *Sci. Tot. Environ.* **136**, 101-109.

Farrell J. and Reinhard M. (1994) Desorption of halogenated organic from model soil, sediments and soil under unsaturated condition. Part 2. Kinetics. *Environ. Sci. Technol.* **28**, 63-27.

Fletcher C. L. and McKay W. A. (1995) Polychlorinated dibenzo-p-dioxins and dibenzofurans in the aquatic environment: a literature review. *Chemosphere*, **25**, 1311-1316.

Foreman W. T. and Bidleman T. F. (1987) An experimental system for investigating vapor - particle partitioning of trace organic pollutants. *Environ. Sci. Technol.* **21**, 869-875.

Foreman W. T. and Bidleman T. F. (1990) Semivolatile organic compounds in the ambient air of Denver, Colorado. *Atmos. Environ.* **24A**, 2405-2416.

Forrest J., Tanner R. J., Spandau D., D'Ottavio T., and Newman L. (1980) Determination of total inorganic nitrate utilizing collection of nitric acid on NaCl - Impregnated filters. *Atmos. Environ.* **14**, 137-144.

Forstner H. J. L., Flagan R. C., and Seinfeld J. H. (1997) Secondary organic aerosol form the photooxidation of aromatic hydrocarbons: Molecular composition. *Environ. Sci. Technol.* **31**, 1345-1358.

Fraser M. P., Grosjean D. , Grosjean, E., Rasmussen R. A., and Cass, G. R. (1996) Air quality model evaluation data for organics. 1. Bulk chemical composition and gas/particle distribution factor. *Environ. Sci. Technol.* **30**, 1731-1743.

Fredenslund A., Jones R. L., and Prausnitz (1975) Group-contribution estimation of activity coefficients in nonideal liquid mixtures. *AICHE* **21**, 1086-1099.

Fredenslund A. and Sorensen J. M. (1994) Group contribution estimation methods. in *Models For Thermodynamic and Phase Equilibria Calculations*. Sandler S. I. Ed., Marcel Dekker, Inc: New York, 287-361.

Freedman A. M. (1995) Tobacco firm shows how ammonia spurs delivery of nicotine. *Wall Street Journal.* A1, Oct. 18.

Freudenthal R. and Jones P. W. (1978) *Carcinogenesis - Polynuclear Aromatic Hydrocarbons*. Raven Press: New York.

Fowler W. K. (1982) Fundamental of passive vapor sampling. *Am. Lab*. **14**, 80-87.

Gallant R. F., King J. W., Levins P. L., and Piecewice J. F. (1978) Characterization of sorbent resins for use in environmental sampling. *US Environmental Protection Agency Report* (*EPA- 600/7-78-54*), Springfield, VA.

Gartrell G. Jr. and Friedlander S. K. (1975) Relating particulate pollution to sources: the 1972 California aerosol characterization study. *Atmos. Environ.* **9**, 279-299.

Glantz S. A. and Parmley W. W. (1991) Passive smoking and heart disease: epidemiology, physiology and biochemistry. *Circulation* **83**, 1-12.

Glausch A., Hahn J., and Schurig V. (1995) Enantioselective determination of choral 2,2',3,3',4,6-hexachlorobiphenyl in human milk samples y multidimensional gas chromatography/electron capture detection and mass spectrometry. *Chemosphere* **30**, 2079-2086.

Gmehling J. (1986) Group contribution methods for the estimation of activity coefficients. *Fluid Phase Equilibria* **30**, 119-134.

Gold K. W., Naugle D. F., and Berry M. A. (1990) *Indoor Concentrations of Environmental Carcinogens*. Research Triangle Institute, Report Number 4479/07-F, P. O. Box 12194, Research Triangle Park, NC 27790-2194.

Goss K. U. (1992) Effects of temperature and relative humidity on the sorption of organic vapors on quartz sand. *Environ. Sci. Technol.* **26**, 2287-2294.

Goss K. U. (1994) Adsorption of organic vapors on polar mineral surfaces and on a bulk water surface: Development of an empirical predictive model. *Environ. Sci. Technol.* **28**, 640-645.

Goyer N. (1990) Chemical contaminants in office building. *Am. Ind. Hyg. Assoc. J.* **51**, 615-619.

Gray H. A. (1986) *Control of Atmospheric Fine Primary Carbon Particle Concentrations*. Ph.D. Thesis, California Institute of Technology, Pasadena, CA.

Gray H. A., Cass G. R., Huntzicker J. J., Heyedrahl E. K., and Rau J. A. (1984) Elemental and organic carbon particle concentration: A long-term perspective. *Sci. Tot. Environ.* **36**, 17-25.

Gray H. A., Cass G. R., Huntzicker J. J., Heyerdahl E. K., and Rau J. A. (1986) Characteristics of atmospheric organic and elemental carbon particle concentrations in Los Angeles. *Environ. Sci. Technol.* **20**, 580-589.

Griest W. H., Jenkins R. A., Tomkins B. A., Moneyhun J. H., Ilgner R. H., Gayle T. M., Higgins C. E., and Guerin M. R. (1988) Sampling and analysis of diesel engine exhaust and the motor pool workplace atmosphere. *Final report ORNL/TM-10689.*

Grimmer G., Naujack K. W., and Dettbarn G. (1987) Gas chromatographic determination of polycyclic aromatic hydrocarbons, aza-arenes, aromatic amines in the particle and vapor phase of mainstream and sidestream smoke of cigarette. *Toxicol. Let.* **35**, 117-124.

Grosjean D. and Friedlander S. K. (1975) Gas-particle distribution factor for organic and other pollutants in the Los Angeles atmosphere. *J. Air Pollut. Control Ass.* **25**, 1038-1044.

Guerin M. R. and Jenkins R. A. (1984) Analytical chemical methods for determination of environmental tobacco smoke constituents. *Eur J. Resp. Dis. Suppl.* **133**, 33-46.

Guerin M. R., Jenkins, R. A., and Tomkins, B. A. (1992) *The Chemistry of Environmental Tobacco Smoke: Composition and Measurement*. Lewis Publisher: Boca Raton.

Hammond S. K., Coghlin J., and Leaderer B. P. (1987) Field study of passive smoking exposure with passive sampler. *Proceedings of 4th International Conference on Indoor Air Quality and Climate*, **Vol. 2**, 131-136.

Hammond S. K. and Leaderer B. P. (1987) A diffusion monitor to measure exposure to passive smoking. *Environ. Sci. Technol.* **21**, 494-497.

Harley R. A., Hannigan M. P. and Cass G. R. (1992) Respeciation of organic gas emissions and the detection of excess unburned gasoline in the atmosphere. *Environ. Sci. Technol.* **26**, 2395-2408.

Hart K. M. (1989) *A Study of Atmospheric n-alkanes and PAHs and Their Distributions Between the Gaseous and Particulate Phases*. Ph.D. Thesis, Oregon Graduate Institute, Portland, OR.

Hart K. M., Isabelle L. M., and Pankow J. F. (1992) High-volume air sampler for particle and gas sampling. 1. Design and gas sampling performance. *Environ. Sci. Technol.* **26**, 1048-1052.

Hart K. M. and Pankow J. F. (1994) High-volume air sampler for particle and gas sampling. 2. use of backup filter to correct for the adsorption of gas-phase polycyclic aromatic hydrocarbons to the front filter. *Environ. Sci. Technol.* **28**, 655-661.

Hayes S. R. (1989) Estimating the effect of being indoor on total personal exposure to outdoor air pollution. *JAPCA*, **39**, 1453-1461.

Hildemann L. M., Markowski G. R., and Cass G. R. (1991) Chemical composition of emission from urban sources of fine aerosol. *Environ. Sci. Technol.* **25**, 744-759.

Hinckley D. A., Bidleman T. F., Foreman W. T., and Tuschall J. R. (1990) Determination of vapor pressure of nonpolar and semipolar organic compounds from gas chromatographic retention data. *J. Chem. Eng. Data* **35**, 232-237.

Hochhauser A. M., Benson J. D., Burns V. R., Gorse, R. A., Koehl W. J., Painter L. J.,Ribbon, B. H., Reuter R. M. and Rutherford J. A. (1991) Effects of gasoline sulfur level on mass exhaust emissions - Auto/oil air quality improvement research program. *SAE technical paper no. 912322*, Society of Automotive Engineers, Warren, PA.

Honeychuck R. V., Cruger T. W., and Milliken J. (1993) Molecular weight of C_{60} in solution by vapor pressure osmometry. *J. Am. Chem. Soc.* **115**, 3034-3035.

Houdt van J. J., Jongen W. M. F., Boley J. S. M., and Alink G. M. (1984) Mutagenic activity of airborne particles inside and outside homes. *Environ. Mutagen.* **6**, 861-869.

Ingebrethsen B. J. and Sears S. B. (1985) Particle size distribution measurements of sidestream cigarette smoke. Presented at *39th Tobacco Chemists' Research Conference: Montreal.*

Izumi K. and Fukuyama T. (1990) Photochemical aerosol formation from aromatic hydrocarbons in the presence of NO_x. *Atmos. Environ.* **24A**, 1433-1441.

Japar S. M., Szkariat A. C., Gorse R. A. Jr, Heyerdahl E. K., Johnson R. L., Rau J. A., and Huntzicker J. J. (1984) Comparison of solvent extraction and thermal-optical carbon analysis methods: Application to diesel vehicle exhaust aerosol. *Environ. Sci. Technol.* **28**, 231-234.

Jenkis R. A. and Gill B. E. (1980) Determination of oxides of nitrogen (NO_x) in cigarette smoke by chemiluminescent analysis. *Anal. Chem.* **52**, 925-928.

Johnson N. D., Barton S. C., Thomas G. H. S., Lane D. A., and Schroeder W. H. (1986) Evaluation of a denuder-based gas/particle sampler for chlorinated organic compounds. *Proc.* 1986 *EPA/APCA Symp. Measurement of Toxic Air Pollutants*, APCA Publication VIP-7, EPA report 600/9-86-013, 156-167.

Johnson W. R., Hale r. W., Nedlock J. W., Grubbs H. J., and Powell D. H. (1973) The distribution of products between mainstream and sidestream smoke. *Tob. Sci.* **17**, 141-144.

Johnson W. R. (1977) The pyrogenesis and physicochemical nature of tobacco smoke. *Recent Adv.Tob. Sci.* **3**, 1-27.

Johnstone R. A. W. and Plimmer J. R. (1959) The chemical constituents of tobacco and tobacco smoke. *Chem. Rev.* **59**, 885-936.

Jones K. C., Stratford J. A., Waterhouse K. S., Furlong E. T., Giger W., Hites R. A., Schaffner C., and Johnson A. E. (1989) Increase in the polynuclear aromatic hydrocarbon content of an agricultural soil over the last century. *Environ. Sci. Technol.* **23**, 95-101.

Junge C. E. (1977) Basic consideration about trace constituents in the atmosphere as related to the fate of global pollutants, in Fate of Pollutant in the Air and Water Environment, Part I, Suffet I. H. Ed; Wiley: New York; 7-26

Kado N. Y., Colome S. D., Kleinman M. T., Hsieh D. P. H., and Jaques P. (1994) Indoor-outdoor concentrations and correlations of PM10-associated mutagenic activity in nonsmokers' and asthmatics' homes. *Environ. Sci. Technol.* **28**, 1073-1078.

Kamens R., Odum J. R., and Fan Z. (1995) Some observations on times to equilibrium for semivolatile polycyclic aromatic hydrocarbons. *Environ. Sci. Technol.* **29**, 43-50.

Kasten P. P., Lapidus, L., and Amundson N. R. (1952) Mathematics of adsorption in beds. V. Effect of intraparticle diffusion in flow system in fixed beds. *J. Phys. Chem.* **56**, 683-688.

Kaupp H. and Vmlauf G. (1992) Atmospheric gas-particle partitioning of organic compounds: comparison of sampling methods. *Atmos. Environ.* **26A**, 2259-2267.

Katritzky A. R. and Rees C. W. (1984) *Comprehensive Heterocyclic Chemistry,* vol. IV; Pergamon Press: New York.

Kadowaki S. (1990) Characterization of carbonaceous aerosols in the Nagoya urban area. 1. Elemental and organic carbon concentrations and the origin of organic aerosols. *Environ. Sci. Technol.* **24**, 741-744.

Kadowaki S. (1994) Characterization of carbonaceous aerosols in the Nagoya urban area. 2. Behavior and origin of particulate *n*-alkanes. *Environ. Sci. Technol.* **28**, 129-135.

Keller C. D. and Bidleman, T. F. (1984) Collection of airborne polycyclic aromatic hydrocarbons and other organics with a glass fiber filter-polyurethane foam system. *Atmos. Environ.* **18**, 837-845.

Kirsten W. J. (1983) *Elemental Analysis: Ultramicro, Micro, and Trace Methods.* Academic Press: New York.

Konig J., Funcke W., Balfanz E., Grosch B., and Pott F. (1980) Testing a high volume sampler for quantitative collection of polycyclic aromatic hydrocarbons. *Atmos. Environ.* **14**, 609-613.

Koop E. J. (1988) *The Health Consequences of Smoking: Nicotine Addiction.* A Surgeon General Report.

Krieger M. S. and Hites R. A. (1994) Measurement of polychlorinated biphenyls and polycyclic aromatic hydrocarbons in air with a diffusion denuder. *Environ. Sci. Technol.* **28**, 1129-1133.

Larson S. M., Cass G. R., and Gray H. A. (1989) Atmospheric carbon particles and the Los Angeles visibility problem. *Aerosol Sci. Technol.* **10**, 118-130.

Larson S. M. and Cass G. R. (1989) Characteristics of summer midday low-visibility events in the Los Angeles area. *Environ. Sci. Technol.* **23**, 281-289.

Lebowitz M. D., Holberg C. J., Boyer B., and Hayes C. (1985) Respiratory symptoms and peak flow associated with indoor and outdoor air pollutants in the south west. *J. Air Pollut. Control. Ass.* **35**, 1154-1158.

Lewis J. and Jackson M. D. (1982) Modification and evaluation of a high-volume air sampler for pesticides and semi-volatile industrial organic chemicals. *Anal. Chem.* **54**, 592-594.

Lewtas J., Goto S., Williams K., Chuang J. C., Petersen B. A., and Wilson, N. K. (1987) The mutagenicity of indoor air particles in a residential pilot field study: application and evaluation of new methodologies. *Atmos. Environ.* **21**, 443-449.

Liang C. and Pankow J. F. (1996) Gas/particle partitioning of organic compounds to environmental tobacco smoke: Partition coefficient measurements by desorption and comparison to urban particulate material. *Environ. Sci. Technol.* **30**, 2800-2805.

Liang C., Pankow J. F., Odum J. R., and Seinfeld J. H. (1997) Gas/Particle Partitioning of Semi-Volatile Organic Compounds to Model Inorganic, Model Organic, and Ambient Smog Aerosols. *Environ. Sci. Technol.* in review.

Lide R. L. (1994) *CRC Handbook of Chemistry and Physics.* 75th edition, CRC Press: Boca, Raton.

Ligocki M. P. and Pankow J. F. (1985) Assessment of adsorption/solvent extracting with polyurethane foam and adsorption/thermal desorption with Tenax-GC for the collection and analysis of ambient organic vapors. *Anal. Chem.* **57**, 1138-1144.

Ligocki M. P. and Pankow J. F. (1989) Measurements of the gas/particle distributions of atmospheric organic compounds. *Environ. Sci. Technol.* **23**, 75-83.

Löfroth G., Nilsson L., and Alfheim I. (1983) *Short-term Bioassays in the Analysis of Complex Environmental Mixtures.* (edited by Waters M. D., Sandhu S. S., Lewtas J., Claxton L., and Nesnow S.) 515-525, Plenum: New York.

Löfroth G. and Lazaridis G. (1986) Environmental tobacco smoke: Comparative characterization by mutagenicity assays of sidestream and mainstream cigarette smoke. *Environ. Mutagen* **8**, 693-704.

Löfroth G., Burton R. M., Forhand L., Hammond S. K., Sella R. L., Zweidinger R. B., and Lewtas J. (1989) Characterization of environmental tobacco smoke. *Environ. Sci. Technol.* **23**, 610-614.

Loganathan B. G., Kannan K., Watanabe I., Kawano M., Irvine K., Kumar S., and Sikka H. (1995) Isomer-specific determination and toxic evaluation of polychlorinated biphenyls, polychlorinated/brominated dibenzo-p-dioxins and dibenzofurans, polybrominated biphenyl ethers, and extractable organic halogen in carp from the Buffalo River, New York. *Environ. Sci. Technol.* **29**, 1832-1838.

Luo W., Liang C., and Pankow J. F. (1996) Unpublished data. Oregon Graduate Institute, Portland, OR.

Maroni M., Seifert B., and Lindvall T. (1995) I*ndoor Air Quality: A Comprehensive Reference Book.* Air Quality Monographs, **Vol 3**; Elsevier: New York.

Mason B. and Moore C. B. (1982) *Principles of Geochemistry.* John Wiley & Son: New

York.

McDow S. R. (1986) *The Effect of Sampling Procedures on Organic Aerosol Measurement.* Ph.D. Thesis, Oregon Graduate Institute, Portland, OR.

McDow S. R. and Huntizcker J. J. (1990) Vapor adsorption artifact in sampling of organic aerosol: face velocity effects. *Atmos. Environ.* **24A**, 2563-2571.

McDow S. R., Sun Q. R., Vartiainen M., Hong Y. S., Yao Y. L., Fister T., Yao R. Q., and Kamens R. M. (1994) Effect of composition and state of organic compounds on polycyclic aromatic hydrocarbon decay in atmospheric aerosols. *Environ. Sci. Technol.* **28**, 2147-2153.

McGarry J. (1983) Correlation and prediction of the vapor pressure of pure liquids over large pressure ranges. *Ind. Eng. Chem. Process Des. Dev.* **22**, 313-322.

Means J. C., Wood S. G., Hassett J. J., and Banward W. L. (1980) Sorption of polynuclear aromatic hydrocarbons by sediments and soils. *Environ. Sci. Technol.* **14**, 1524-1531.

Menzie C. A., Potocki B. B., and Santodonato J. (1992) Exposure to carcinogenic PAHs in the environment. *Environ. Sci. Technol.* **26**, 1278-1284.

Mitra S. and Ray B. (1995) Patterns and sources of polycyclic aromatic hydrocarbons and their derivatives in indoor air. *Atmos. Environ.* **29**, 3345-3356.

Morie G. P.(1972) Fraction of protonated and unprotonated nicotine in tobacco smoke at various pH values. *Tobacco Sci.* **16**, 167.

Mumford J. L., Harris D. B., Willians K., Chuang J. C., and Cooke M. (1987) Indoor air sampling and mutagenicity studies of emissions from unvented coal combustion. *Environ. Sci. Technol.* **21**, 308-311.

National Research Council (NRC) (1986) *Environmental Tobacco Smoke: Measuring Exposures and Assessing Health Effects.* National Academy Press: Washington, DC.

Ngabe B. and Bidleman T. F. (1992) Occurrence and vapor particle partitioning of heavy organic compounds in ambient air in Brazzaville, Congo. *Environ. Sci. Technol.* **76**, 147-156.

Nowak R. (1994) Nicotine scrutinized as FDA seeks to regulate cigarettes. *Science* **264**, 1555-1556.

O'Brien R. J., Crabtree J. H., Holmes J. R/, Hoggan M. C., and Bockian A. H. (1975)

Formation of photochemical aerosol from hydrocarbons. *Environ. Sci. Technol.* **9**, 577-582.

Oddson J. K., Letey J., and Weeks L. V. (1970) Predicted distribution of organic chemicals in solution and adsorbed as a function of position and time for various chemical and soil properties. *Soil Sci. Soc. Am. Proc*. **34**, 412-417.

Odum J. R., Yu J., and Kamens R. M. (1994) Modeling the mass transfer of semivolatile organics in combustion aerosols. *Environ. Sci. Technol.* **28**, 2278-2284.

Odum J. R., Hoffmann T., Bowman F., Collins D., Flagan R. C., and Seinfeld J. H. (1996) Gas/particle partitioning and secondary organic aerosol yields. *Environ. Sci. Technol.* **30**, 2580-2585.

Ogden M. W., Eudy L. W., Heavner D. L., Conrad F. W. Jr, and Green C. R. (1989a) Improved gas chromatographic determination of nicotine in environmental tobacco smoke. *Analyst*, **114**, 1005-1008.

Ogden M. W., Maiolo K. C., Oldaker G. B., and Conrad F. W. Jr. (1986b) Evaluation of methods for estimating the contribution of ETS to respirable suspended particles. *43rd Tobacco Chemists' Research Conference*, *Richmond, VA.*

Pandis S. N., Paulson S. E., Seinfeld J. H., and Glagan R. C. (1991) Aerosol formation in the photooxidation of isprene and β-pinene. *Atmos. Environ.* **25A**, 997-1008.

Pandis S. N., Harley R. A., Cass G. R., and Seinfeld, J. H. (1992) Secondary organic aerosol formation and transport. *Atmos. Environ.* **26A**, 2269-2282.

Pankow J. F. (1986) Magnitude of artifacts caused by bubbles and headspace in the determination of volatile compounds in water. *Anal. Chem.* **58**, 1822-1826.

Pankow J. F. (1987) Review and comparative analysis of the theories on partitioning between the gas and aerosol particulate phases in the atmosphere. *Atmos. Environ.* **21**, 2275-2283.

Pankow J. F. (1988) Gas phase retention volume behavior of organic compounds on the sorbent poly(oxy-m-terphenyl-2',5'-xylene). *Anal. Chem.* **60**, 950-958.

Pankow J. F. (1991) Common y-intercept and single compound regression of gas-particle partitioning data vs 1/T. *Atmos. Environ*. **25A**, 2229-2239.

Pankow J. F (1992) Application of common y-intercept regression parameters for log K_p vs 1/T for predicting gas-particle partitioning in the urban environment. *Atmos.*

Environ. **26A**, 2489-2497.

Pankow J. F. (1993) A simple box model for the annual cycle of partitioning of semi-volatile organic compounds between the atmospheric and the earth's surface. *Atmos. Environ.* **27A**, 1139-1152.

Pankow J. F. (1994) An absorption model of gas/particle partitioning of organic compounds in the atmosphere. *Atmos. Environ.* **28**, 185-188.

Pankow J. F. In *Gas and Particle Partitioning Measurements of Atmospheric Organic Compound*; Lane D.A. Ed; Gordon and Breach:Newark, in press.

Pankow J. F., Ligocki M. P., Rosen M. E., Isabelle L. M., and Hart K. M. (1988) Adsorption/thermal desorption with small cartridges for the determination of trace aqueous semivolatile organic compounds. *Environ. Sci. Technol.* **60**, 40-47.

Pankow J. F. and Bidleman T. F. (1992) Interdependence of the slopes and intercepts from log-log correlations of measured gas-phase partitioning and vapor pressure-I. Theory and analysis of available data. *Atmos. Environ.* **26A**, 1071-1080.

Pankow J. F., Isabelle L. M., Buchholz D. A., Luo W., and Reeves B. D. (1994) Gas/particle partitioning of polycyclic aromatic hydrocarbons and alkanes to environmental tobacco smoke. *Environ. Sci. Technol.* **28**, 363-365.

Pella E. (1990a) Elemental organic analysis. Part 1: Historical development. *Am. Lab.* **22**, 116-124.

Pella E. (1990b) Elemental organic analysis. Part 2. Start of art. *Am. Lab.* **22**, 28-32.

Pellizzari E., Carpenter B. H., Bunch J. E., and Sawicki E. (1975a) Collection and analysis of trace organic vapor pollutants in ambient atmospheres. Technique for evaluation concentration of vapors by sorbent media. *Environ. Sci. Technol.* **9**, 552-555.

Pellizzari E., Carpenter B. H., Bunch J. E., and Sawicki E. (1975b) Collection and analysis of trace organic vapor pollutants in ambient atmospheres. Thermal desorption of organic vapors from sorbent media. *Environ. Sci. Technol.* **9**, 556-560.

Pellizzari E. D., Sheldon L. S., Sparacino C. M., Bursey J. T., Wallace L, and Bromberg S. (1984) *Proceedings of the 3rd International Conference on Indoor Air Quality and Climate,* **Vol. 4**, 303-308.

Philips J. L., Goldstone F. M., Reynolds G. L., Lester J. N., and Perry R. (1993) Relationships between indoor and outdoor air quality in four naturally ventilated office in the United Kingdom. *Atmos. Environ.* **27A**, 1743-1753.

Possanzini M., Febo A., and Liberti A. (1983) New design of a high-performance denuder for the sampling of atmospheric pollutants. *Atmos. Environ.* **17**, 2605-2610.

Pritchard J. N., Black A., and McAughey J. J. (1988) The physical behavior of sidestream tobacco smoke under ambient conditions. In *Indoor and Ambient Air Quality*, Perry R. and Kirt P. W. Ed, London: Selper.

Proctor C. J., Martin C., Bevan J. L., and Dymond H. F. (1988) Evaluation of an apparatus designed for the collection of sidestream tobacco smoke. *Analyst* **113**, 1509-1513.

R. J. Reynolds (1988) *Chemical and Biological Studies of New Cigarette prototypes that Heat Instead of Burn Tobacco.* R. J. Reynolds Tobacco Company, Winston-Salem, North Carolina.

Ramsey R. S., Moneyhun J. H., and Jenkins R. A. (1990) Generation, sampling and chromatographic analysis of particulate matter in dilute sidestream tobacco smoke. *Anal. Chim. Acta* **236**, 213-220.

Repace J. L. and Lowrey A. H. (1985) Observational vs. extrapolative models in estimating mortality from passive smoking. *Environ. Int.* **11**, 3-22.

Robert G. (1990) Indoor pollution: sources, effect and mitigation strategies. In *Environmental Tobacco Smoke, Proceedings of the International Symposium at McGill University*, Lexington books: Lexington, Massachusetts.

Roberts D. L. (1988) Natural tobacco flavor. *Recent Adv. Tob. Sci.* **14**, 49-81.

Rogge W. F., Hildemann L. M., Mazurek M. A., and Cass G. R. (1993a) Sources of fine organic aerosol. 2. Noncatalyst and catalyst-equipped automobiles and heavy-duty diesel trucks. *Environ. Sci. Technol.* **27**, 636-651.

Rogge W. F., Hildemann L. M., Mazurek M. A., and Cass G. R. (1993b) Sources of fine organic aerosol. 4. Particulate abrasion products from leaf surfaces of urban plants. *Environ. Sci.Technol.* **27**, 2700-2711.

Rogge W. F., Hildemann L. M., Mazurek M. A., and Cass G. R., and Simonelt B. R. T. (1994) Sources of fine organic aerosol. 6. Cigarette smoke in the urban atmosphere. *Environ. Sci. Technol.* **28**, 1375-1388.

Rounds S. A. and Pankow J. F. (1990) Application of a radial diffusion model to describe gas/particle sorption kinetics. *Environ. Sci. Technol.* **24**, 1378-1386.

Rounds S.A., Tiffany B. A., and Pankow J. F. (1993) Description of gas/particle sorption kinetics with an intraparticle diffusion model: Desorption experiments. *Environ. Sci. Technol.* **27**, 366-377.

Schmeltz I. and Hoffmann D. (1977) Nitrogen-containing compounds in tobacco and tobacco smoke. *Chem. Rev.* **77**, 295-311.

Sakuma H., Kusama M., Mnakata S., Ohsumi T. and Sugawara S. (1983) The distribution of cigarette smoke component between mainstream and sidestream smoke. Part I. Acidic components. *Beitr. Tabakforsh.* **12**, 63-71.

Sakuma H., Kusama M., Yamaguchi K., Matsuki T., and Sugawara S. (1984) The distribution of cigarette smoke component between mainstream and sidestream smoke. Part II. Bases. *Beitr. Tabakforsh.* **12**, 199-209.

Schauer J. J., Rogge W. F., Hildemann L. M., Mazurek M. A., and Cass G. R. (1996) Source apportionment of airborne particulate matter using organic compounds as tracers. *Atmos. Environ.* **30**, 3837-3855.

Schievelbein H. and Eberhardt R. (1972) Cardiovascular action of nicotine and smoking. *J. Natl.Cancer Inst.* **48**, 1785-1794.

Schuetzle D., Cronn D., and Crittenden A. L. (1975) Molecular composition of secondary aerosol and its possible origin. *Environ. Sci. Technol.* **9**, 838-845.

Schwartz G. P., Daisey J. M., and Lioy P. J. (1981) Effects of sampling duration on the concentration of particulate organic collected on glass fiber filters. Amer. Ind. Hyg. Assoc. J. **42**, 258-263.

Seinfeld J. H. (1986) *Atmospheric Chemistry and Physics of Air Pollution.* John Wiley & Sons: New York, NY.

Shah J. J., Johnson R. L., Heyerdahl E. K., and Huntzicker J. J. (1986) Carbonaceous aerosol at urban and rural sites in the United State. *J. Air Pollut. Control Assoc.* **36**, 254-257.

Sheffield A. E. and Pankow J. F. (1994) Specific surface area of urban atmospheric particulate matter in Portland, Oregon. *Environ. Sci. Technol.* **28**, 1759-1766.

Smith J. P., Grosjean D., and Pitts J. N. (1978) Observation of significant losses of particulate nitrate and ammonium from high volume glass fiber filter samples stored at room temperature. *J. Air Pollut. Control Assoc.* **28**, 930-933.

Snedecor G. W. and Cochran W. G. (1989) *Statistical Methods*. Iowa State University press: Ames, IA.

Stedman R. L. (1968) The chemical composition of tobacco and tobacco smoke. *Chem. Rev.* **68**, 153-207.

Sterling T. C., Dimich H., and Kobayashi, D. (1982) Indoor byproduct levels of tobacco smoke: a critical review of the literature. *J. Air Poll. Assoc.* **32**, 250-259.

Storey J. M. E. (1993) *Gas/Particle Partitioning of Semi-Volatile Organic Compounds to Model Atmospheric Paticulate Material*. Ph.D. Thesis, Oregon Graduate Institute, Portland, OR.

Storey J. M. E. and Pankow J. F. (1992) Gas-particle partitioning of semi-volatile organic compounds to model atmospheric particulate materials - Part I. Sorption to graphite, sodium chloride, alumina, and silica particles under low humidity conditions. *Atmos. Environ.* **26A**, 435-443.

Storey J. M. E., Luo W., Isabelle L. M., and Pankow J. F. (1995) Gas/solid partitioning of semivolatile organic compounds to model atmospheric solid surfaces as a function of relative humidity. Part 1. Clean Quartz. *Environ. Sci. Technol.* **29**, 2420-2428.

Supelco, Inc (1990) High-purity carbon molecular sieves for monitoring many volatile airborne contaminants. *The Supelco Reporter*, **9**, 13-16.

Tang H., Richards G., Lee M. L., Lewis E. A., Hansen L. D., and Eatough D. J. (1990) Solanesol - A tracer for environmental tobacco smoke. *Environ. Sci. Technol.* 24, 848-852.

Thompson C. V., Jenkins R. A., and Higgins C. E. (1989) A thermal desorption method for the determination of nicotine in indoor environments. *Environ. Sci. Technol.* **23**, 429-435.

Tiegs D., Gmehling J., Medina A., Soares M., Bastos J., Alessi P., and Kikic I. (1986) *Activity Coefficients at Infinite Dilution*. Vol. IX, Part 1 & Part 2; DECHEMA: Germany.

Timmermans, J. (1950) *Physico-chemical Constants of Pure Organic Compounds*; Elsevier Pub. Co.: New York.

Thrane K. E. and Mikalson A. (1981) High-volume sampling of airborne polycyclic aromatic hydrocarbons using glass fiber filters and polyurethane foam. *Atoms. Environ.* **15**, 909-918.

Turner B. C. and Glotfelty D. E. (1977) Field sampling of pesticide vapors with polyurethane foam. *Anal. Chem.* **15**, 909-918.

Turpin B. C. and Huntzicker J. J. (1991) Secondary formation of organic aerosol in the Los Angeles basin: A descriptive analysis of organic and elemental carbon concentrations. *Atmos. Environ.* **25A**, 207-215.

Turpin B. J. and Huntzicker J. J. (1994) Investigation of organic aerosol sampling artifacts in the Los Angeles basin. *Atmos. Environ.* **28**, 3061-3071.

Turpin B. J. and Huntzicker J. J. (1995) Identification of secondary organic aerosol episodes and quantitation of primary and secondary organic aerosol concentrations during SCAQS. *Atmos. Environ.* **29**, 3527-3544.

U.S. Department of Health and Human Services (1986) *The Health Consequences of Involuntary Smoking: A Report of the Surgeon General*. DHHS Pub. No. 87-8398. U.S Department of Health and Human Services, Public Health Service: Washington, DC.

U.S. Environmental Protection Agency (1972) Indoor-outdoor carbon monoxide pollution study. *General Electric Company final report EPA-RA-73-020*, office of Research and Monitoring.

Vainio H., Hemminki K., and Wilbourn J. (1985) Data on the carcinogenicity of chemicals in the IARC Monographs programme. *Carcinogenesis*, **6**, 1653-1665.

Van de Rostyne C. and Prausnitz J. M. (1980) Vapor pressure of some nitrogen-containing, coal-derived liquids. *J. Chem. Eng. Data* **25**, 1-3.

Van Vaeck L., Van Cauwenberghe K., and Janssens J. (1984) The gas-particle distribution of organic aerosol constituents: measurement of the volatilization artifact in Hi-Vol Cascade Impactor Sampling. *Atmos. Environ.* **18**, 417-430.

Van Vaeck L. and Van Cauwenberghe K. (1985) Characteristic parameters of particle size distributions of primary organic constituents of ambient aerosols. *Environ. Sci. Technol.* **19**, 707-716.

Vassilaros D. L., Kong R. B., Later D. W., and Lee M. L. (1982) Linear retention index system for polycyclic aromatic compounds: Critical evaluation and additional indices. *J. Chromatogr.* **252**, 1-20.

Wang S. C., Paulson S. E., Grosjean D., Flagan R. C., and Seinfeld J. H. (1992) Aerosol formation and growth in atmospheric organic/NO_x system - Part I. Outdoor smog chamber studies of C_7- and C_8-hydrocarbons. *Atmos. Environ.* **26A**, 403-420.

Wallace L. A., Pellizzari E. D., Hartwell T. D., Sparacino C. M., Sheldon L. S., and Zelon H. (1985) Personal exposures, indoor-outdoor relationships, and breath levels of toxic air pollutants measured for 355 persons in New Jersey. *Atmos. Environ.* **19**, 1651-1661.

Wells A J. An estimate of adult mortality in the united states from passive smoking. *Environ. Int.* **14**, 249-265.

West P. W., Sen B., and Gibson N. A. (1958) Gas-liquid chromatographic analysis applied to air pollution. *Anal. Chem.* **30**, 1390-1397.

Wiley J. A., Robinson J. P., Piazza R., Garrett K., Cirksena K., Cheng Y., and Martin G. (1991) Activity Patterns of California Residents. *Final Report No. A6-177-33; California Air Resources Board: Sacramento, CA.*

Williams F. W. and Umstead M. E. (1968) Determination of trace contaminants in air by concentrating on porous polymer beads. *Anal. Chem.* 40, 2232-2234.

Wilson N. K., Kuhlman M. R., Chuang J. C., Mack G. A., and Howes, J. E. Jr. (1989) A quiet sampler for the collection of semivolatile organic pollutants in indoor air. *Environ. Sci. Technol.* **23**, 1112-1116.

Windholz M. (1976) *The Merck Index,* 9th ed.; Merck & Co. Inc: New Jersey.

Wolfe N. L., Steen W. C., and Burns L. A. (1980) Phthalate ester hydrolysis: linear free energy relationships. *Chemosphere* **9**, 403-408.

World Health Organization (WHO) (1987) Air Quality Guidelines for Europe. *WHO Regional Publications*, *European Series 13*; WHO Regional Office for Europe: Copenhagen, Denmark.

Wu S. C. and Gschwen P. M. (1986) Sorption kinetics of hydrophobic organic compounds to natural sediments and soils. *Environ. Sci. Technol.* **20,** 717-725.

Yamasaki H., Kuwata K., and Miyamoto K. (1982) Effect of temperature on aspects of airborne polycyclic aromatic hydrocarbons. *Environ. Sci. Technol*. **16**, 189-194.

Ye Y., Tsai C. J., Pui D. Y. H., and Lewis C. W. (1991) Particle transmission characteristics of an annular denuder ambient sampling system. *Aerosol Sci. Technol.* **14**, 102-111.

Yocom J. E. (1982) Indoor-outdoor air quality relationships. *J. Air Pollut. Control. Ass.* **32,** 500-520.

Zhang X. and McMurry P. H. (1991) Theoretical analysis of evaporative losses of adsorbed or absorbed species during atmospheric aerosol sampling. *Environ. Sci. Technol.* **25**, 456-459.

Zlatkis A., Lichtenstein H. A., and Tishbee A. (1973) Collection and analysis of trace volatile organics in gases and biological fluids with a new solid sorbent. *Chromatogr.* **6**, 67-70.

Zwolinski B. J. and Wilhoit R. C. (1971) *Handbook of Vapor Pressures and Heats of Vaporization of Hydrocarbons and Related Compounds.* API44-TRC Publication No. 101. Thermodynamic Research Center, College station, Texas A&M University, TX 77843.

BIOGRAPHY

The author was born in Canton, China on December 3, 1969. She grew up in a suburban area from 1975 to 1987, which comprised her elemental and high school years. She moved back into the city in 1987 and began her college education in Zhongshan University. The author earned a B.S. degree in Geology in 1991 with honors. Although she had valuable undergraduate research experience with Dr. Jiangke Wang working on the classification of dinosaur eggs, she still had a dream of becoming a good chemist. This dream came true when the author was accepted as a Master's student at the Oregon Graduate Institute (OGI) in 1992.

At OGI, Cikui earned her Master's degree in Environmental Science and Engineering in 1993, and elected to pursue her Ph.D. degree in Environmental Chemistry under the supervision of Dr. James F. Pankow. She spent two years working on the gas/particle partitioning of semivolatile organic compounds to environmental tobacco smoke. A paper written on this work earned her a "Student Paper Award" granted by the American Chemical Society in 1996. The author then spent the summer of 1996 at the California Institute of Technology collaborating with Dr. John H. Seinfeld's group working on gas/particle partitioning to model aerosol and urban particulate matter. This collaboration provided her excellent opportunity to learn new techniques from other researchers. Cikui completed the requirements for her Ph.D. in 1997.

PUBLICATIONS

Liang C. and Pankow J. F. (1996) Gas/particle partitioning of organic compounds to environmental tobacco smoke: Partitioning coefficient measurements by desorption and comparison to urban particulate matter. *Environ. Sci. Technol.* **30**, 2800-2805.

Liang C. and Pankow J. F. (1996) Gas/particle partitioning of organic compounds to environmental tobacco smoke: Partitioning coefficient measurements by desorption and comparison to urban particulate matter. *Advance ACS Abstract*, June, 1996.

Pankow J. F., Mader B. T., Luo W., Pavlick A., and Liang C. (1997) Gaseous ammonia and the conversion of nicotine in tobacco smoke to its available free base form. *Environ. Sci. Technol.* 31, 2428-2433

Liang C. and Gallagher D. A. (1997) Quantitative Structure Property Relationship: Water solubility Prediction. *Am. Lab*. March 34-40.

Liang C., Pankow J. F., Odum J. R., and Seinfeld J. H. (1997) Gas/particle partitioning of semi-volatile organic compounds to model inorganic, model organic, and ambient smog aerosol. *Environ. Sci. Technol*. in press.

Liang C. and Gallagher D. A. (1997) Prediction of vapor pressure by QSPR and comparison to neural networks. In preparation.